NORTHWESTERN UNIVERSITY

# Regulation of Anaphase Progression during *Caenorhabditis elegans* Oocyte Meiosis

A DISSERTATION

SUBMITTED TO THE GRADUATE SCHOOL
IN PARTIAL FULFILLMENT OF THE REQUIREMENTS

for the degree

DOCTOR OF PHILOSOPHY

Field of Biological Sciences

By

Amanda Roca

EVANSTON, ILLINOIS

September 2018

**Abstract:**

Meiosis is a specialized form of cell division where chromosomes are duplicated once and segregated twice, in order to reduce the chromosome number by half to generate haploid gametes. In contrast to mitosis, oocyte meiosis in many species occurs in the absence of centrosomes, the microtubule organizing centers that nucleate microtubules and help to define the spindle poles. We have used *C. elegans* oocytes as a model system to study the mechanisms by which chromosomes congress and segregate on these acentrosomal spindles.

*C. elegans* oocytes use a chromosome segregation mechanism that is independent of end-on kinetochore microtubule attachments and instead utilizes lateral attachments and depends on a complex of proteins containing AIR-2/Aurora B kinase that forms a ring around the center of each homologous chromosome pair (Ring Complex, RC). These RCs facilitate congression during metaphase and then are released from chromosomes in anaphase and progressively disassemble as the chromosomes segregate. In this dissertation, we first demonstrate that RC disassembly and other aspects of normal anaphase progression are delayed in response to a variety of meiotic errors, revealing a regulatory mechanism for anaphase progression as well as a novel checkpoint-like mechanism that may function to allow errors more time to resolve. Next, we uncover mechanisms underlying the dynamic regulation of the RCs, revealing a general strategy by which protein complexes can be progressively remodeled. We find that the stability of the RC is regulated by a balance of SUMOylation and deSUMOylation activity and that the SUMO protease ULP-1 enables RC disassembly during anaphase. Finally, we provide further evidence that these unique chromosome segregation mechanisms function in the context of stabilized lateral microtubule attachments that persist through anaphase. These findings contribute to the overall understanding of cellular checkpoints, anaphase progression, and protein complex regulation during dynamic cellular processes.

**Acknowledgments:**

First and foremost, I have to acknowledge Sadie Wignall. Sadie you have shaped me into a great cell biologist, and it has been a pleasure to have you as a boss. Your enthusiasm for cell biology is infectious, and your positive attitude and supportive nature have been crucial to my success as a graduate student. Thank you so much for introducing me to cell biology and showing me how amazing microscopy can be! As a woman in science, I'm very fortunate to have found a great role model like you. You are an amazing speaker, teacher, writer, scientist, person, and mother. I hope I'm half as successful as you one day!

I also have to thank my lab mates for always challenging me to be a better scientist and creating such a great work environment. You are all amazing people and I had way too much fun working alongside you. To Carissa, Tim, and Ian- it has been a pleasure growing together as scientists and making six years of fun memories. You are all extremely talented people, and I know you will succeed at whatever you do next. To Nikita- thank you for loving the rings as much as I do! Your enthusiasm for science keeps me motivated every day. To Jeremy- you have been so much fun to work with, and you bring such a great perspective to our group. I will miss you all very much. And to my former lab mates and friends, Mike and Chrissy, thank you guys for always making me feel at home during the first few years in the lab. And finally, thank you to my undergraduate mentee Rachel, you helped me so much with the not so fun parts of biology but smiled your way through it!

Thank you to the best family in the whole world. You have made six years of graduate school very easy to get through. Our vacations and visits, phone calls, and cards have made working so far away that much easier. I am so incredibly lucky to have such an encouraging group of people rooting for me every day. And a special thank you to my husband Antonio who has been my partner throughout many big life changes in the last decade. You are the calm to my crazy and I love you.

To my committee, Jason Brickner, John Marko, and Tom O'Halloran. Thank you for giving me great insight throughout my graduate career. I appreciate that you all have such different backgrounds and perspectives on my work and kept me on my toes every time we met.

Finally, thank you to the BIF Facility and staff, to all the labs that have provided us with reagents throughout these projects, and to the Caenorhabditis Genetics Center for many of the strains used in this dissertation. This work has been supported by a National Science Foundation Graduate Research Fellowship grant and the Molecular Biophysics Training Program at Northwestern University.

**Abbreviations:**

*Caenorhabditis elegans* (*C. elegans*)

Catalytic domain (CD)

Chromosomal Passenger Complex (CPC)

Meiosis I (MI)

Meiosis II (MII)

Neck-head domain (NH)

Microtubule associated protein (MAP)

Nuclear envelope breakdown (NEBD)

Ring Complex (RC)

Spindle Assembly Checkpoint (SAC)

Small ubiquitin-like modifier (SUMO)

SUMO interacting motifs (SIMs)

**Dedication:**

I would like to dedicate this dissertation to my family, who throughout my graduate career has made it seem as though we weren't 1,000 miles apart.

**Table of Contents:**


| | Page |
|---|---|
| **Abstract** | **3** |
| **Acknowledgments** | **4** |
| **Abbreviations** | **6** |
| **Dedication** | **7** |
| **List of Figures** | **11** |
| **Chapter 1: Introduction** | **13** |
| 1.A Introduction to Cell Division | 14 |
| 1.B Meiosis | 15 |
| 1.C *C. elegans* as a model organism to study acentrosomal cell division | 18 |
| 1.D *C. elegans* oocyte meiosis | 19 |
| 1.E The Midbivalent Ring Complex | 24 |
| 1.F Aurora B and the Chromosomal Passenger Complex | 27 |
| 1.G The Spindle Assembly Checkpoint | 28 |
| 1.H The Abscission Checkpoint/ NoCut | 32 |
| 1.I The SUMOylation pathway | 33 |
| 1.J SUMOylation in *C. elegans* | 36 |
| 1.K SUMO during cell division | 36 |
| **Chapter 2: *Caenorhabditis elegans* oocytes detect meiotic errors in the absence of canonical end-on kinetochore attachments** | **40** |
| 2.A Introduction | 41 |
| 2.B The presence of univalents alters AIR-2/Aurora B behavior in anaphase | 42 |
| 2.C Defects prior to anaphase onset and environmental stresses can delay RC disassembly | 44 |

2.D Microtubule channels remain open and kinetochore disassembly is delayed in response to error 47

2.E The response to errors requires the kinetochore but not components of the spindle assembly checkpoint 50

2.F Conclusions and discussion 53

**Chapter 3: Dynamic SUMO remodeling drives a series of critical events during meiotic divisions** **59**

3.A Introduction 60

3.B RC disassembly in anaphase is a step-wise process 61

3.C SUMO association with RCs is correlated with the stability of the structures 62

3.D GEI-17-dependent SUMOylation regulates AIR-2 release from chromosomes 68

3.E The SUMO protease ULP-1 is required for RC disassembly and anaphase progression 68

3.F BUB-1 targets ULP-1 to the RC to promote disassembly 76

3.G ULP-1 has a role on RCs independent of SUMO maturation and RC disassembly 78

3.H ULP-1 protease is active prior to anaphase 80

3.I E2/E3 enzymes leave RCs before ULP-1 protease 83

3.J Conclusions and discussion 83

**Chapter 4: Expanded studies of chromosome segregation in *C. elegans* oocytes reinforce a role for lateral microtubule bundles** **90**

4.A Introduction 91

4.B Lateral microtubule bundles represent a stabilized population of spindle microtubules 92

4.C Lateral microtubule bundles run alongside chromosomes throughout anaphase 94

4.D Lateral microtubule bundles are stabilized during anaphase 97

4.E Conclusions and discussion 101

**Chapter 5: Final conclusions and future directions 106**

5.A Summary of findings 107

5.B Future directions 108

5.B.1 Error-sensing during oocyte meiosis 108

5.B.2 The error response and chromosome segregation mechanisms 111

5.B.3 SUMO-mediated RC regulation 114

5.C Final remarks 115

**Chapter 6: Materials and Methods 117**

**Chapter 7: References 128**

**Appendix 143**

Appendix A 143

Appendix B 144

Appendix C 145

**List of Figures:**

**Figure 1.1** Mitosis vs. Meiosis

**Figure 1.2** *C. elegans* mitosis versus acentrosomal oocyte meiosis

**Figure 1.3** Body diagram of *C. elegans*

**Figure 1.4** Chromosome organization during *C. elegans* meiosis

**Figure 1.5** *C. elegans* meiotic kinetochores

**Figure 1.6** Stages of *C. elegans* oocyte spindle assembly

**Figure 1.7** Model for chromosome segregation in *C. elegans* oocytes

**Figure 1.8** Ring Complex localization

**Table 1.1** Extensive list of Ring Complex proteins

**Figure 1.9** The Spindle Assembly Checkpoint

**Figure 1.10** The SUMOylation pathway

**Figure 1.11** Model for SUMO-mediated RC assembly

**Figure 2.1** AIR-2/Aurora B anaphase behavior is altered in the presence of univalents

**Figure 2.2** Quantification of AIR-2 localization in wild-type anaphase

**Figure 2.3** Defects prior to anaphase onset and environmental stresses can delay RC disassembly

**Figure 2.4** Microtubule channels remain open and kinetochore disassembly is delayed in response to error

**Figure 2.5** Kinetochore analysis under additional error conditions

**Figure 2.6** The response to errors requires the kinetochore

**Figure 2.7** The response to errors requires the kinetochore but not Spindle Assembly Checkpoint proteins

**Figure 2.8** MDF-1 (Mad1) localization and targeting in oocyte meiosis

**Figure 2.9** Model for kinetochore and AIR-2/Aurora B-mediated anaphase regulation

**Figure 3.1** SUMO and SUMO E2/E3 enzymes leave the RCs during anaphase

**Figure 3.2** SUMO associates with stabilized anaphase RCs

**Figure 3.3** GEI-17-dependent SUMOylation regulates AIR-2 release from chromosomes

**Figure 3.4** Characterization of the SUMO proteases ULP-2, ULP-4, and ULP-5

**Figure 3.5** The SUMO protease ULP-1 is required for RC disassembly

**Figure 3.6** ULP-1 antibody specificity and ULP-1 Meiosis II and Mitosis localization

**Figure 3.7** Other RC components colocalize with persisting SUMO and AIR-2 structures

**Figure 3.8** ULP-1 can deSUMOylate RC components AIR-2 and KLP-19 *in vitro*

**Figure 3.9** BUB-1 targets ULP-1 to the RC to promote disassembly

**Figure 3.10** ULP-1 has a role on RCs independent of SUMO maturation and RC disassembly

**Figure 3.11** SUMO intensity on RCs increases following *ulp-1* (RNAi)

**Figure 3.12** SUMO and AIR-2 intensity on RCs following ULP depletions

**Figure 3.13** E2/E3 enzymes leave RCs before ULP-1 protease

**Figure 3.14** Model for SUMO-mediated anaphase regulation

**Figure 4.1** Stabilized lateral microtubule bundles run alongside chromosomes prior to anaphase

**Figure 4.2** MEL-28 encircles mid to late anaphase chromosomes

**Figure 4.3** Lateral chromosome-microtubule interactions persist until the end of anaphase

**Figure 4.4** End-on microtubule interactions at the metaphase to anaphase transition are cold stable and depend on the kinetochore

**Figure 4.5** Lateral microtubule bundles represent a stabilized population of anaphase spindle microtubules

**Figure 4.6** Model for lateral microtubule-mediated chromosome segregation

**Figure 4.7** Dynein is localized to pole microtubules until mid anaphase

**Appendix Figure A** Validation of new RC protein antibodies

**Appendix Figure B** Other RC proteins can be SUMOylated *in vitro*

**Appendix Figure C** EBP-1 localization on oocyte spindles

# CHAPTER 1:

## Introduction

**1.A Introduction to Cell Division**

Cell division is the process by which one cell is divided into two or more daughter cells and is crucial for organism development and growth. In eukaryotes, there are two distinct forms of cell division; mitosis, where each daughter cell is genetically identical to the parent cell and meiosis, a reproductive cell division, where the number of chromosomes in the daughter cells is reduced by half to produce haploid gametes, either egg or sperm. Unlike mitosis, where chromosomes are duplicated once and divided once, in meiosis, chromosomes are duplicated once but go through two rounds of division. In order to carry out these divisions in both mitosis and meiosis, cells must align chromosomes during metaphase and equally segregate them during anaphase[1].

In order to coordinate chromosome movement, the cell builds an apparatus called a spindle, which is made of protein filaments called microtubules. Microtubules are composed of α and β-tubulin heterodimers that form tubular structures 25nm in diameter. They exhibit polarity arising from the head-to-tail arrangement of the α and β-tubulin dimers[2]. Therefore, in a protofilament, one end will have the α-subunits exposed ("minus-end") while the other end will have the β-subunits exposed ("plus-end"). Both ends are dynamic, but the plus-ends typically exhibit more periods of rapid growth and shrinkage. In the spindle, these dynamics are affected by proteins called MAPs (microtubule associated proteins)[3].

During most cell division, spindle microtubules are nucleated and organized by organelles called centrosomes. The centrosome is composed of two microtubule-based cylindrical structures called centrioles surrounded by a proteinaceous non-membrane-bound compartment called pericentriolar material[4]. Mitotic cells and spermatocytes use these structures to build a bipolar spindle and then coordinate chromosome movements. But interestingly, female egg cells (oocytes), plants, and higher fungi have lost centrosomes over evolution and use other mechanisms to organize their spindles and carry out chromosome movements. In general though, microtubules in both centrosomal and acentrosomal spindles are organized, sorted, and bundled by MAPs and motor proteins such as dynein and kinesins.

In order to carry out chromosome congression and segregation, microtubules make attachments to chromosomes via protein complexes called kinetochores, which assemble on the chromosome at a

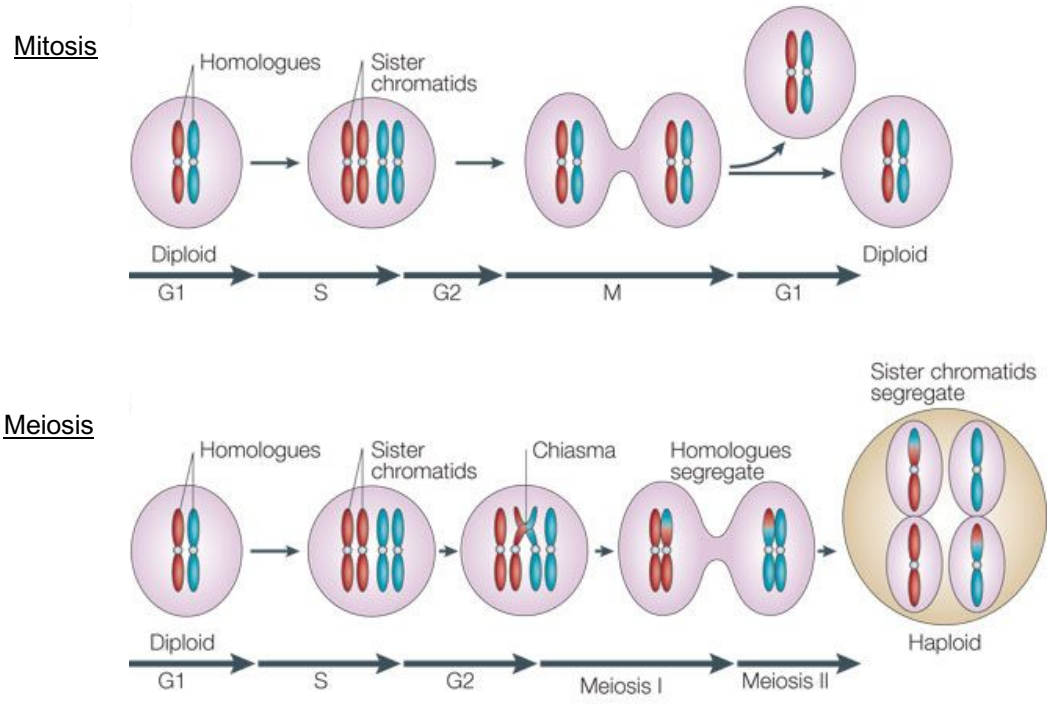


**Figure 1.1 Mitosis vs. Meiosis**
Top row depicts mitotic progression, whereby homologous chromosomes are replicated during S-phase to create sister chromatids, followed by one round of division where sister chromatids are partitioned equally to the two daughter cells. Unlike mitosis, during meiosis (bottom row), homologs undergo recombination to exchange genetic material. During meiosis I homologs separate and during meiosis II sisters separate. Figure has been adapted from Marston *et al*, 2005, *Nature Reviews Molecular Cell Biology*[5]**.**

defined region of the DNA called a centromere[6]. Once stably attached to all kinetochores, the cell initiates anaphase and microtubules depolymerize to pull chromosomes apart. Kinetochores are fairly conserved across organisms in terms of molecular composition, but the number of microtubules that can bind to an individual kinetochore varies widely across species[7].

### 1.B Meiosis

Meiosis is a unique type of cell division in sexually reproducing organisms in which the resulting gametes (egg and sperm) contain a haploid number of chromosomes. This allows for the regeneration of

the diploid genome when the egg and sperm come together to produce the resulting zygote, maintaining the ploidy of the organism. After a single genome duplication event, the meiotic cell undergoes two chromosomal divisions. In meiosis I (MI), the homologous chromosomes separate, and therefore sister chromatids must orient together to the same spindle pole. In meiosis II (MII), sister chromatids separate, yielding the haploid gamete. As opposed to spermatocyte meiosis where this process results in four haploid cells, during female egg meiosis (oocyte meiosis) these divisions produce only one viable haploid cell. During both MI and MII, a polar body is extruded, and the DNA is disposed of, leaving only one remaining haploid set of chromosomes. It is absolutely crucial that the mechanisms involved in these divisions are carried out correctly in order to produce viable gametes. Errors, such as a lagging or mis-segregated chromosomes, can result in an aneuploid zygote, meaning that it does not contain the correct number of chromosomes.

One defining feature of female oocyte meiosis is that it lacks centrosomes[8, 9]. In mitosis and spermatocyte meiosis, centrosomes are the organelles that define the spindle poles and act as the microtubule nucleating centers, giving rise to a bipolar spindle. But in oocytes, the centrosomes are degraded before the meiotic divisions and it is the sperm that retains its centrosomes for the resulting zygote after fusion with the egg. There are two main hypotheses for why this degradation happens, the first being that this prevents the occurrence of too many centrosomes in the resulting zygote. The second hypothesis is that spindles containing centrosomes generally are made of large astral microtubules that encompass the entire cell. One goal of the oocyte is to retain most of its cytoplasm, but that could be difficult to achieve when dividing a large spindle in half[10].

Errors during meiosis can cause an incorrect number of chromosomes in the embryo (aneuploidy), which has profound implications for human health. It is estimated that at least 10% of human embryos are chromosomally abnormal. One study revealed that greater than 35% of embryos from women who had suffered spontaneous abortions had an aneuploidy karyotype, making aneuploidy the leading cause of miscarriage.[11] Notably, the only aneuploidies that are compatible with life are trisomy of chromosomes 13, 18, and 21 and aneuploidies of the sex chromosomes, but even these result in severe health consequences.

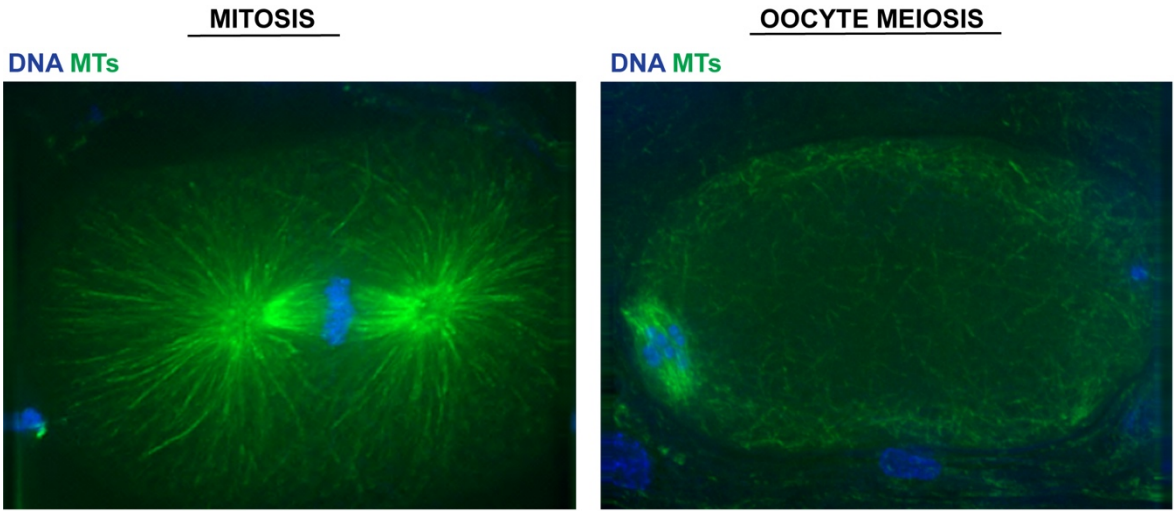


**Figure 1.2 Mitosis versus acentrosomal oocyte meiosis**
*C. elegans* one-cell mitotically dividing embryo (left) compared to a meiotically dividing acentrosomal oocyte (right), stained for DNA (blue) and microtubules (green). As opposed to the mitotic spindle containing centrosomes, the meiotic spindle is small, barrel-shaped, and located near the cortex of the cell.

Most aneuploidy in humans arises from problems with the female meiotic cells. Not only is female meiosis more error-prone than other cell divisions, but also the likelihood for error dramatically increases with age, resulting in an even higher incidence of miscarriage and birth defects, such as Down syndrome. One study reported than even in healthy young women, 25-30% of oocytes are aneuploid[112]. This has significant implications for human health and women's fertility. Despite its significance, much less is known about the distinct mechanisms of oocyte spindle assembly, chromosome movement, and error checkpoints as compared to mitosis. Therefore, it is important to investigate the molecular mechanisms that have given rise to such a fundamentally error prone process.

Remarkably, mammalian oocytes begin meiosis before the female is even born; oocytes arrest after homologous chromosomes have paired and recombined. This means that oocytes are arrested in early prophase until, at a minimum, the female hits puberty[13]. One of the main challenges with this is keeping the homologs paired for what could be decades. Studies in mouse oocytes have revealed that

there is no renewal or turnover of cohesin proteins during the meiotic prophase arrest and this suggests that over time, this connection deteriorates[14, 15]. This is also a problem for sister chromatids that need to remain to together during MI so they can co-segregate to the same spindle pole (before then becoming divided during MII). Studies have reported a loss in sister chromatid cohesin as an oocyte ages and an increase in the inter-kinetochore distance between the two sisters, causing the two chromatids to align incorrectly[14, 16]. Other studies have reported a decrease in BUB1 and BubR1(MAD3) (spindle assembly checkpoint proteins) and Sgo2 (a protein that protects cohesion) as oocytes age[12, 16]. These studies suggest that in mammalian oocytes in additional to being inherently error-prone, the frequency of errors increases with age.

### 1.C *C. elegans* as a model organism to study acentrosomal cell division

*C. elegans* is a useful model organism for studying the fundamental mechanisms of oocyte meiosis because like many other organisms, including humans and mice, the oocytes are acentrosomal. But unlike mammals, where the oocytes are difficult to obtain and study, *C. elegans* have many features that make them easy to image and genetically manipulate. First, they have a transparent body, which is ideal for live and fixed imaging, and the oocytes can be easily extracted for imaging as well. Second, *C. elegans* germlines are organized into an assembly-line fashion where cells progress through meiosis and then embryogenesis, making them easy to stage. Additionally, depletion of proteins by RNAi is straightforward and effective by means of either injection or simply by feeding the worms bacteria that have been transformed with constructs targeting individual genes; feeding RNAi allows for large functional screens. Furthermore, many useful *C. elegans* strains (mutants and fluorescently-tagged strains) are available and for those that are not, worms can be genetically manipulated to obtain new strains through CRISPR genome editing. Finally, cell division proteins are highly conserved between the nematode and mammalian systems, making the *C. elegans* an ideal model system for studying the basic mechanisms of spindle assembly, chromosome congression, and chromosome segregation in an acentrosomal system.

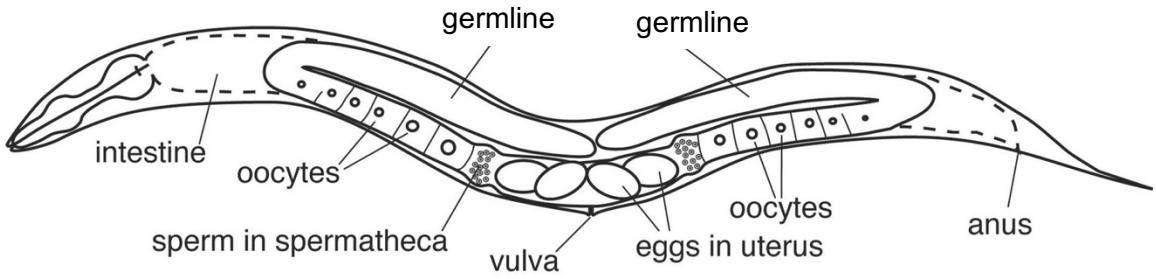


**Figure 1.3 Body diagram of *C. elegans***
Prophase arrested oocytes move through the spermatheca where fertilization triggers meiotic progression. Image adapted from 'wormbook.org'.

### 1.D *C. elegans* oocyte meiosis

In *C. elegans* hermaphrodites, meiosis begins after the six maternal chromosomes and six paternal chromosomes have undergone DNA replication to create sister chromatids. During early meiosis, the homologous chromosomes pair, and one off-centered crossover event occurs on each homolog pair[17]. This results in the propagation of a signal across the rest of the chromosome by the synaptonemal complex to prevent further crossover events. The off-centered nature of the crossover allows for the formation of "long arms" and "short arms" (Fig. 1.4). After recombination has occurred, the two sister chromatids and two homologous chromosomes rearrange and condense down, first going through a cruciform formation, and then reaching the "bivalent" stage, where the short arms have been tucked in so that the bivalent resembles a pill-like structure and the short arms are not distinguishable[18]. A cohesion protein, REC-8, localizes along the long and short arm axes[19], keeping the sisters and homologs together, while an MI specific cohesin, COH-3/4, coats only the short arm axis[20]. These will eventually be cleaved by the protease Separase (SEP-1) to initiate anaphase during MI.[19, 21]

*C. elegans* chromosomes are holocentric, meaning that the centromeric DNA, and therefore centromeric proteins, are dispersed throughout the entire chromosome; each bivalent contains approximately 100 point centromeres[22]. Because of this, the outer kinetochore assembles into structures

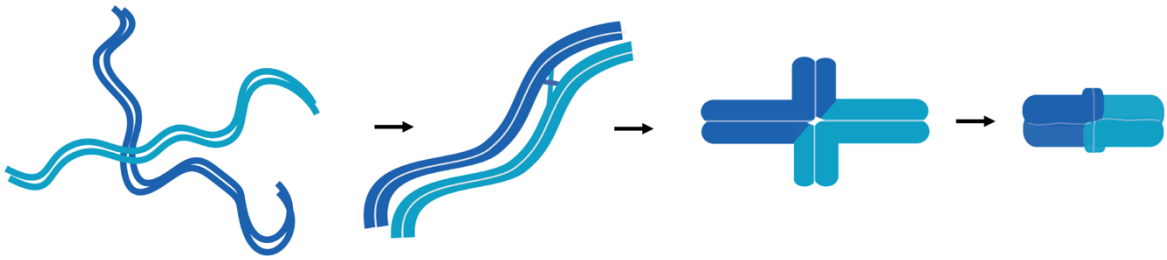

**Figure 1.4 Chromosome organization during *C. elegans* meiosis**
Homologous chromosomes pair up and recombination occurs. One crossover event causes the formation of short and long arms which then condense down to form the final bivalent structure where short arms are not distinguishable.

that cup each half of the bivalent (Figure 1.5)[23]. However, the kinetochore cups are excluded from the midbivalent region where a large protein complex localizes. The molecular composition of *C. elegans* kinetochores is very similar to that of other organisms, consisting of KNL-1, the MIS-12 complex, the NDC-80 complex, and the RZZ complex (the only major difference is that *C. elegans* lack a CENP-E homolog)[24-26]. Interestingly, while the worm uses kinetochores to make canonical end-on microtubule attachments to chromosomes to facilitate congression and segregation in mitosis and spermatocyte meiosis, kinetochores are not required for chromosome segregation in the oocytes. Instead they are more important for chromosome alignment during oocyte metaphase, likely orienting the bivalents within the lateral bundles[27]. It is not understood how kinetochores restrict end-on attachments in oocytes. It is also unclear how holocentric kinetochores in general prevent incorrect microtubule attachments when the “target” is so large.

Centromeres are usually defined by the presence of a centromere-specific variant histone CENP-A (also called cenH3), and this variant replaces Histone H3 to form centromeric nucleosomes. *C. elegans* contains two highly homologous CENP-A homologs, HCP-3 and a meiosis-specific variant, CPAR-1. Although HCP-3 is required for kinetochore assembly during the mitotic divisions, neither HCP-3 nor CPAR-1 are essential for building the kinetochore during oocyte meiosis. Intriguingly, HCP-3 is present on chromatin during MI but not MII in oocytes, and CPAR-1 is present during Metaphase I and II but is not

present during Anaphase I and II[23]. These mysterious localization patterns illustrate that there is still much to be learned about the contributions of centromeric histones during *C. elegans* meiosis including what alternative signals the kinetochore would use to assemble onto the bivalent.

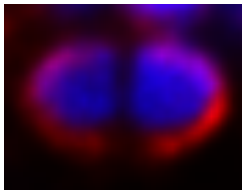


**Figure 1.5 *C. elegans* meiotic kinetochores**
In *C. elegans*, holocentric kinetochores form cup-like structures around the two halves of the bivalent but are excluded from the midbivalent region. Image shown is during oocyte meiosis, but a similar localization pattern in seen in spermatocytes.

In late prophase of MI, the oocyte arrests in until it passes through the spermatheca, in which fertilization by the sperm triggers nuclear envelope breakdown (NEBD) and the meiotic divisions. Immediately following NEBD, microtubules nucleate, and form a cage-like structure that mimics the shape of the nuclear envelope[28]. It is unclear how microtubules are nucleated during this cage-stage. We do know that unlike *Xenopus* and *C. elegans* mitotic cells, the oocytes do not fully rely on Ran-mediated microtubule nucleation where microtubule nucleating factors are activated near chromosomes due to a Ran-GTP gradient[29]. Once microtubules are nucleated, the microtubule bundles are progressively sorted by proteins such as KLP-18 and MESP-1, so that the minus ends are moved to the outer periphery. The spindle then goes through a multipolar stage before ultimately reaching bipolarity[28]. This process of coalescence of multiple early foci has also been observed in mice, frogs, and flies, and seems to be fairly universal in terms of acentrosomal spindle assembly. Many other proteins are involved in organizing the bipolar spindle, including the microtubule depolymerizer MCAK[30], the microtubule severing proteins MEI-1/2 (katanin)[31], the minus-end directed kinesins KLP-15/16[32], the minus end motor protein Dynein[33], and the Aurora A kinase, AIR-1[34]. These proteins all contribute to the overall size, length, and shape of the spindle.

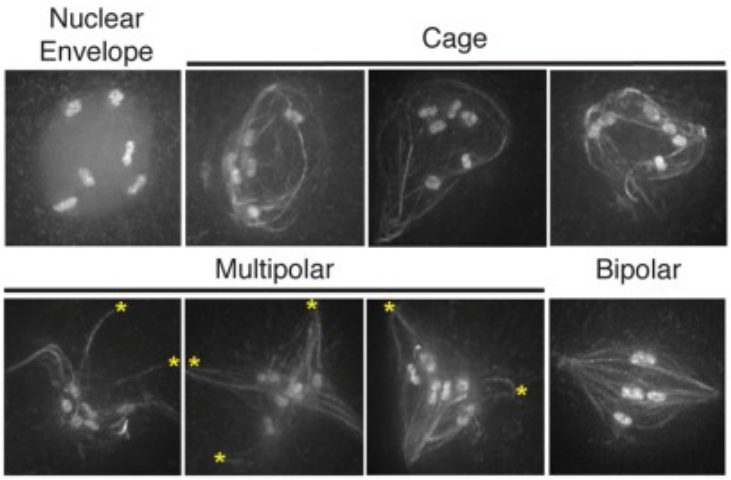


**Figure 1.6 Stages of *C. elegans* oocyte spindle assembly**
Upon NEBD microtubules nucleate in a cage formation and then the bundles are sorted and form multiple poles, which coalesce until the spindle reaches bipolarity.
Figure adapted from Wolff *et al*. *Molecular Biology of the Cell*, 2016[28]

One interesting feature of *C. elegans* oocyte spindles is that microtubules make lateral associations with the bivalents and end-on kinetochore attachments are not observed[35]. Moreover, chromosome congression and segregation is mediated by a large protein complex that forms a ring at the center of each bivalent called the ring complex (RC). During prometaphase, RC component and plus-end directed kinesin, KLP-19, is thought to "walk" chromosomes along the lateral bundles to the center of the spindle where the microtubule plus-ends overlap[35]. Once chromosomes have aligned, a mechanism mediated by LIN-5 (NuMA), ASPM-1, CMD-1 and dynein allows the spindle to rotate 90° and shrink from approximately 10μm to 3-4μm, causing the pole microtubules to come in contact with the kinetochores[36, 37]. At this point, it is hypothesized that transient microtubule attachments may occur, as the two sides of the bivalent appear to stretch just before anaphase onset[38]. Anaphase is initiated upon Securin degradation, allowing for REC-8 and COH-3/4 cleavage by SEP-1/separase at the midbivalent region between the two homologous chromosomes[19, 21]. The RCs between the homologs are released from chromatin, releasing the plus-end directed force, and minus end forces function to move chromosomes along the lateral bundles towards the poles.[39]

During the first stage of anaphase (Anaphase A), the spindle poles broaden, organizing the microtubules in a parallel array, and homologous chromosomes move towards spindle poles through open microtubule channels along lateral bundles[38]. The kinetochores are still present during this stage. During the second stage of anaphase (Anaphase B), the chromosomes reach the poles and the entire spindle elongates via ZYG-8 dependent microtubule polymerization, and this drives the majority of segregation[38]. By Anaphase B, kinetochores have been completely disassembled. Although kinetochores are present during Anaphase A, depletion of KNL-1 does not affect the overall segregation rate, illustrating a kinetochore-independent mode of chromosome segregation[27]. Once the homologs have fully segregated (usually around 5μm), the first polar body is extruded, and the retained sister chromatids begin to reorganize. They become oriented in opposite directions with REC-8 between them[20]. A similar sequence

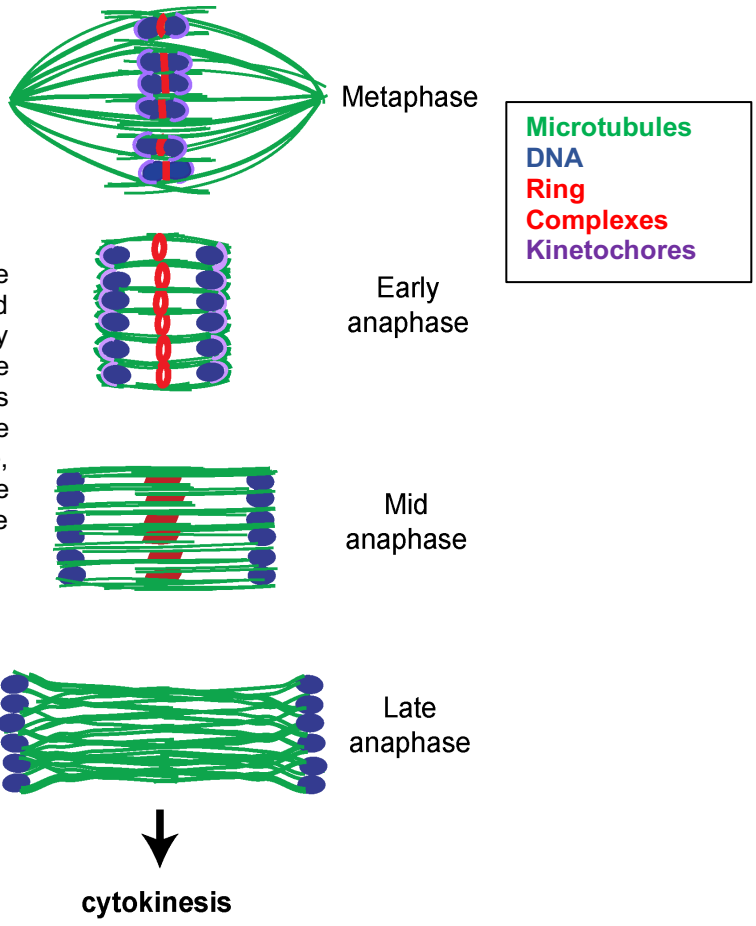


**Figure 1.7 Model for chromosome segregation in *C. elegans* oocytes**
Ring complexs (RCs) formed around the midbivalent region provide plus-end directed forces during metaphase. In early anaphase the spindle shrinks, RCs are removed as cohesin between homologs is released, and chromosomes move towards spindle poles. By mid anaphase, RCs are disassembling, kinetochores are absent and the spindle elongates to drive further segregation.

of events occurs during MII with the only major differences being that 1) spindle assembly does not include a cage-stage and 2) the metaphase and anaphase spindle sizes scale down relative to the chromosome size. Finally, a second polar body is extruded and a nucleus reforms around the remaining six chromosomes. The female and male pronuclei will later fuse to ultimately regenerate a diploid organism.

### 1.E The Midbivalent Ring Complex

In addition to the previously mentioned kinesin KLP-19, the ring complexes are comprised of many other conserved cell division proteins including the kinase BUB-1 (a component of the spindle assembly checkpoint, discussed in a later section), the CENP-F homologs HCP-1/2, the CLASP homolog CLS-2[27], the microtubule depolymerizing kinesin MCAK[30], a condesin I component CAPG-1[40], and the Chromosomal Passenger Complex containing AIR-2/Aurora B, ICP-1/INCENP, BIR-1/Survivin, and CSC-1/Borealin[41-43] (an extensive list is shown in Table 1.1). Some of these proteins, such as BUB-1, HCP-1/2, and CLS-2 are also localized to the kinetochore but are recruited to these two locations using distinct mechanisms. Others, such as MCAK and KLP-19, also coat the chromatin. The RC is particularly interesting because although

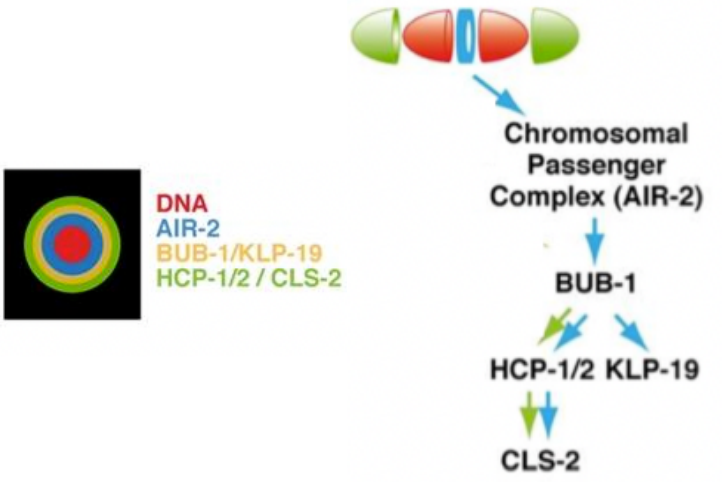


**Figure 1.8 Ring Complex localization**
(Left) Placement of RC proteins relative to one another and (right) localization dependency between RC components for RC and kinetochore localization (noted by blue and green arrows, respectively). Figure adapted from Dumont *et al Nature Cell Biology,* 2010[27]

these proteins are all quite conserved and their individual roles in cell division have been described, they have never been observed together in a large protein complex, independent of the kinetochore/centromeric region. Additionally, the canonical roles of these proteins typically involve regulation of end-on kinetochore microtubule attachments which are not apparent in the oocyte and even if they were, the RCs are located in a distinct location from the kinetochores.

RC assembly occurs during early prometaphase, concurrently with NEBD. The Chromosomal Passenger Complex first rearranges from what appears to be a linear localization along the short arm axis[44], to a ring-like structure encircling this region. Then, the other proteins are progressively recruited in a SUMO-dependent manner[45] (discussed further in the SUMO section) as shown in Figure 1.8. Dumont *et al* found that the CPC is required for BUB-1 to localize to the RCs. BUB-1 is required for KLP-19 and HCP1/2 to localize to the complex, and HCP1/2 is required for CLS-2 localization[27]. The same study also illustrated the relative positions of these components by fluorescently labeling them and measuring the diameters of the resulting ring. This placed components into an outer, middle, and inner layer. AIR-2 is in the inner layer, BUB-1 and KLP-19 are in the middle layer, and HCP-1/2 and CLS-2 are on the outer layer[27]. These experiments suggest that the overall architecture of the RC is structured by layers of subcomplexes.

During prometaphase, the RCs provide a plus-end directed force to move the chromosomes towards microtubule plus ends in the center of the spindle[35]. Once anaphase is initiated SEP-1 relocalizes from the kinetochores to the RCs[39], cleaves cohesin between the two homologs[21], and the homologs begin to separate. The RCs are then released from chromosomes thereby removing the plus-end directed force from chromosomes. For a brief period of anaphase, RCs remain intact at the center of the anaphase spindle within channels formed by the lateral microtubule bundles. RCs are thought to keep these channels wide and open for chromosomes to move through as they segregate[39, 46]. The fact that the RCs remain intact during this stage demonstrates structural integrity as an independent complex. But as anaphase progresses the RCs disassemble, flatten out, and are not apparent by late anaphase. This disassembly process includes three major events: 1) various proteins leave the complex (or are potentially degraded), 2) the RCs are physically squished by the collapsing microtubule channels, and 3) AIR-2/the CPC relocalizes from the

RCs to coat anaphase spindle microtubules. Throughout this dissertation we use AIR-2 relocalization to microtubules as a readout of RC disassembly.

| ***C. elegans*** **RC Protein** | **Yeast/Human homolog** | **Localization during oocyte meiosis** | **General protein function** |
|---|---|---|---|
| AIR-2 | Ipl1/Aurora B | RC (M)<br>Spindle microtubules (A) | CPC, Serine/Threonine kinase |
| CSC-1 | Nbl1/Borealin | RC (M)<br>Spindle microtubules (A) | CPC, localization subunit |
| BIR-1 | Bir1/Survivin | RC (M)<br>Spindle microtubules (A) | CPC, localization subunit |
| ICP-1 | Sli15/INCENP | RC (M)<br>Spindle microtubules (A) | CPC, scaffold, MT binding |
| BUB-1 | Bub1/BUB1 | RC and KT | Serine/Threonine kinase<br>Spindle Assembly Checkpoint |
| HCP-1/2 | (none)/CENP-F | RC and KT | Kinetochore associated |
| CLS-2 | Stu1/CLASP1 | RC and KT | MT polymerizer |
| CAPG-1 | Ycg1/CAP-G | RC (M)<br>Spindle microtubules (A) | Condensin I component |
| SEP-1 | Esp1/Separin | RC (A) | Cleaves cohesion at anaphase onset |
| UBC-9 | Ubc9p/UBC9 | RC (M) | SUMO E2 conjugase |
| GEI-17 | Siz1p/PIAS1 | RC (M) | SUMO E3 ligase |
| ULP-1 | Ulp1p/SENP1 | RC | SUMO protease |
| SMO-1 | Smt3p/SUMO1 | RC | Reversible post-translational modification |
| MCAK | (none)/KIF2C | RC and chromatin | MT depolymerizer |
| KLP-19 | (none)/KIF4a | RC and chromatin | Plus-end directed kinesin |

**Table 1.1 Extensive list of Ring Complex proteins**
Abbreviations: M=metaphase, A=anaphase, CPC= chromosomal passenger complex, MT= microtubule

**1.F Aurora B and the Chromosomal Passenger Complex**

The Chromosomal Passenger Complex (CPC) is a major regulator of mitosis and meiosis in most eukaryotes and includes the proteins AIR-2 (Aurora B), ICP-1 (INCENP), BIR-1 (Survivin), and CSC-1 (Borealin)[47]. Because an immense amount of research has been done on this complex, I will highlight discoveries that appear to be general features of the complex but come from work in multiple organisms and from both mitosis and meiosis. The CPC is thought to have two functional modules bridged by INCENP. First, Borealin and Survivin bind to the N-terminal region of INCENP to form a triple helix, and this part of the complex aids in localization to the chromosome during prometaphase. It is well established that the Histone H3 Threonine 3 mark by Haspin kinase is recognized by Survivin,[48, 49] and some evidence suggests that the BUB-1-dependent mark on Histone H2A at Threonine 120 may be recognized by Borealin[50]. On the other end of the complex, the Serine/Threonine protein kinase Aurora B is associated with the C-terminal part of INCENP, and this interaction causes an autophosphorylation event that is required for full Aurora B kinase activity[51]. Besides its scaffolding role, INCENP also contains a microtubule binding domain that is thought to regulate and mediate the interaction between the CPC and spindle microtubules when the CPC relocalizes during anaphase[52]. In general, the CPC localizes to chromatin through metaphase and then relocalizes to spindle microtubules in anaphase[47]. Dynamic changes in CPC localization throughout mitosis and meiosis ensure that phosphorylation substrates are spatially restricted, as the CPC has substrates essential for chromosome condensation, correction of improper kinetochore-microtubule attachments, activation of the Spindle Assembly Checkpoint, and cytokinesis.

Aurora B is involved in many processes throughout cell division. First, it is involved in recruiting condensin to the chromosomes which is crucial for proper chromosome condensation[53]. Aurora B has also been shown to phosphorylate the Shugoshin proteins that protect cohesion between sister chromatids in Meiosis I. Interestingly though, Aurora B is also involved in degradation of cohesion at anaphase onset, by phosphorylating cohesin along the inter-homolog access, allowing it to be cleaved by Separase[19, 21]. Aurora B is also implicated in recruiting the Spindle Assembly Checkpoint proteins to the kinetochore, and it functions to destabilize improper microtubule attachments through localization of MCAK and inhibition of

kinetochore proteins[54-57]. During anaphase, the CPC relocalizes to the microtubules and is required for recruitment of the centralspindlin complex to the spindle midzone and has been shown to phosphorylate centralspindlin component MKLP1 (*C. elegans* ZEN-4) in order to enhance its microtubule bundling activity[58]. Furthermore, the CPC phosphorylates other spindle proteins such as Kif2a and Kif4, which are implicated in regulating spindle size[59, 60].

The CPC transition from the chromosomes to the spindle microtubules is crucial for proper cytokinesis and mitotic/meiotic exit[47]. It also prevents the reactivation of the Spindle Assembly Checkpoint and allows for decondensation of the chromosomes. This transition requires two events, that the CPC is released from chromatin and that it then binds microtubules. To remove the CPC from chromatin, most studies suggest that the previously mentioned histone phosphorylation marks that localize the CPC to chromatin during metaphase are removed[48, 49]. Furthermore, in yeast, the Cdk-1 phosphorylation mark on Sli15 (ICP-1/INCENP), which aids in chromosomal recruitment, is also removed at anaphase onset and this drives the relocalization process, as overall Cdk-1 activity is decreased[61]. These phosphorylation marks on both histone proteins and INCENP have been shown to be antagonized by Protein Phosphatase 1 (PP1) and PP2A.

A few hypotheses have been proposed for CPC transport and binding to the microtubules. In mammalian cells, CPC relocalization to the spindle midzone is thought to depend on MKLP2-driven, plus end-directed transport upon dephosphorylation of CDK1 marks on both proteins[62, 63]. In yeast (which lack an MKLP2 homolog), Ipl1 (AIR-2/Aurora B) becomes associated with Bim1 (EB1 homolog), a protein that localizes to the plus-ends of microtubules [61]. Another mechanism of CPC relocalization is through regulation of INCENP's microtubule binding domain. Upon dephosphorylation, the CPC affinity for microtubules increases dramatically[64]. In *C. elegans*, it is not understood which of these mechanisms occurs.

### 1.G The Spindle Assembly Checkpoint

As noted in the previous two sections, multiple components of the RC have known roles in an error detection mechanism called the spindle assembly checkpoint (SAC) that has been well characterized in mitosis in many systems. The spindle assembly checkpoint monitors kinetochore-microtubule attachments

and delays anaphase onset until all proper attachments have been made[65]. A proper kinetochore-microtubule attachment is called an amphitelic attachment, defined as the two sister chromatids being attached to microtubules emanating from opposite poles, and thus becoming “bioriented”. This ensures that each daughter cell receives only one copy of a chromosome. During prometaphase and metaphase, other types of attachments can occur: 1) monotelic, where only one sister chromatid is attached to microtubules from a spindle pole and the other is unattached, 2) syntelic, where the two sisters are both attached to microtubules emanating from the same pole, or 3) merotelic, where a single sister chromatid is attached to microtubules from both poles. It is hypothesized that the cell can sense the tension across the chromosome when a proper amphitelic attachment forms and it then relays this information to the cell cycle machinery[66].

Components of the spindle assembly checkpoint are responsible for monitoring the attachment status and signaling when proper attachments are made[65]. These components include the Mitotic Checkpoint Complex proteins, MAD2, MAD3, BUB3, and CDC20, as well as MAD1, BUB1, and MPS1 (absent in *C. elegans*)[65]. During prometaphase, SAC proteins localize to kinetochores and keep SAC activated or “on” until they are removed. In mitosis, even a single unattached kinetochore can maintain the spindle checkpoint. When the SAC signal is “on” MAD1 and MAD2 form a complex at unattached kinetochores. MAD2 exists in two conformations, an “open” form (o-MAD2) and “closed” form (c-MAD2), and the MAD1/MAD2 complex at kinetochores catalyzes this conformational conversion. It is hypothesized that a cytoplasmic pool of o-MAD2 cycles on and off kinetochores, thus converting to c-MAD2, and this allows the protein to bind and inhibit CDC20, along with MAD3 (BubR1) and BUB3[67]. CDC20 is the mitotic activator of the APC/C, so inhibiting CDC20 prevents anaphase onset. Once all of the kinetochores are correctly attached, the SAC proteins at kinetochores are displaced and the checkpoint has been satisfied, CDC20 is released from inhibition and the APC/C becomes active. The APC/C then ubiquitinates Securin and Cyclin B to trigger their degradation by the proteasome, and this allows Separase (previously inhibited by Securin) to cleave Cohesin between chromosomes. The degradation of Cyclin B inactivates the master mitotic kinase, CDK1, which promotes exit from mitosis.

Aurora B kinase is critically important for error-detection during mitosis and meiosis. This kinase is particularly important for correcting merotelic attachments that are not sensed by SAC due to the tension

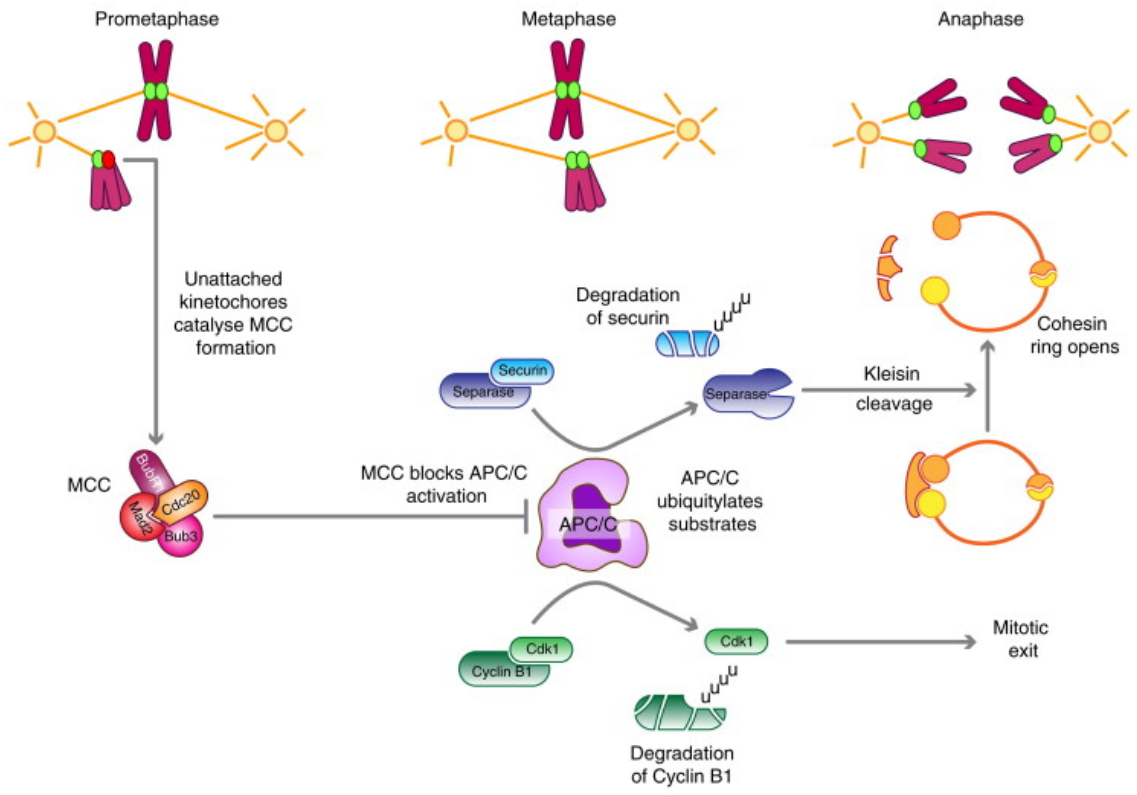


**Figure 1.9 The Spindle Assembly Checkpoint**
Unattached kinetochores promote the assembly of the Mitotic Checkpoint Complex (MCC) which inhibits the APC/C by binding its activator Ccd20. Upon proper attachments, SAC proteins at the kinetochore are displaced and Cdc20 binds and activates the APC/C. The APC/C ubiquitinates Cyclin B and Securin (Separase inhibitor). Separase cleaves cohesin and chromosomes segregate. Adapted from Lara-Gonzalez *et al,* Current Biology, 2012[65].

they create[68]. Aurora B has been shown to phosphorylate substrates on the kinetochore that aid in microtubule release and microtubule destabilization. Aurora B recruits MCAK to kinetochores to depolymerize microtubules[56] and phosphorylation of the kinetochore components NDC-80 and KNL-1 strongly reduces their microtubule binding activity[54, 55, 57]. Essentially, Aurora B activity on the kinetochore creates unattached kinetochores that can then be sensed by SAC. Studies have suggested that the ability of the system to sense tension depends on the localization of Aurora B relative to its substrates at the outer kinetochore. The most popular hypothesis for how this might work is called “the spatial separation model”,

which predicts that Aurora B is physically moved away from its kinetochore substrates when the chromosome is under tension[69]. But more recent studies have suggested that the kinetochore has an intrinsic capacity to stabilize microtubules when mechanical tension is applied (kinetochore-intrinsic model)[70]. Although it is still debated, some studies propose that Aurora B is more directly involved in the SAC response, outside of creating phosphorylating kinetochore substrates, and may do so by recruiting SAC components and promoting Mitotic Checkpoint Complex assembly[71].

It is still unclear if and how cells use SAC during meiosis. SAC proteins were traditionally defined as only essential under conditions when there was an error; depletion of these proteins on their own did not cause increased lethality, and they only became essential when a microtubule drug was added or microtubule attachments were perturbed in another way. However, in yeast cells, *Drosophila* oocytes, and mouse oocytes, SAC components are required for proper meiotic divisions and depletion of these proteins results in highly accelerated anaphase and chromosome mis-segregation[72-75]. Despite this requirement during normal conditions, it is thought that in mouse oocytes and meiotically dividing yeast, SAC functions in a similar mechanism to mitotic cells, because a detectable delay in anaphase onset is observed after perturbing microtubule attachments[73, 76].

It is clear that SAC is much more permissive in female meiosis than in other cell types; a few unattached kinetochores in mouse oocytes can escape detection[77]. Thus, one important area of research is understanding why SAC is so inefficient in mammalian oocytes. One study showed that SAC proteins BUB1 and BubR1 (MAD3) recruitment to kinetochores decreases with age in human oocytes[12]. Many other studies suggest that SAC may be leaky due to the large cytoplasmic size of the cell and SAC components are simply diluted out; this size problem has been characterized in large, mitotically dividing embryos[78]. Another problem may be that mouse oocyte kinetochores do not spatially separate from Aurora B when properly attached[79]. If the ‘spatial separation’ model is true, this would present a problem for the SAC mechanism in the oocyte.

**1.H The Abscission Checkpoint/ NoCut**

NoCut is a more recently discovered error-detection mechanism that can inhibit cytokinesis in the presence of chromatin at the spindle midzone by causing an abscission delay. The original paper describing this mechanism showed that in budding yeast, chromatin proximity would activate Ipl1 (AIR-2/Aurora B) and its activity would remain high as long as the chromatin was near the midzone[80]. During an error, such as a chromatin bridge, Ipl1 would remain active and cause anillin-like proteins Boi1 and Boi2 to remain at the bud neck and delay abscission. The authors noticed that cells that lacked an established midzone also initiated a checkpoint response and hypothesized that this was still due to Ipl1's association with chromatin. In this scenario, Ipl1 would remain on anaphase chromosomes instead of relocalizing. The authors pondered whether this novel error-detection mechanism could still work in higher eukaryotes because satisfying the NoCut checkpoint requires inactivation of Aurora B at the midzone and in other organisms Aurora B activity is required at the midzone for furrowing and cytokinesis.

A few years later, the same group further characterized the checkpoint mechanism as 1) being triggered by the presence of unsegregated chromatin over the spindle midzone 2) requiring targeting of the CPC to the central spindle and 3) involving a histone acetylation complex protein Ahc1[81]. But they also found that NoCut could be triggered when they forced Ipl1 to stay in contact with chromatin, independent of anaphase defects, Ahc1, the FEAR pathway, and CPC localization at the spindle midzone. It is still under debate which types of DNA structures are recognized by NoCut. Since these studies, various reports of an Aurora-B dependent abscission checkpoint mechanism have been reported in higher eukaryotes.

In HeLa cells, an Aurora B dependent, NoCut equivalent pathway works through chromatin activation, where Aurora B phosphorylates MKLP1 (ZEN-4), which stabilizes the intercellular bridge and prevents abscission[82]. But in contrast to the mechanism in yeast, which prevents chromatin breakage, in HeLa cells, this seems to be used to prevent tetraploidization, as the mammalian abscission machinery is incapable of cutting through chromatin and will instead regress and form a binucleate cell. More recent studies have shown that this Abscission Checkpoint also works through the ESCRT complex, which mediates membrane scission, showing that Borealin (BIR-1) can interact with the complex, promoting

phosphorylation by Aurora B and preventing cytokinesis[83]. In *C. elegans* mitotic cells, disruption of AIR-2, the spindle midzone, or condensin leads to cytokinesis failures in a chromatin-obstruction-dependent manner[84]. This study found that Condensin I normally localizes to the spindle midzone in anaphase, but was enriched on chromatin bridges near the midzone in an AIR-2 dependent manner. They proposed that AIR-2 recruits Condensin I to aid in the resolution of chromatin obstructions and helps to generate a signal to delay cytokinesis. Given these studies, it has become clear that a mechanism similar to NoCut exists in higher eukaryotes, but whether this checkpoint uses the same means to prevent abscission is still unknown.

**1.I The SUMOylation pathway**

The small ubiquitin-like modifier (SUMO) is a reversible post-translational modification. SUMO was first discovered in yeast, which only have one SUMO protein called Smt3 (suppressor of Mif2, a kinetochore protein) and interestingly, was identified in a screen as a gene that when mutated suppressed the severe anaphase progression defects cause by Mif2 mutations[85, 86]. Since then, SUMO has emerged as a major regulator in cell division. Conjugation of SUMO to target proteins can influence substrate protein localization, interactions, and degradation, and this highly conserved protein modification is generally required for proper development and has been implicated in many cellular processes and signaling pathways. The SUMO protein is approximately 12kD and at least one has been found in every eukaryotic organism studied, including fungi and plants. In humans, there are four confirmed SUMO isoforms: SUMO1, SUMO2/3 (which are so similar that they are experimentally indistinguishable) and SUMO4. In *C. elegans* there is only one, SMO-1 (which resembles SUMO1 in sequence but SUMO2/3 in electrostatic mapping[87]). Although the SUMO field is relatively new, it is becoming increasingly clear that SUMOylation and deSUMOylation play an important role in regulating cell division and other dynamic cellular processes.

Before SUMO can be conjugated to substrate proteins, it must first be matured by a SUMO protease (ULP-1/Ulp1 in worms and yeast, SENP1 in mammals), where the last amino acid(s) are cleaved off the newly translated SUMO revealing a C-terminal “GG” [88]. The “GG” of the SUMO is then covalently linked to an E1-activating enzyme (SAE1/SAE2 heterodimer in humans, AOS-1/UBA-2 in worms) and then transferred to an E2-conjugating enzyme (UBC9 in most organisms) through a thioester linkage. The E2

conjugase has the ability to transfer SUMO to the substrate protein, but a SUMO-specific E3 ligase accelerates this process, facilitating the transfer of SUMO to a lysine residue on the substrate protein through an isopeptide bond[89]. Experimental studies suggest that many SUMOylation sites follow a consensus motif of φ-K-X-E (where 'φ' is a hydrophobic residue), but there is growing evidence for variability in this sequence, including phosphorylations that can positively influence the motif. It is estimated that 65% of the human proteome carries the SUMO consensus sequence, suggesting that SUMOylation must have more regulation than just the motif[90, 91]. Importantly, SUMO itself usually carries this motif and this allows for SUMO chain formation. Interestingly though, *C. elegans* SUMO, SMO-1, does not have this exact motif and can still be chained, illustrating further that this motif is only suggestive.

SUMO modifications are removed by SUMO-specific cysteine proteases which cleave the isopeptide bond between SUMO and substrate proteins (SENP1, 2, 3, 5, 6, and 7 in vertebrates and ULP-1, 2, 4, and 5 in worms); ULP-1/SENP1 is also the enzyme that initially cleaves the C-terminus of SUMO during maturation. Regulation of these enzymes is still relatively unclear, but three general modes of regulation have been shown[92]. First, ULP/SENP activity has been shown to be modified by phosphorylation; in yeast, Ulp2 accumulates hyperphosphorylation during mitosis to suppress its activity[93] and in HeLa cells, SENP3 has also been shown to be phosphorylated to regulate mitotic activity[94]. Second, the proteases are regulated by restricting their localization, which is usually defined by their N-terminal region. For example, ULP-1 encodes a nuclear pore localization sequence and is restricted to that location until NEBD, when it moves to the meiotic spindle (Chapter 3). The final mode of regulation is through substrate preference. In organisms with multiple isoforms of SUMO, specific ULPs/SENPs have a preference for certain SUMO isoforms. Furthermore, individual protease families prefer to either cleave SUMO directly from substrate proteins or break SUMO-SUMO bonds, editing the number of SUMOs in a chain (for example, SENP6 and 7 are thought to prefer SUMO2/3 and chain-editing)[92].

Many SUMO interactions in the cell occur non-covalently, through SUMO Interacting Motifs (SIMs). SIMs are generally made of branched hydrophobic residues with serine and/or acidic residues on either side. A SIM forms a beta-strand that sits in the groove between a beta-strand and alpha helix of the SUMO

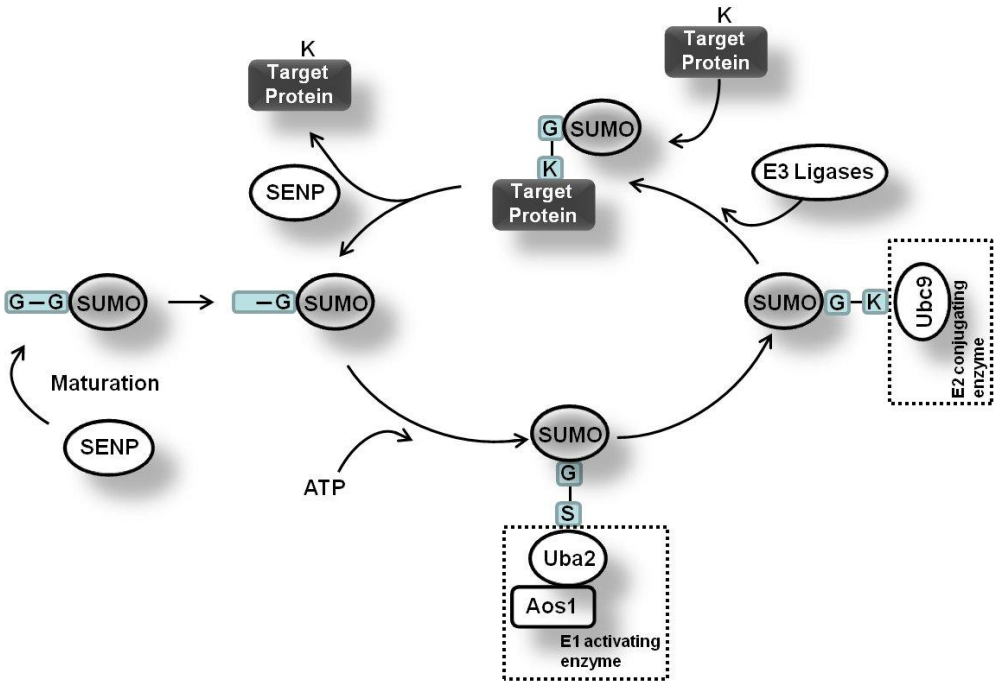


**Figure 1.10 The SUMOylation pathway**
SUMO becomes conjugatable after a C-terminal cleavage by a SUMO protease. Then it is conjugated to an E1 activating enzyme, is passed to an E2 conjugating enzyme, and an E3 ligase aids in conjugation to a lysine residue on the substrate protein. Figured adapted from Feligioni *et al*, *AIMS Molecular Science*, 2015[95].

molecule, and this interaction has a $K_d$ in the uM range[96]. This allows for an interaction that can be quickly modified if necessary.

Although the SUMO pathway and overall SUMO protein structure is very similar to ubiquitin, most of the research to date has shown that SUMO mainly affects protein-protein interactions and localization, rather than degradation. But, an interesting class of ubiquitin ligases have been recently discovered that recognize specific SUMO modifications as degradation signals. The STUbL (SUMO targeted Ubiquitin ligase) family of proteins ubiquitinate SUMO chains to create a dual signal for the recruitment of proteins able to bind SUMO and Ubiquitin simultaneously[97]. Once this mark is recognized, it leads to either extraction or degradation of the modified protein. Another interesting aspect to this phenomenon is that ULP/SENP proteins have been shown to antagonize this form of degradation by deSUMOylating these proteins; for

example, in mammals SENP6 is thought to protect the inner kinetochore from degradation through deSUMOylation[98].

### 1.J SUMOylation in *C. elegans*

In *C. elegans*, there is one SUMO (SMO-1) ortholog that can be conjugated to target proteins by the hierarchical actions of ULP-1 (removes the C-terminal phenylalanine), an E1 activating heterodimer, an E2 conjugating enzyme (UBC-9), and SUMO-specific E3 ligases (Siz/PIAS-type GEI-17 or MMS-21). Initial studies showed that *smo-1* (RNAi) results in embryonic arrest and homozygous deletion mutations cause sterility and abnormal gonad, germ cell, and vulva development[99, 100]. A 2018 mass spectrometry-based screen identified 874 proteins modified by SUMO in the worm; this study estimated that roughly 15-20% of the worm proteome is SUMOylated and that the amount globally increases in response to various stresses[101]. In the past decade, many more detailed studies have emerged showing just how crucial SUMO is in terms of organism development and cellular processes. SUMO has been implicated in *C. elegans* pharyngeal muscle development[102], vulva development[103], genes required for the E.R. stress response[104], X-chromosome dosage compensation[105], Hox gene expression[106], intermediate filament regulation[107], adherens junction assembly[108], sensory receptor localization to cilia[109], the mevalonate pathway during larval development[110], as well as mitotic and meiotic processes (discussed later). Microarray data suggest that there are high expression levels of SUMO during periods of increased cell division in the worm[101]. While these examples are limited to *C. elegans*, similar findings have been reported across all eukaryotes and illustrate just how useful SUMO is in regulating dynamic cellular processes.

### 1.K SUMO during cell division

SUMOylation has been previously reported to be essential for proper chromosome segregation during mitosis[111]. More recent studies have identified many mitotic proteins that are modified and may be responsible for these earlier observed phenotypes. First, cohesion proteins have been shown to be SUMOylated across many organisms, including yeast and humans[112-114]. Second, many centromere and kinetochore-localized proteins have been identified as SUMO substrates. These include CENP-H, CENP-

I, and CENP-K, Ndc10p, Cep3p, Ndc80[115], CENP-C (*in vitro*)[116], CENP-E (also binds SUMO chains on the kinetochore through a SIM motif)[117], Nuf2, BubR1(MAD3)[117], and Kif18A[118]. Many of these studies also involved perturbation of the SUMO state of the protein, which led to severe chromosome alignment, biorientation, and/or segregation defects, as well as mitotic exit delays or binucleate cells. SUMO not only plays a role at the kinetochore, but it also regulates anaphase midzone proteins, such as Kif4a, a plus-end directed kinesin that helps to limit the length of the anaphase spindle[119]. SUMO is also implicated in the metaphase to anaphase transition, as shown by two very recent papers identifying an APC subunit, APC4, as being regulated by the modification and necessary for timely entry into anaphase[120, 121]. Finally, in fungi, humans, and *Drosophila*, septins have been shown to be SUMOylated in order to promote proper cytokinesis[122-125].

The chromosomal passenger complex (consisting of Aurora B/AIR-2, Survivin/BIR-1, Borealin/CSC-1, and INCENP/ICP-1; discussed in detail earlier) has also been recently identified as SUMO-regulated. Two studies have reported that Aurora B is modified by SUMO in HeLa cells during mitotic division[19, 126]. One of these studies also suggests that SUMO is conjugated within the active site of the enzyme and this may regulate its kinase activity[19]. Another study identified Bir1p (the yeast homolog to BIR-1/Survivin) as a SUMO substrate during mitosis, although this group did not attempt investigate whether this modification has a functional role[115]. Beyond these direct modifications, SUMO regulates the CPC's dynamic localization during mitosis. In yeast, the CPC is targeted to the chromosomes via a Haspin kinase phosphorylation mark laid onto Histone H3 Threonine 3[49]. SUMOylation of DNA Topoisomerase IIα regulates Haspin during this process, and therefore, regulates CPC loading onto chromosomes[127]. Another study showed that in human cells Borealin is SUMOylated, peaking at early mitosis[94]. The protein also seems to interact with and be regulated by SENP-3, suggesting SUMOylation and deSUMOylation occurs throughout the cell cycle.

SUMO-mediated regulation is also implicated in meiotic processes; severe spindle assembly and chromosome segregation defects have been observed in budding yeast, rat oocytes, mouse oocytes, and human spermatocytes upon SUMO perturbation[128]. Accordingly, in imaging experiments SUMO can be observed across the spindles of many of these cells[129-131]. In early meiosis, homologous chromosomes

must pair up and exchange genetic material in a process called recombination. In budding yeast, the protein complex that holds the chromosomes together, the Synaptonemal Complex, is regulated by SUMOylation[132]. However, this has not been observed in other organisms. Another stage of meiosis affected by SUMO is NEBD (also referred to as 'germinal vesicle breakdown' in some organisms), which occurs just prior to building the meiotic spindle. In mouse oocytes, SUMO is required for this process[130, 131]. Finally, SUMO is involved in the maintenance of centromeric cohesion through the MI to MII transition, when Sgo2 (a protein that protects cohesin from cleavage) levels are reduced, but sister chromatids still need to remain together[129]. Beyond these studies, very few SUMOylated proteins involved in chromosome congression and segregation have been identified in meiotic cells, but given the high number of identified in mitosis, one can hypothesize that some of these carry over to the meiotic cells and contribute to the severe defects observed upon SUMO depletion or overexpression.

Only a few studies have investigated SUMO during cell division in *C. elegans*, but they reveal an important role for SUMO-mediated regulation during mitosis and meiosis. The first study showed that in the one-cell dividing embryo, SUMO is involved in the relocalization of the CPC from chromatin to microtubules. Pelisch *et al* found that this process involves ULP-4, proposing that ULP-4 deSUMOylates AIR-2/Aurora B at anaphase onset to promote relocalization to the midzone[133]. Another study found that depletion of SUMO or the SUMO conjugase UBC-9 affects the meiotic bivalent structure; these worms seemed to be unable to repair multiple DNA breaks before entering meiosis and therefore had an increased number of recombination intermediates and abnormal bivalent structure[134]. Finally, SUMO-mediated regulation has been directly implicated in RC assembly during oocyte meiosis[45]. Pelisch *et al* showed that: 1) SUMO, UBC-9 (E2 conjugase), and GEI-17 (E3 ligase) localize to the RC, 2) the RC does not assemble in the absence of GEI-17, 3) RC components AIR-2 and KLP-19 can be SUMOylated *in vitro* and KLP-19 is also SUMOylated *in vivo*, and 4) other RC components such as BUB-1 have SUMO interaction motifs (SIMs) that are necessary for interaction with SUMOylated RC proteins. The authors concluded that a network of SUMO-SIM interactions between RC proteins drives the assembly of the complex during prometaphase. These studies demonstrate that SUMO plays an important role during *C. elegans* cell division and encourage further investigation.

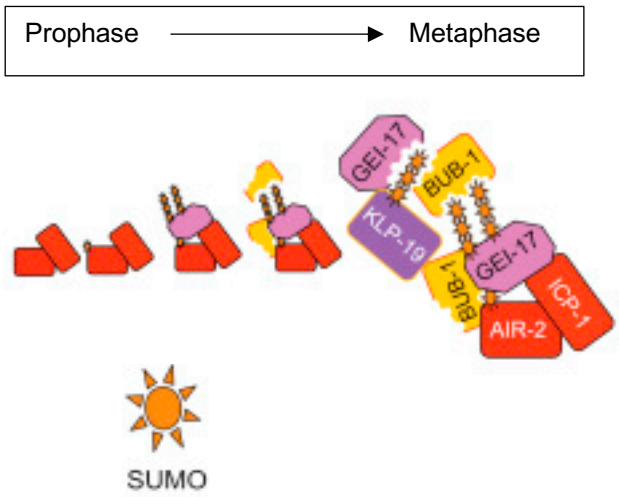


**Figure 1.11 Model for SUMO-mediated RC assembly**
Progressive assembly of the RC complex through SUMO-SIM interactions. AIR-2, GEI-17, and KLP-19 are proposed to be SUMOylated, while BUB-1 contains a SIM. In this model, SUMOylation of some components drives recruitment of SIM-containing proteins, driving progressive ring assembly. This figure has been adapted from Pelisch *et al,* Molecular Cell, 2017[135]

# CHAPTER 2:

## *Caenorhabditis elegans* oocytes detect meiotic errors in the absence of canonical end-on kinetochore attachments

The data presented in this chapter was published in the *Journal of Cell Biology*, PMID: 28356326
Some initial observations that led to this project were made by Christina Muscat, earning her authorship on this paper. However, almost all of the data in this chapter and in the published paper was generated by Amanda Roca, excluding the images in Figure 2.3E rows 2 and 3, which were taken by Christina Muscat.

**2.A Introduction**

Proper partitioning of chromosomes during cell division is essential for organismal viability. During mitosis, chromosomes attach to spindle microtubules at sites called kinetochores, forming end-on attachments that mediate chromosome congression and segregation[136]. These attachments are also central to a surveillance mechanism, the spindle assembly checkpoint (SAC), in which cells monitor the attachment of kinetochores to spindle microtubules as a means of detecting errors[137]. However, homologous chromosome pairs (bivalents) in *C. elegans* oocytes do not appear to form end-on attachments, and instead are surrounded by laterally-associated microtubule bundles running along their sides[35]. Whether these oocytes are able to detect and respond to errors is currently unknown.

*C. elegans* have holocentric kinetochores that, in meiosis, cup the ends of each bivalent[23]. Compromising kinetochore function by depleting KNL-1 (which is required for the loading of the MIS-12 complex, the RZZ complex, and BUB-1), results in chromosome alignment defects during metaphase, suggesting that these holocentric kinetochores help orient bivalents within the lateral microtubule bundles. Despite this, chromosome segregation appears to be largely kinetochore-independent, as kinetochores are normally removed from chromosomes during anaphase. Moreover, although KNL-1 depletion results in some lagging chromosomes, most segregate at normal rates, suggesting that kinetochore attachments are not generating the forces that drive segregation[27].

Instead, chromosome congression and segregation are aided by a protein complex that forms a ring around the center of each bivalent in Meiosis I (MI) and around the interface between sister chromatids in Meiosis II (MII); we refer to these as the midbivalent ring complexes (RCs). These RCs contain the kinesin-4 family member KLP-19, which has been proposed to provide chromosomes with a plus-end directed force that promotes movement to the metaphase plate along the laterally-associated bundles[35]. Then, in anaphase, these RCs are removed from chromosomes, removing this plus-end directed force and allowing poleward movement; additionally, the spindle also significantly elongates during anaphase, driving chromosomes further apart. In addition to KLP-19, the RCs include a number of other conserved cell division proteins and the chromosomal passenger complex, which consists of AIR-2/Aurora B kinase, ICP-1, CSC-1, and BIR-1, and is required for the targeting of all other known RC components[27].

Now, we have discovered that the behavior of these RCs changes in anaphase when errors are present. Surprisingly, despite the apparent lack of end-on attachments in this system, this error response requires the kinetochore. Our studies have therefore revealed a new mechanism that appears to regulate the progression of anaphase events in this specialized form of cell division and also suggest that the kinetochore plays a non-canonical role in error detection in these cells.

**2.B The presence of univalents alters AIR-2/Aurora B behavior in anaphase**

In a previous study, we assessed the contribution of the RCs to chromosome congression and segregation by examining the behavior of univalents, which do not undergo crossover formation and therefore lack RCs[39]. We used the *him-8* mutant, in which the X chromosomes fail to pair, [138]resulting in five RC-containing bivalents that segregate normally and two univalents that exhibit alignment and segregation defects.[39] Unexpectedly, during these studies we noticed unusual RC behavior in the *him-8* mutant during anaphase (Fig. 2.1).

During wild-type meiosis, separase (SEP-1) moves from the kinetochores to the RCs at anaphase onset, and as the chromosomes begin segregating the RCs remain at the center of the spindle.[27, 39] Shortly after, RC component AIR-2/Aurora B relocalizes across the spindle and the RC structures begin disassembling and are gone by late anaphase (Fig. 2.1A). In contrast, in the *him-8* mutant, AIR-2 often associated with the RCs in mid-to-late anaphase, and under these conditions the RCs appeared more intact, instead of flattening (Fig. 2.1B).

To quantify this behavior, we evaluated 246 wild-type spindles and established a chromosome segregation distance that we defined as the transition from early to mid anaphase, when AIR-2 should no longer be RC-associated. From this analysis, we found that AIR-2 had relocalized to microtubules in a majority of wild-type spindles when the chromosomes were ≥ 2.5μm apart (Fig. 2.2); at ≥ 2.5μm only 8% of mid anaphase spindles had AIR-2 in RC structures. In contrast, using these same criteria we found that AIR-2 was RC-associated (though sometimes faintly relocalized to the microtubules) in 34% of mid anaphase spindles in the *him-8* mutant (Fig. 2.1C). We observed similar behavior in the *zim-1* mutant (where chromosomes I and III fail to pair, resulting in four univalents[139]), demonstrating that autosomal

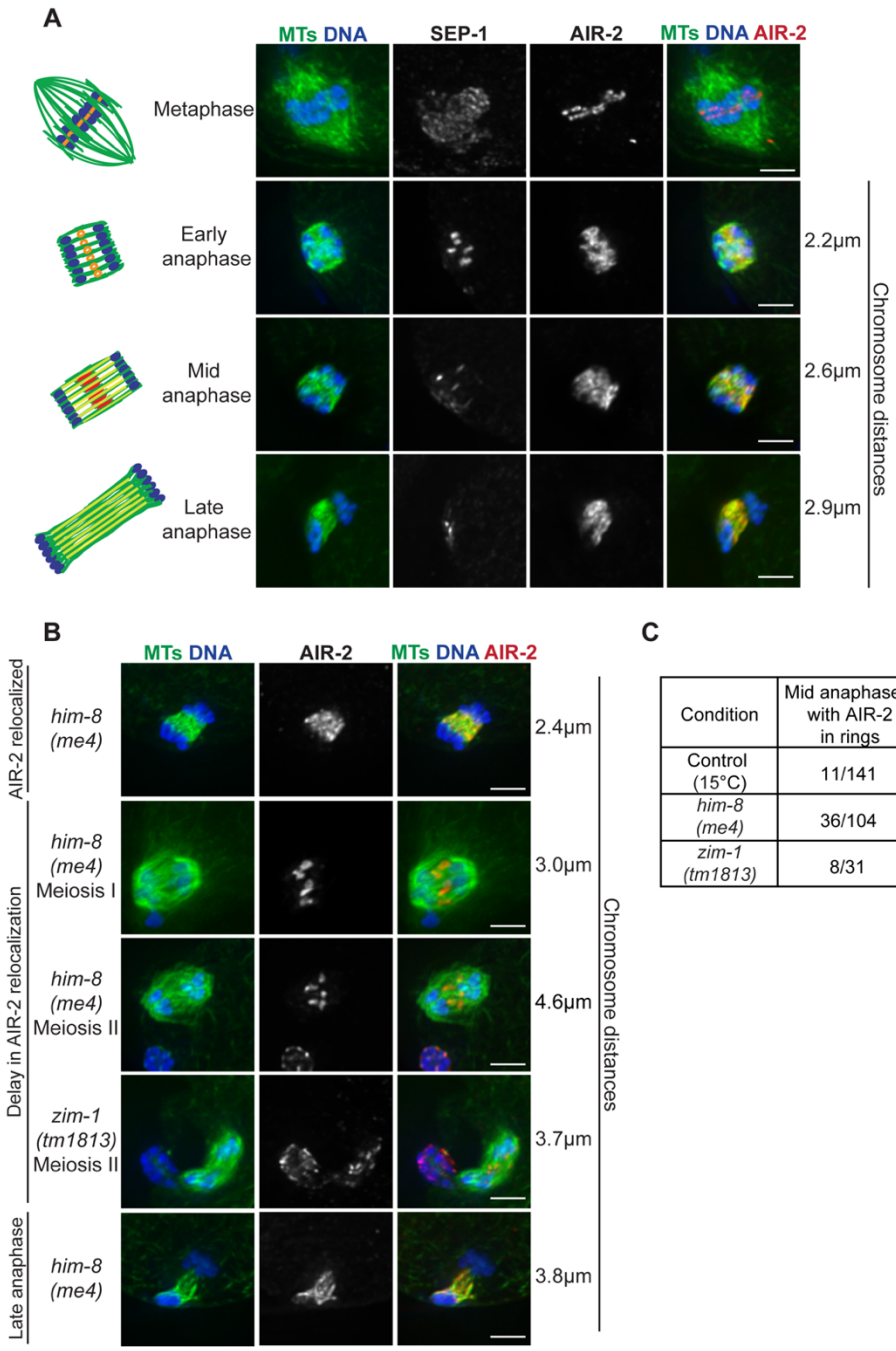


| Condition | Mid anaphases with AIR-2 in rings | Percent mid anaphases with AIR-2 in rings |
|---|---|---|
| Control (15°C) | 11/141 | 8% |
| *him-8 (me4)* | 36/104 | 34% |
| *zim-1 (tm1813)* | 8/31 | 26% |

**Figure 2.1 AIR-2/Aurora B anaphase behavior is altered in the presence of univalents**
(A) Wild-type anaphase in spindles stained for DNA (blue), tubulin (green), SEP-1, and AIR-2 (red in merge). The chromosome segregation distances and spindle morphology were used to determine the anaphase stages. Diagrams depict DNA (blue), microtubules (green), AIR-2 (yellow), the RCs without AIR-2 (red), and the RCs containing AIR-2 (orange). (B) AIR-2 behavior in spindles containing univalents, in either the *him-8(me4)* or the *zim-1(tm1813)* mutant. In some spindles, AIR-2 relocalizes to microtubules by mid anaphase (row 1), while in others AIR-2 remains RC-associated in MI (row 2) and MII (rows 3 and 4); note that in MII, AIR-2 also displays polar body localization. AIR-2 always relocalizes by late anaphase (row 5) (C) Quantification of mid anaphase spindles with AIR-2 in RCs for control, *him-8(me4)*, and *zim-1(tm1813)* MI and MII spindles. Bar = 2.5µm.

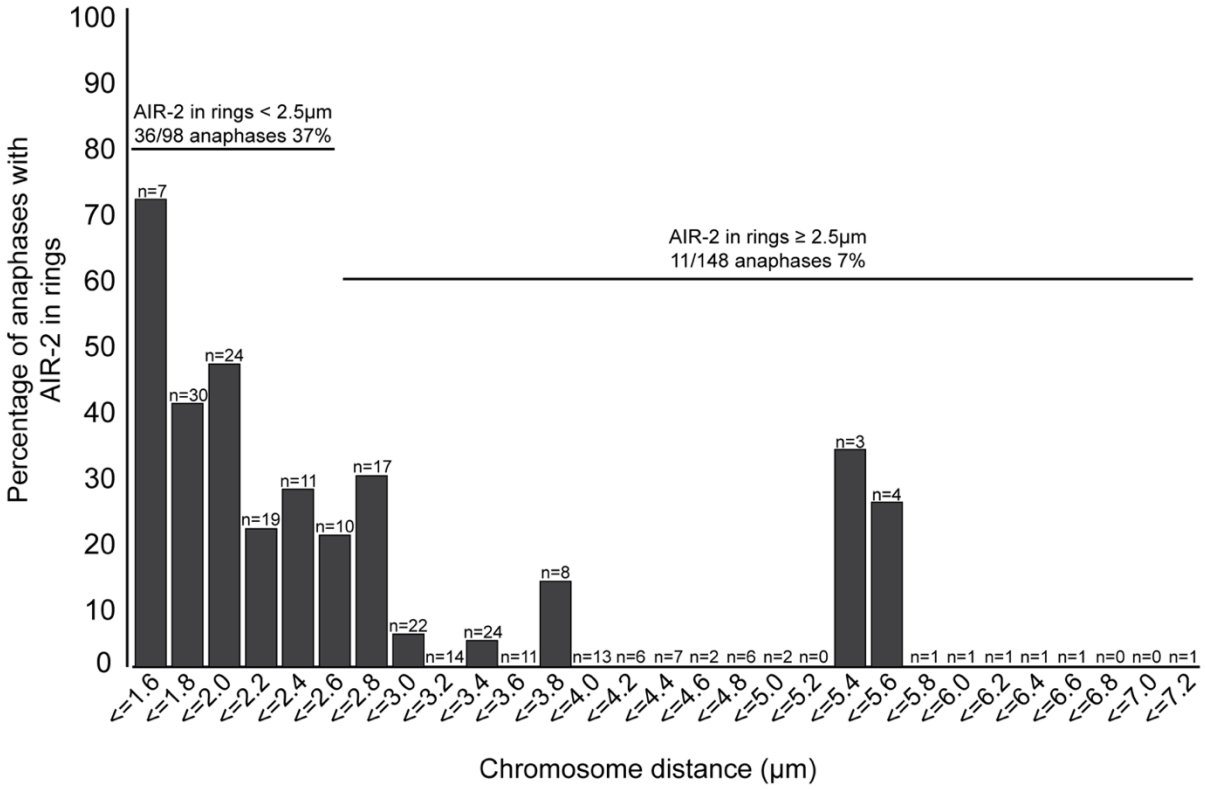


**Figure 2.2 Quantification of AIR-2 localization in wild-type anaphase**
Percent of anaphase spindles with AIR-2 in RCs at each given chromosome segregation distance.

univalents also trigger this behavior (Fig. 2.1B, C); in both mutants we observed these changes in both MI and MII (Fig. 2.1B, C). Importantly, AIR-2 was never associated with the RCs at late anaphase, when the polar body begins to pinch off (Fig. 2.1B). Therefore, AIR-2 relocalization is delayed but not prevented in the presence of univalents.

### 2.C Defects prior to anaphase onset and environmental stresses can delay RC disassembly

Next, we wanted to determine whether this altered AIR-2 behavior was specific to mutants containing univalents or whether this behavior would also occur following other types of perturbations, which would be suggestive of a general regulatory mechanism. First, we induced spindle defects by either depleting spindle-pole protein ASPM-1[30, 36] or by analyzing a partial-loss of function mutant of the microtubule severing protein, MEI-2/katanin[31, 140]. In both cases, AIR-2 remained in RCs in a significant

fraction of mid anaphase spindles (Fig. 2.3A, D), demonstrating that spindle disorganization can alter AIR-2 behavior. Second, because the RC has been implicated in chromosome congression and segregation, we depleted RC components KLP-19 and CAPG-1, and we observed a similar delay in AIR-2 relocalization (Fig. 2.3A, B, D, and E); AIR-2 metaphase localization is unaffected following depletion of these proteins[27, 53], allowing us to assess anaphase behavior. Therefore, AIR-2 anaphase behavior is altered in response to many types of perturbations.

Some spindles with altered AIR-2 behavior had severely lagging chromosomes (Fig. 2B) but others did not (Fig. 1B, 2A), indicating that this delay can occur in the absence of obvious chromosome segregation defects and is not due to chromosomes directly contacting the RCs. Additionally, under conditions where AIR-2 remained RC-associated, other RC proteins were also retained in the structures (Fig. 2E) and all RCs within the spindle behaved similarly, suggesting a global mechanism that leads to general RC stabilization. Our observations are therefore consistent with the idea that AIR-2 relocalizing to the microtubules and RC disassembly are regulated processes that can be delayed in the presence of errors.

To determine whether errors occurring after anaphase onset can also alter AIR-2 and RC behavior, we individually depleted proteins required for cytokinesis, the centralspindlin components ZEN-4 and CYK-4[141, 142] and the anillin-related protein, ANI-1[143]. In each case, AIR-2 and RC behavior were indistinguishable from control anaphase spindles in MI (Fig. 2.3C, D). This was not due to ineffective RNAi, as we observed MII spindles with twice the normal number of chromosomes (caused by MI cytokinesis failure), and in many of those anaphase II spindles, AIR-2 remained RC-associated (Fig. 2.3C). Together, our results suggest that errors occurring prior to anaphase can alter AIR-2 anaphase behavior, but defects in late anaphase do not trigger a change, likely because at that point AIR-2 would have already relocalized.

Finally, we investigated whether other types of stresses affect anaphase RC behavior. The standard range of growth temperatures for *C. elegans* is 15-25˚C [144], but worms begin to lose fecundity above 24˚C[145]. After short exposures to either low (4˚C) or high (25˚C, 30˚C) temperatures, AIR-2 relocalization to microtubules and RC disassembly were delayed (Fig. 2.3A, D). Therefore, disassembly of the RC is a regulated process that is altered in response to meiotic errors and unfavorable environmental conditions.

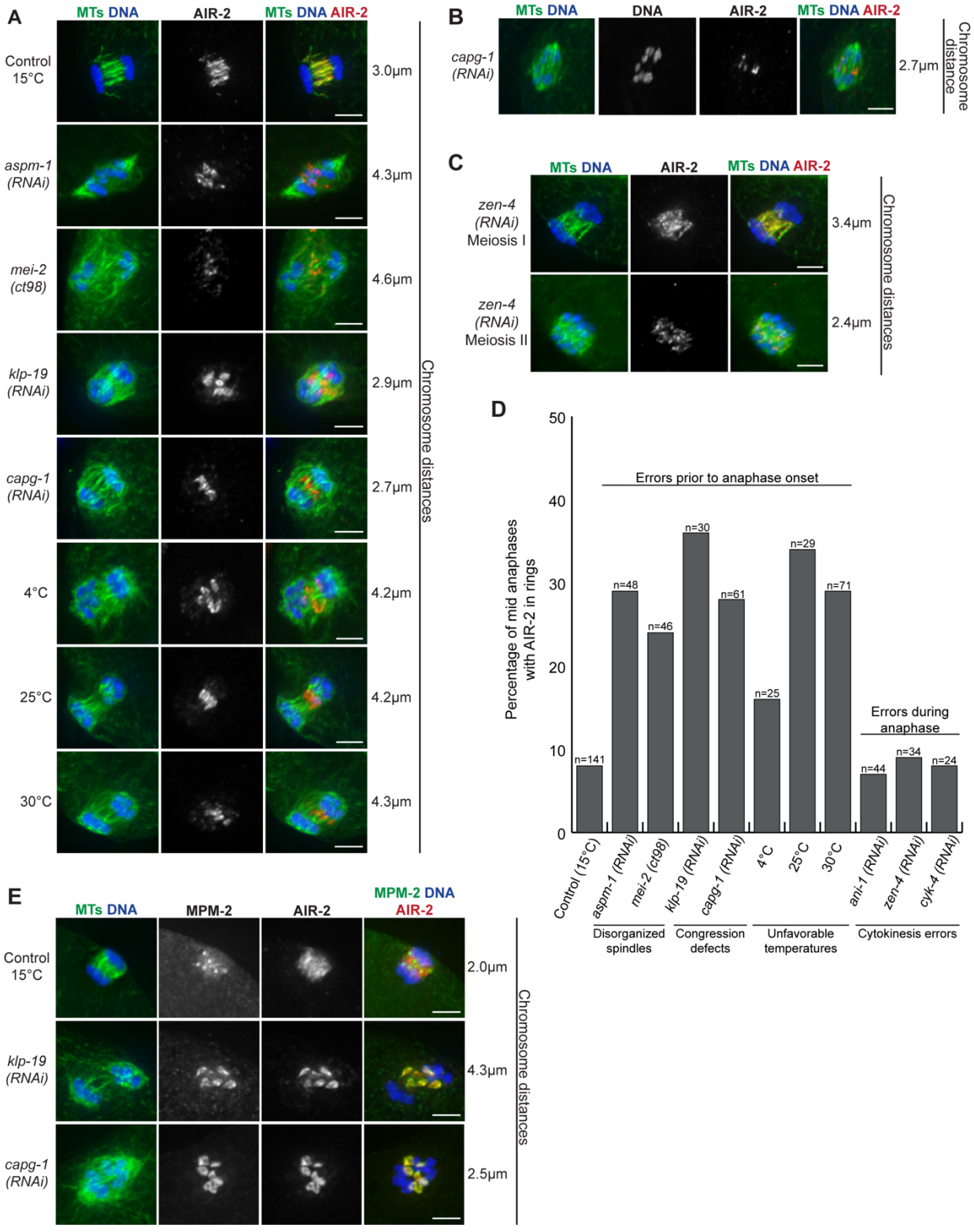
A
MTs DNA
AIR-2
MTs DNA AIR-2
Control 15°C
3.0µm
aspm-1 (RNAi)
4.3µm
mei-2 (ct98)
4.6µm
klp-19 (RNAi)
2.9µm
capg-1 (RNAi)
2.7µm
4°C
4.2µm
25°C
4.2µm
30°C
4.3µm
Chromosome distances
B
MTs DNA
DNA
AIR-2
MTs DNA AIR-2
capg-1 (RNAi)
2.7µm
Chromosome distance
C
MTs DNA
AIR-2
MTs DNA AIR-2
zen-4 (RNAi) Meiosis I
3.4µm
zen-4 (RNAi) Meiosis II
2.4µm
Chromosome distances
D
Percentage of mid anaphases with AIR-2 in rings
Errors prior to anaphase onset
Errors during anaphase
n=141
n=48
n=46
n=30
n=61
n=25
n=29
n=71
n=44
n=34
n=24
Control (15°C)
aspm-1 (RNAi)
mei-2 (ct98)
klp-19 (RNAi)
capg-1 (RNAi)
4°C
25°C
30°C
ani-1 (RNAi)
zen-4 (RNAi)
cyk-4 (RNAi)
Disorganized spindles
Congression defects
Unfavorable temperatures
Cytokinesis errors
E
MTs DNA
MPM-2
AIR-2
MPM-2 DNA AIR-2
Control 15°C
2.0µm
klp-19 (RNAi)
4.3µm
capg-1 (RNAi)
2.5µm
Chromosome distances

**Figure 2.3 (previous page) Defects prior to anaphase onset and environmental stresses can delay RC disassembly**
(A-C) DNA (blue), tubulin (green), and AIR-2 (red) in control and error-induced spindles. AIR-2 stays RC-associated following a variety of perturbations, and RC disassembly is delayed both in spindles with (B) and without (A) lagging chromosomes. (C) *zen-4(RNAi)* does not delay RC disassembly in MI but can cause AIR-2 to remain in RCs in MII when there is double the chromosome number. (D) Quantification of mid anaphase spindles with AIR-2 in RCs for all conditions tested. Includes MI and MII spindles for all conditions except depletion of *zen-4, cyk-4*, and *ani-1*. (E) DNA (blue), tubulin (green, column 1), AIR-2 (red), and MPM-2 (green, column 4) in control and error-induced spindles. MPM-2 marks the RC structures, illustrating that additional RC proteins are stabilized when AIR-2 persists in RCs under error conditions. Bar = 2.5μm.

**2.D Microtubule channels remain open and kinetochore disassembly is delayed in response to error**

When assessing RC behavior in various mutant conditions, we noticed that anaphase spindle morphology often differed from the control (Fig. 2.1B, 2.3A, B, E). Therefore, we decided to compare spindle organization in cases where the RCs persisted, to those in which RCs disassembled normally. In control oocytes, spindle poles broaden in early anaphase, creating microtubule channels that are open from pole to pole; these channels then close as anaphase progresses, reducing the width of the central region of the spindle (Fig. 2.1A). In most of the mutant spindles we examined, the poles still broadened, organizing the microtubules in a parallel array. However, while in wild-type oocytes the channels in the center of the spindle are typically compressing in mid anaphase, the central region of the spindles often appeared wide in the mutant conditions (Fig. 2.1B, 2.3 A, B, and E and 2.4A). We quantified this effect and found that when AIR-2 remained with the RCs, spindles were significantly wider than when RCs disassembled normally (Fig. 2.4B). Moreover, we observed open microtubule channels in the center of the spindle under these conditions, suggesting that the persistence of RCs maintains this microtubule organization.

Another unusual feature we observed in spindles with delayed RC disassembly was increased microtubule density at the poleward surfaces of separating chromosomes. In contrast to control spindles, where the chromosomes move past the poles during mid anaphase[39] (Fig. 2.1A), these spindles instead appeared to have “closed poles”, with the microtubule channels blocked at the ends (Fig. 2.1B, 2.3A,B, and E). Since this microtubule density resembled the cupping shape of the kinetochores, we hypothesized that kinetochores might be making inappropriate attachments to microtubules, enabling this extra accumulation. Therefore, we tested whether kinetochore disassembly was delayed under error conditions, by examining

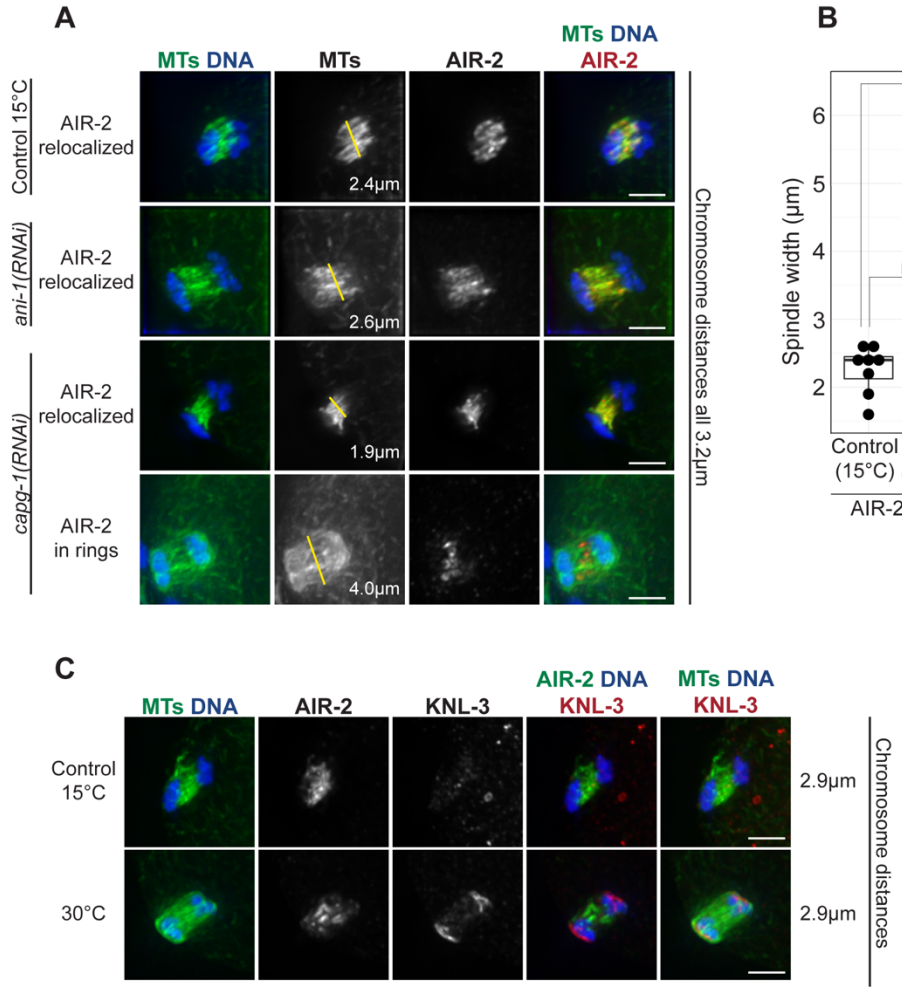


**Figure 2.4 Microtubule channels remain open and kinetochore disassembly is delayed in response to error**

(A) Spindles stained for DNA (blue), tubulin (green), and AIR-2 (red). When AIR-2 remains in RCs (row 4, *capg-1(RNAi)* shown) the spindle is significantly wider than when AIR-2 is microtubule-associated (rows 1-3); spindle widths denoted within each image. (B) Box plot shows the widths of spindles in which AIR-2 is relocalized, compared to those in which AIR-2 remains in RCs. Spindles measured had chromosome distances between 2.7µm-4.2µm. Box represents first quartile, median, and third quartile. Lines extend to data points within 1.5 interquartile range. N.S., not significant; asterisk represents significant difference (two-tailed t-test, $p<0.001$) (C) Spindles stained for DNA (blue), tubulin (green, columns 1 and 5), AIR-2 (green, column 4) and KNL-3 (red). KNL-3 remains chromosome-associated when AIR-2 remains in RCs; 30˚C treatment shown. Bar = 2.5µm.

the outer kinetochore component KNL-3, which normally cups the chromosome ends prior to anaphase and is removed from chromosomes by mid anaphase[23, 27]. Notably, when we induced an RC disassembly delay, KNL-3 persisted on chromosomes (Fig. 2.4C, Fig. 2.5A). This finding reveals that kinetochore disassembly

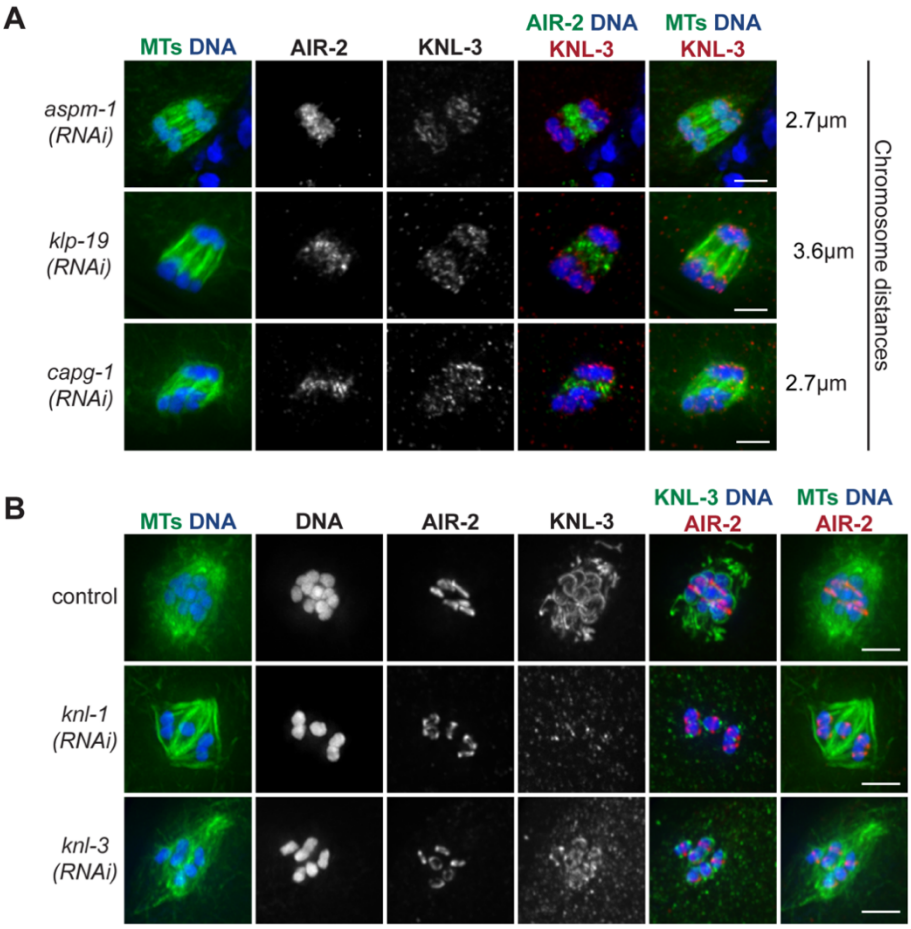


C

| Condition | Mid anaphases with AIR-2 in rings | Percent mid anaphases with AIR-2 in rings |
|---|---|---|
| *klp-19 (RNAi)* | 11/30 | 36% |
| *klp-19/knl-1 (RNAi)* | 3/46 | 7% |
| *capg-1 (RNAi)* | 17/61 | 28% |
| *capg-1/knl-1 (RNAi)* | 5/31 | 16% |

**Figure 2.5 Kinetochore analysis under additional error conditions**
(A) Spindles stained for DNA (blue), tubulin (green, columns 1 and 5), AIR-2 (green, column 4) and outer kinetochore component KNL-3 (red). KNL-3 is usually removed from chromosomes in anaphase but remains chromosome-associated when AIR-2 remains in RCs; *aspm-1*, *capg-1*, and *klp-19 RNAi* treatment shown. (B) Metaphase spindles stained for DNA (blue), tubulin (green, columns 1 and 6), KNL-3 (green, column 5) and AIR-2 (red) after partial *knl-1 (RNAi)* or *knl-3 (RNAi)*. (C) Quantification of mid anaphase spindles with AIR-2 in RCs (chromosome distances ≥ 2.5µm) for *klp-19(RNAi)*, *capg-1(RNAi), klp-19/knl-1(RNAi)* and *capg-1/knl-1(RNAi)*. Kinetochore depletion by *knl-1(RNAi)* reduces the percent of AIR-2 in RCs in *klp-19(RNAi)* and *capg-1(RNAi)* spindles. Data includes both MI and MII spindles. *aspm-1*/*knl-1(RNAi)* could not be quantified due to disorganization of the spindle but showed a similar trend. Bar = 2.5µm.

is also a regulated process that can be delayed in the presence of meiotic errors and illustrates that kinetochores may not have to be completely removed in order for chromosomes to segregate.

**2.E The response to errors requires the kinetochore but not components of the spindle assembly checkpoint**

Next, we wanted to investigate how errors are detected in this unique form of cell division. Because univalents lack RCs but still elicit an error response (Fig. 2.1B, C), it is unlikely the RC itself acts as a sensor. Alternatively, in mitosis, errors are detected via end-on kinetochore attachments that generate tension across the chromosome. While end-on attachments have not been observed in *C. elegans* oocytes, the holocentric kinetochores cup the ends of the bivalents prior to anaphase, placing them in a location where they could mediate side attachments to the lateral bundles. Moreover, kinetochore proteins coat the surfaces of univalents[39], so they could theoretically participate in error sensing in those mutants as well.

To determine whether the kinetochore is required for the response to meiotic errors, we partially depleted outer kinetochore components KNL-1 and KNL-3 and assessed whether RC disassembly could be delayed in anaphase. These depletions caused metaphase defects, with bivalents misaligned within the lateral microtubule bundles (Fig. 2.5B), and the spindles had lagging chromosomes in anaphase (Fig. 2.6), as previously reported[27]. However, despite these errors, we did not observe a delay in AIR-2 relocalization to the spindle or in RC disassembly (Fig. 2.5C, 2.6, 2.7B,). Instead, depleting these kinetochore components prevented a RC disassembly delay, even under error conditions that would normally elicit this response (Fig. 2.6, 2.7B). These data therefore demonstrate that the kinetochore is required for delaying RC disassembly in response to errors; in this context the kinetochores could play a role in sensing the errors or, alternatively, since they persist in the error conditions, they could be required for transducing the error signal.

This requirement for the kinetochore raises the possibility that the anaphase delays we observe are mediated by the spindle assembly checkpoint (SAC), since that mechanism also relies on kinetochore function. Although we do not observe a metaphase arrest in response to errors, *C. elegans* embryos have been shown to have a weak SAC response[78, 146, 147], so it is possible that the anaphase delays we observe

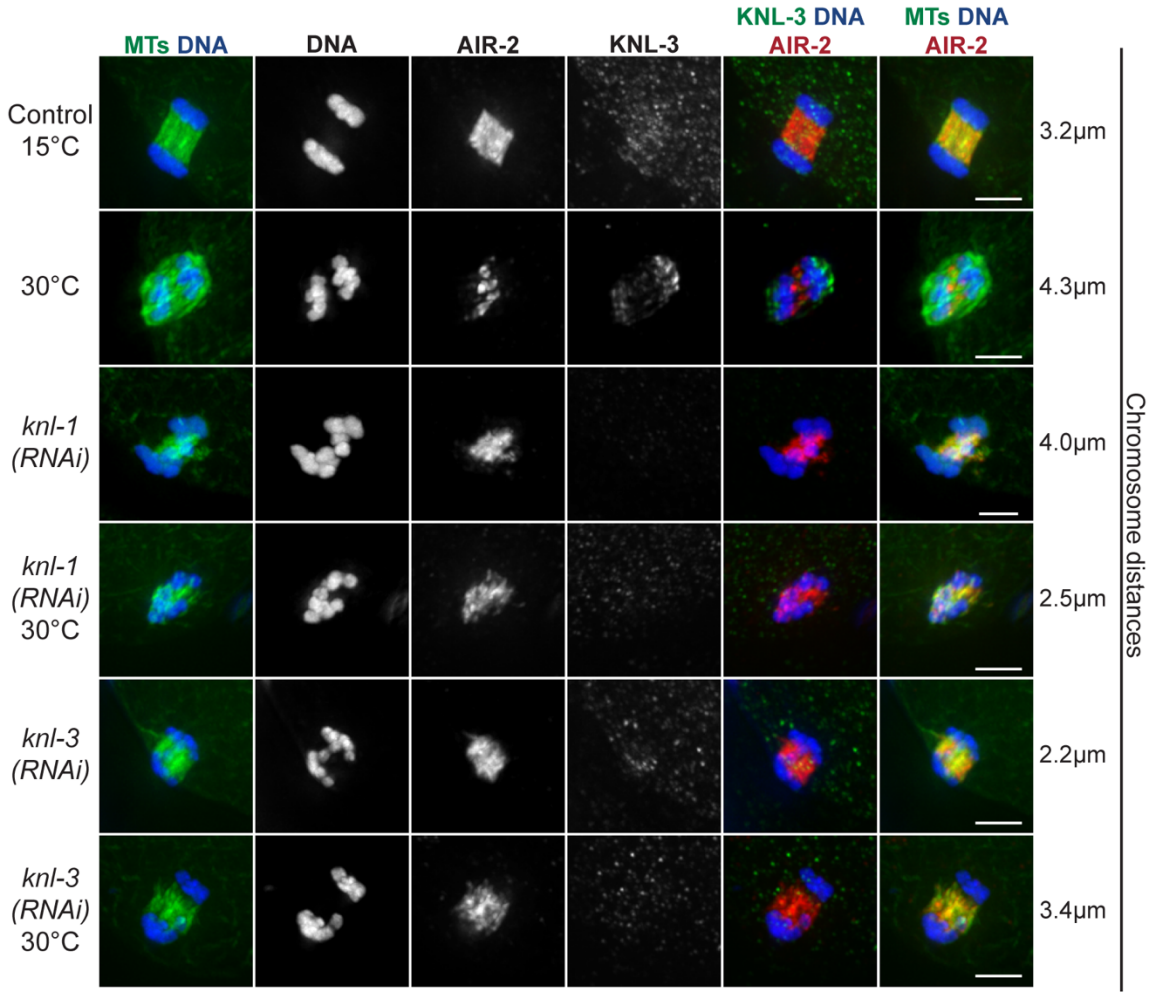


**Figure 2.6 The response to errors requires the kinetochore**
Mid anaphase spindles stained for DNA (blue), tubulin (green, columns 1 and 6), KNL-3 (green, column 5) and AIR-2 (red). Neither *knl-1(RNAi)* nor *knl-3(RNAi)* cause a RC disassembly delay. At 30˚C, AIR-2 does not remain in RCs following partial depletion of KNL-1 and KNL-3. Images were not restricted to the mid anaphase cutoff of ≥ 2.5µm to illustrate that AIR-2 relocalizes in early anaphase as well. Bar = 2.5µm.

could reflect a mild SAC response. To test this hypothesis, we inhibited SAC components and scored AIR-2 and RC anaphase behavior, with and without inducing an additional stress; for this analysis we singly and doubly depleted *mdf-1* (Mad1) and *san-1* (Mad3) using RNAi and also assessed *san-1(ok1580)* and *bub-3(ok3437)* mutant strains. Unlike the kinetochore depletions, where nearly all error response was lost (Fig. 2.6, 2.7B), in the SAC mutant/depletion conditions, AIR-2 still persisted in RCs after 30°C treatment. Notably, some SAC depletions induced an error response on their own (Fig. 2.7), suggesting that SAC

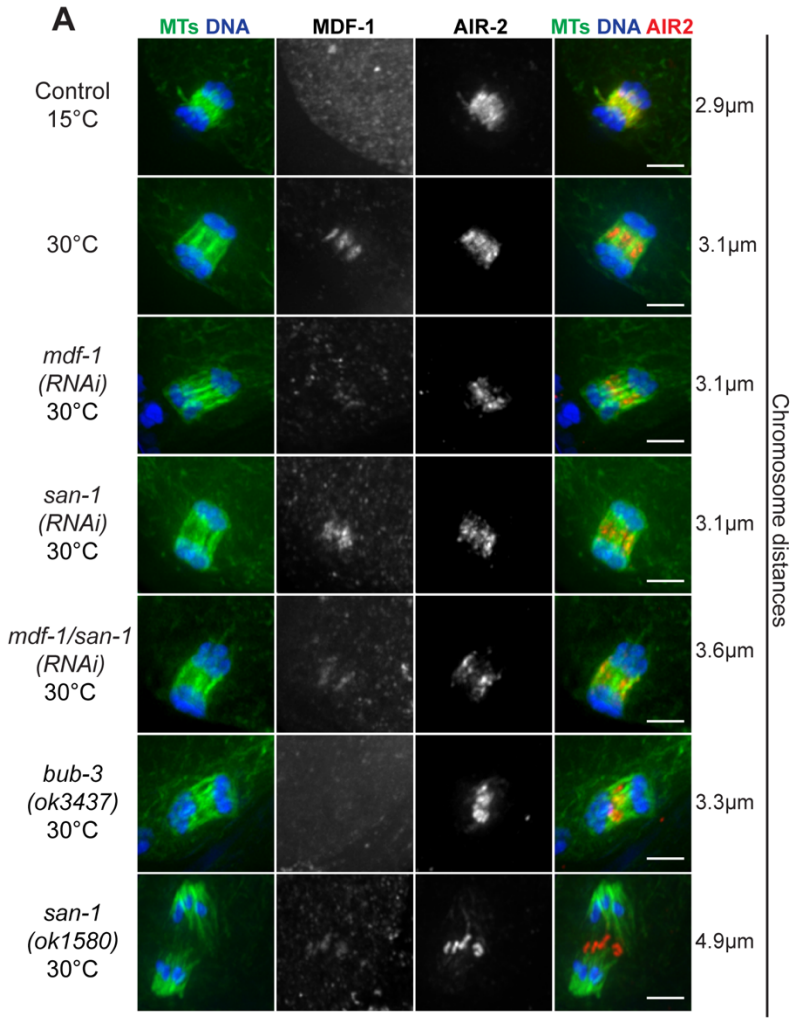
A
MTs DNA
MDF-1
AIR-2
MTs DNA AIR2
Control 15°C
30°C
mdf-1 (RNAi) 30°C
san-1 (RNAi) 30°C
mdf-1/san-1 (RNAi) 30°C
bub-3 (ok3437) 30°C
san-1 (ok1580) 30°C
2.9µm
3.1µm
3.1µm
3.1µm
3.6µm
3.3µm
4.9µm
Chromosome distances

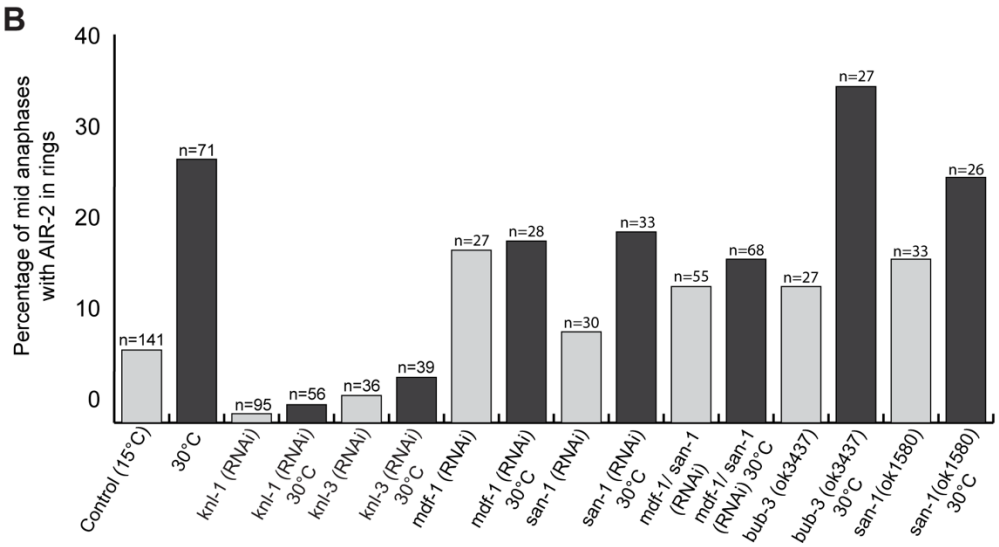
B
Percentage of mid anaphases with AIR-2 in rings
0
10
20
30
40
n=141
n=71
n=95
n=56
n=36
n=39
n=27
n=28
n=30
n=33
n=55
n=68
n=27
n=27
n=33
n=26
Control (15°C)
30°C
knl-1 (RNAi)
knl-1 (RNAi) 30°C
knl-3 (RNAi)
knl-3 (RNAi) 30°C
mdf-1 (RNAi)
mdf-1 (RNAi) 30°C
san-1 (RNAi)
san-1 (RNAi) 30°C
mdf-1/ san-1 (RNAi)
mdf-1/ san-1 (RNAi) 30°C
bub-3 (ok3437)
bub-3 (ok3437) 30°C
san-1(ok1580)
san-1(ok1580) 30°C

**Figure 2.7 (previous page) The response to errors requires the kinetochore but not Spindle Assembly Checkpoint proteins**
(A) Mid anaphase spindles stained for DNA (blue), tubulin (green), AIR-2 (red), and MDF-1. AIR-2 remains in RCs after 30˚C treatment in worms depleted of MDF-1, SAN-1, and MDF-1/SAN-1 and in *bub-3* and *san-1* mutant strains. (B) Quantification of mid anaphase spindles with AIR-2 in RCs for the kinetochore and SAC depletions at 15˚C and 30˚C. Includes MI and MII spindles with chromosome distances ≥ 2.5μm. Note that depletion of SAC components alone (15˚C) increased the percentage of spindles with AIR-2 in RCs. In the case of MDF-1, this percentage did not increase significantly when combined with a 30˚C treatment, suggesting that while MDF-1 does not appear to be absolutely required for an error response, its depletion may affect the magnitude of the response. Bar = 2.5μm.

components may play roles in oocyte meiosis but are likely not required for the observed anaphase delays.

As a part of this analysis, we also assessed MDF-1 (Mad1) localization, since this protein has been shown to transiently localize to the RCs at anaphase onset[148] (Fig. 2.8), placing it in a location where it could potentially regulate AIR-2 relocalization to the microtubules and participate in the error response. However, we found that the MDF-1 localization pattern did not correlate with AIR-2 behavior, since while it associated with the RCs just before AIR-2 relocalized to the microtubules, it also remained with the flattening RCs well after AIR-2 removal (Fig. 2.8A, B). MDF-1 persisted in RCs during mid to late anaphase under error conditions, but since other components of the RC are also RC-associated under these conditions (Fig. 2.3E and Fig. 2.8A), this behavior likely reflects a general stabilization of the RC structures and not a specific retention of MDF-1. Additionally, we found that in the *bub-3(ok3437)* mutant strain, MDF-1 no longer associated with the anaphase RCs, demonstrating that BUB-3 is required for MDF-1 RC targeting but that this targeting is not required for the AIR-2 error response (Fig. 2.7A, 2.8C). Therefore, while the intriguing MDF-1 localization pattern and its targeting by BUB-3 suggests that SAC components may have roles in oocyte meiosis, they do not appear to be necessary for the RC regulation we have uncovered, implying that in this mechanism, the kinetochore is required for the error response independent of MDF-1, SAN-1, and BUB-3.

### 2.F Conclusions and discussion

In summary, our studies have revealed that there is a regulatory mechanism that alters multiple aspects of anaphase progression in response to a variety of perturbations, suggesting that errors can be

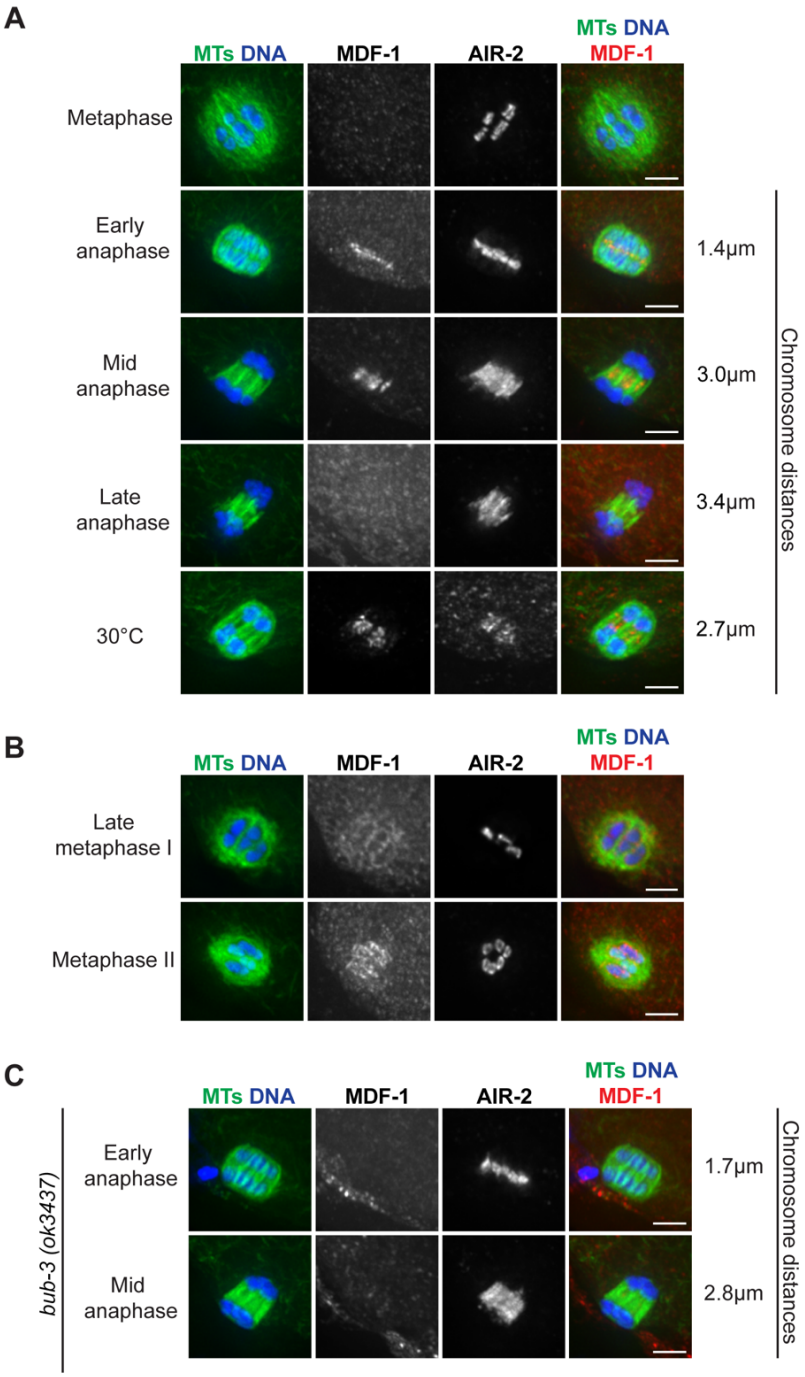


**Figure 2.8 MDF-1 (Mad1) localization and targeting in oocyte meiosis**
Spindles stained for DNA (blue), tubulin (green), MDF-1 (red), and AIR-2. (A) MDF-1 is diffuse until early anaphase when it localizes to the RCs and persists there as the RCs disassemble. Similar to other RC proteins we have assayed, MDF-1 remains on RCs longer under error conditions, suggesting that the entire RC is stabilized under these conditions. (B) Although MDF-1 is usually diffuse in metaphase, occasionally we observed kinetochore or RC localization at that stage. Two examples are shown; MI (row 1) and MII (row 2). Top panel shows a single z-slice. This localization did not appear to be increased under error conditions and may represent transient targeting. (C) MDF-1 is delocalized from the RCs in anaphase in the *bub-3(ok3437)* mutant strain. Bar = 2.5μm.

detected in this system (Fig. 2.9). We speculate that delaying RC disassembly and keeping the microtubule channels open could prevent the collapse of microtubule bundles around lagging chromosomes, allowing errors more time to resolve. This suggests that *C. elegans* oocytes employ a mechanism that could serve to increase the fidelity of chromosome segregation, similar to checkpoints that operate in other cell types. However, this regulation does not appear to elicit a strong metaphase arrest, as is seen in mutants of the anaphase promoting complex[149, 150], since anaphase progresses and cytokinesis occurs in all cases. This is reflected in our quantification, as we do not observe RCs persisting in all anaphase spindles in any mutant condition. While it is possible that not every error is detected, it is also likely that many of the spindles we observe are past the point of delay.

Although it is possible that the timing of cell cycle events may be altered in response to error, we hypothesize that this mechanism instead primarily represents a shift in the progression and coordination of anaphase events. A recent study defined *C. elegans* meiotic anaphase as having two distinct phases: Anaphase A and B[38]. Chromosomes exhibit poleward movement during Anaphase A, when microtubule channels are open in the center of the spindle, kinetochores are still present on the chromosomes but are beginning to disassemble, and RCs are still intact but AIR-2 is beginning to relocalize. Then in Anaphase B, spindle elongation occurs to further separate chromosomes; at this stage the chromosomes have moved to the ends of the microtubule channels, the RCs are disassembling, and the kinetochores are gone. Under normal conditions, Anaphase A and B appear to be sequential mechanisms, with chromosome-to-pole movement preceding spindle elongation[38]. In contrast, we speculate that under error conditions, maintaining RCs, kinetochores, and open microtubules channels could represent an extension of Anaphase A mechanisms, keeping them active as the spindle elongates to facilitate chromosome segregation. Our results therefore demonstrate that it is not essential to completely turn off the Anaphase A mechanisms for Anaphase B to proceed, implying that Anaphase B spindle elongation can occur in the context of the Anaphase A type of spindle organization, with open microtubule channels in the center of the spindle and lateral associations on the sides of chromosomes.

Another interesting aspect of our findings is that the delay in kinetochore removal led to extra microtubule density at the ends of the chromosomes in anaphase, suggesting that if kinetochores are not

removed, the ends of the chromosomes become competent for microtubule association at this stage. This finding raises the intriguing possibility that kinetochores may form transient functional attachments that participate in the early stages of chromosome segregation; if this were the case, it could represent another

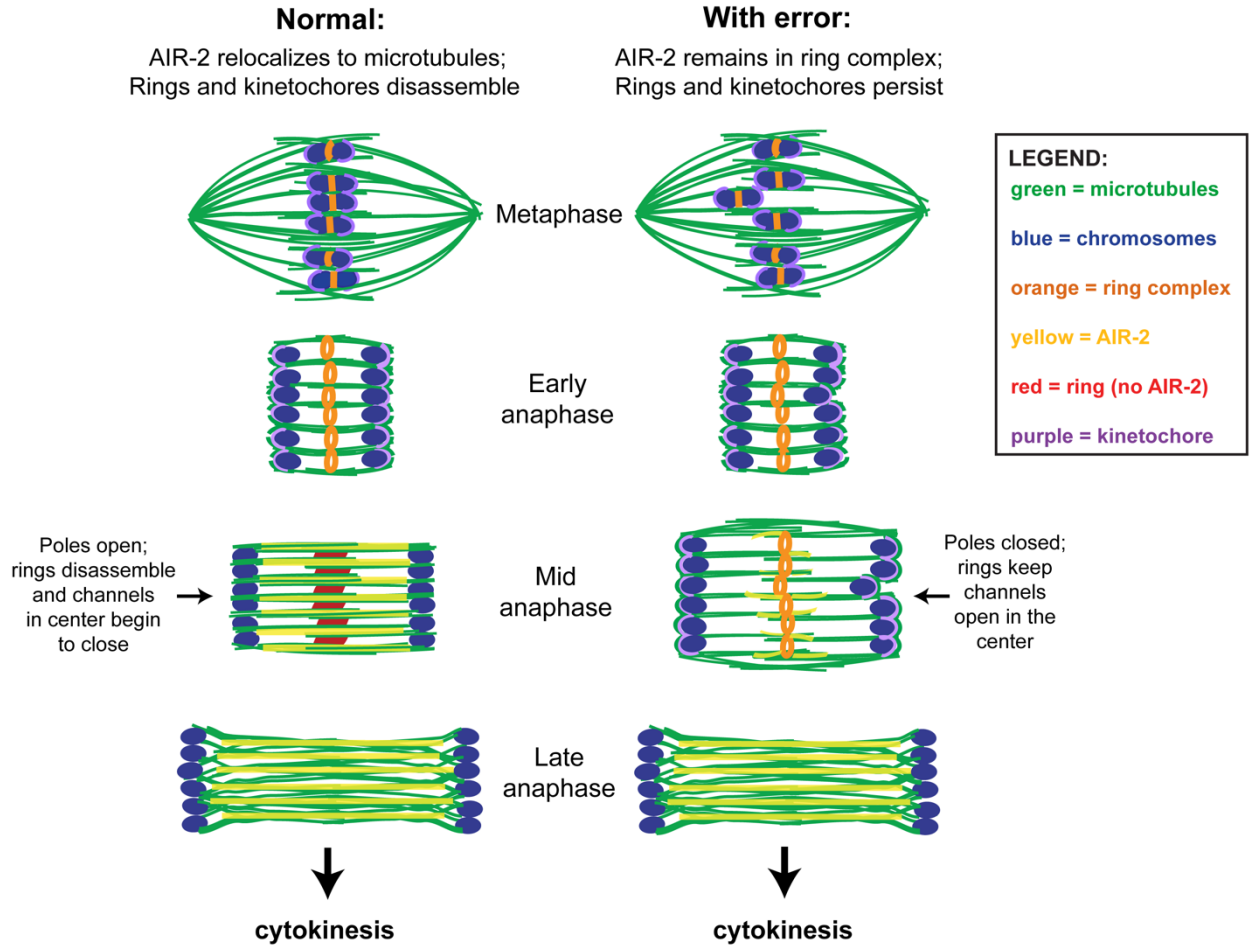


**Figure 2.9 Model for kinetochore and AIR-2/Aurora B-mediated anaphase regulation**
Model depicting DNA (blue), microtubules (green), the RCs with AIR-2 (orange), AIR-2 (yellow), the RCs without AIR-2 (red) and kinetochores (purple). In normal meiosis (left), kinetochores are removed from chromosomes, AIR-2 relocalizes to the microtubules, and the RCs begin to disassemble by mid anaphase. Under many types of perturbations (right, a congression defect is depicted), AIR-2 remains with the RCs throughout mid anaphase, keeping the microtubule channels open. Chromosomes continue segregating, despite retention of kinetochores on chromosomes. By late anaphase, AIR-2 relocalizes to the microtubules and cytokinesis occurs.

mechanism that is retained under error conditions that could help promote chromosome segregation. However, since previous work demonstrated that chromosomes segregate at normal rates following KNL-1 depletion (even during Anaphase A, when kinetochores would have been present on chromosomes)[27], even if these transient attachments form, they are unlikely to make a major contribution to chromosome segregation. Regardless of whether these extra microtubules are force-generating, the fact that they appear to "block" the ends of the microtubule channels reveals a potential reason why kinetochores usually disassemble by mid anaphase; this could serve to clear a path so that the chromosomes can move past the poles.

Our finding that kinetochore disassembly is delayed under error conditions also reveals that although this form of chromosome segregation is usually kinetochore-independent, kinetochore removal does not appear to be absolutely required for chromosome separation. This is an important finding, since a recent study proposed that kinetochores must be removed in order for chromosome segregation to occur[151]. This hypothesis was based on the analysis of mutants where targeting of a phosphatase (GSP-2/PP1) to chromosomes was prevented; under these conditions kinetochores did not disassemble and chromosomes did not segregate, but segregation was rescued when kinetochore components were also depleted. Given our finding that kinetochores are required for an error response, an alternate possibility to explain these data is that PP1 regulates aspects of anaphase progression as part of the mechanism we have described. If this were the case, kinetochore depletion would enable anaphase to proceed in mutants lacking PP1 targeting, since under these conditions the oocytes would bypass error detection. Therefore, future studies testing this possibility may shed light on the molecular mechanisms of RC and kinetochore disassembly.

Some important questions that arise from our discovery are when and how oocytes monitor and sense errors and what types of errors are detected. Because errors late in anaphase do not appear to be detected by this mechanism, our data point to detection occurring in either metaphase or very early anaphase. Intriguingly, it was recently shown that just before chromosome segregation, when the spindle shrinks and the poles come into close proximity with the kinetochores, the chromosomes and kinetochores appear to transiently stretch[38]. This finding suggests that a tension-sensing mechanism acting at the

metaphase to anaphase transition could monitor proper chromosome alignment; under this scenario, proper tension across the chromosome would promote AIR-2/Aurora B relocalization to the microtubules. In this mechanism, tension could be generated utilizing side-attachments to the lateral bundles, mediated by kinetochore proteins cupping the bivalent ends or through transient end-on kinetochore attachments made when the spindle shrinks. In the latter situation, these transient attachments would be quickly lost as the kinetochores disassemble under normal conditions, but under the error conditions where kinetochores persist, they could be retained. Importantly, since neither of these potential mechanisms relies on canonical tension-generating end-on attachments that are in place prior to anaphase onset, our studies have revealed a new strategy for error detection during cell division. Future studies building on this work will shed light on how chromosomes are accurately segregated during this important specialized cell division.

# CHAPTER 3:

## Dynamic SUMO remodeling drives a series of critical events during meiotic divisions

The data presented in this chapter is currently under revision for *PLOS Genetics*.
All data shown was generated by Amanda Roca with the exception of Figure 3.2 C, D, and E, which were generated by Nikita Divekar.

**3.A Introduction**

*C. elegans* oocytes utilize mechanisms for chromosome congression and segregation that are distinct from those used in mitosis. In these cells, end-on kinetochore-microtubule attachments are not apparent, and instead microtubules associate laterally with the chromosomes[35]. Additionally, segregation is kinetochore-independent, as kinetochores are normally disassembled during early anaphase, and kinetochore depletion does not affect chromosome segregation rates.[27] Although the exact mechanism driving chromosome segregation remains controversial, it is clear that both congression and segregation depend upon a large protein complex that forms a ring around the center of each bivalent in MI and around the sister chromatid interface in MII. These ring complexes (RCs) are comprised of a number of conserved cell division proteins, including the Chromosome Passenger Complex/CPC (containing AIR-2/Aurora B kinase), the kinesin-4 family motor KLP-19, and the kinase BUB-1[27, 35, 42]. During prometaphase, KLP-19 provides chromosomes with a plus-end directed force that is thought to facilitate congression to the metaphase plate. Then in anaphase, separase (SEP-1) is targeted to the RCs to cleave cohesin, and the RCs are released and left at the center of the spindle as the chromosomes segregation[21, 39]. Depletion of some individual RC components and/or preventing the assembly of the complex as a whole result in severe chromosome segregation defects, demonstrating the importance of this complex during meiosis[21, 27]. Therefore, understanding how the RC assembles and is regulated will provide valuable insights into how chromosomes are accurately partitioned in oocytes.

Although the individual contribution of each RC protein to the overall functions of the complex is not fully understood, previous studies have revealed some of the principles underlying RC assembly. Initial work demonstrated that certain components are required for others to load, with the CPC required for the proper localization of all other known RC components[27]. Moreover, a recent study showed that SUMO, a reversible post-translational modification, regulates RC assembly[45]. In *C. elegans*, there is one SUMO ortholog that can be conjugated to target proteins by an E1 activating enzyme, an E2 conjugating enzyme (UBC-9), and SUMO-specific E3 ligases. Evidence supporting a role for SUMO in RC assembly includes the demonstration that: 1) SUMO, UBC-9, and GEI-17 (a PIAS family E3 ligase) localize to the RC, 2) RC assembly is GEI-17 dependent, 3) RC components AIR-2 and KLP-19 can be SUMOylated *in vitro*, and 4)

other RC components such as BUB-1 have SUMO interaction motifs (SIMs) and can interact with SUMOylated proteins. These findings support a model that a network of SUMO-SIM interactions between RC proteins drives the assembly of the complex. However, much still remains to be discovered about how SUMO contributes to RC organization and function.

Importantly, the mechanisms driving RC disassembly in anaphase are even less understood. Normally, AIR-2/Aurora B leaves the RCs soon after their release from chromosomes in early anaphase and relocalizes to the microtubules. At the same time, the released RCs appear to lose structural integrity, since they flatten by mid anaphase and then are absent by late anaphase. However, we recently discovered that AIR-2 relocalization to microtubules and RC disassembly are delayed in the presence of a variety of meiotic errors, demonstrating that these processes are regulated (Chapter 2[46]). We also found that when the RCs remained intact, anaphase spindle morphology was altered in a manner that could potentially increase the fidelity of chromosome segregation. Therefore, control of RC disassembly is a central feature of anaphase progression, making it important to understand.

In this chapter, we provide the first detailed description of RC disassembly in *C. elegans* oocytes and show that this process and other critical anaphase events rely on the dynamic remodeling of SUMO modifications. We found that SUMO promotes the stability of the RC and that RC disassembly is dependent on targeting the SUMO protease ULP-1 to the structures, suggesting that ULP-1 could promote disassembly by removing SUMO from RC components upon removal of the E2/E3 enzymes from the RCs in early anaphase. Moreover, we found that ULP-1 is active prior to anaphase and may regulate aspects of ring assembly and maintenance independent of its role in SUMO maturation. Our findings therefore demonstrate that dynamic SUMO remodeling is required for key events that facilitate anaphase progression during oocyte meiosis and also demonstrate that a balance between SUMO E2/E3 and ULP-1 protease activity can regulate the SUMOylation status and thus the stability of essential protein complexes.

**3.B RC disassembly in anaphase is a step-wise process**

Since SUMO is RC-associated and is required for RC assembly, we reasoned that SUMO removal might be required for the disassembly of these complexes in anaphase. Consistent with this hypothesis,

previous imaging demonstrated that SUMO leaves the RCs sometime in anaphase, relocalizing across the spindle by late anaphase. However, precisely when SUMO leaves the RCs was not addressed. Therefore, we set out to carefully assess SUMO localization in relation to other RC components (Fig. 3.1A, B). As shown previously, we found that SUMO is present on the RCs after nuclear envelope breakdown (NEBD) and by late anaphase had relocalized to spindle microtubules. Because a similar localization pattern is exhibited by AIR-2, an RC component previously suggested to be SUMO-modified, we compared the behavior of these two proteins. Notably, the localization of these proteins differed in mid anaphase, with SUMO maintaining robust RC localization after AIR-2 relocalized to microtubules (Fig. 3.1A, row 4), demonstrating that proteins other than AIR-2 are likely SUMOylated at this stage. Notably, in early anaphase spindles where a small population of AIR-2 had relocalized to microtubules, we saw that the microtubule-associated population of AIR-2 was not colocalized with SUMO (Fig. 3.1A, arrow). This result supports the idea that if AIR-2 is SUMOylated when it is in the RC, this modification is removed before AIR-2 relocalizes to microtubules.

We also found that SUMO persisted in the RCs longer than SEP-1 (Fig. 3.1B, row 2), demonstrating that RC components leave the complex at different times and suggesting that the disassembly of these structures is a sequential process. In addition, we confirmed that UBC-9 (SUMO E2) and GEI-17 (SUMO E3) localize to the RCs as they form and remain associated with these complexes until early anaphase (Fig. 3.1C). However, in spindles where AIR-2 had relocalized from the RCs to the microtubules (the stage at which the RCs are flattening and disassembling), the E2/E3 enzymes appeared diffuse across the spindle (Fig. 3.1C, row 4-5). These findings demonstrate that UBC-9 and GEI-17 removal from the RCs occurs around the time that the RCs lose structural integrity, consistent with the view that altering the SUMOylation status of the RC could play a role in disassembly.

**3.C SUMO association with RCs is correlated with the stability of the structures**

Given that RC disassembly appeared to be a stepwise process, we next set out to determine how early in anaphase this process was initiated. A recent study reported that following depletion of MEL-28 (a

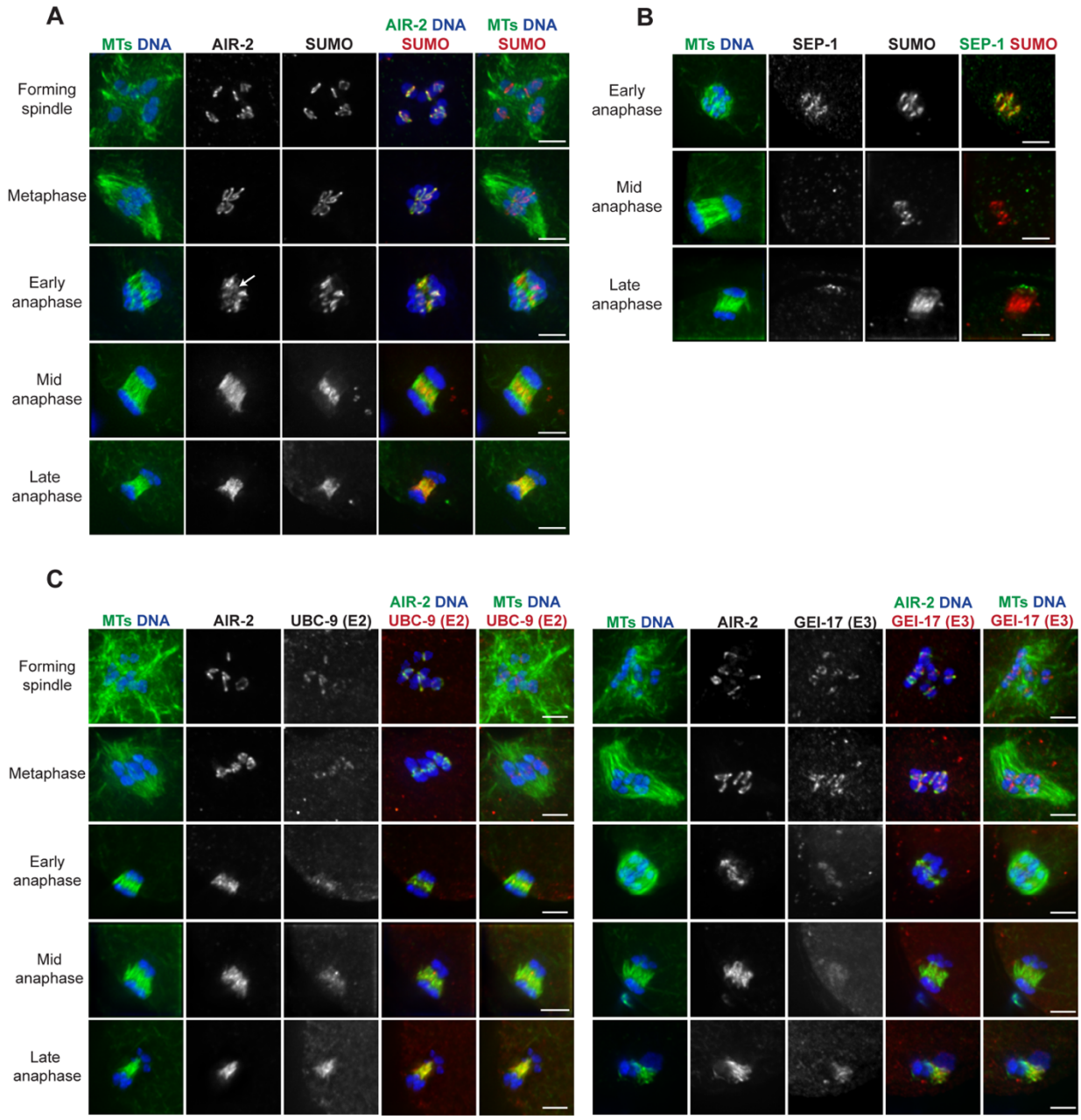


**<u>Figure 3.1</u> SUMO and SUMO E2/E3 enzymes leave the RCs during anaphase**
(A) Localization of SUMO (red) from spindle formation through late anaphase, compared to AIR-2 (green, column 4), DNA (blue), and tubulin (green, columns 1 and 5). SUMO becomes RC associated after NEBD, but leaves the RCs by late anaphase, relocalizing to the microtubules; SUMO remains RC-associated later into anaphase than AIR-2. (B) SUMO (red), compared to SEP-1 (green, column 4), DNA (blue), and tubulin (green, column 1) throughout anaphase. SUMO remains RC-associated after SEP-1 leaves. (C) Localization of UBC-9 (SUMO E2) (red, left panel) or GEI-17 (SUMO E3) (red, right panel) from spindle formation through late anaphase, compared to AIR-2 (green, column 4), DNA (blue), and tubulin (green, columns 1 and 5). UBC-9 and GEI-17 localize to the RCs during spindle assembly and then begin to leave these structures in early anaphase. Bar = 2.5μm.

nucleoporin responsible for targeting Protein Phosphatase 1/ PP1 to meiotic chromosomes), chromosomes separate at the metaphase to anaphase transition but spindles remain in an “early anaphase” configuration, where chromosomes are unable to move very far apart[151]. We therefore asked whether the disassembly of RCs was initiated before this stage, potentially due to their physical release from chromosomes, or after.

To test this, we depleted MEL-28 and then assessed the localization of AIR-2; AIR-2 is a relevant marker since it is the first known RC component to leave the RCs in anaphase, and since RC disassembly and AIR-2 relocalization are thought to occur concurrently. Notably, we found that AIR-2 was RC-associated in the majority of *mel-28(RNAi)* anaphase spindles (36/46 spindles; 78%) (Fig. 3.2A), demonstrating that its relocalization to the spindle is not triggered with anaphase onset. Moreover, while the RCs usually begin to flatten out as they disassemble in mid-anaphase, following *mel-28(RNAi)* they retained their ring-like shape, suggesting that they had not initiated the disassembly process and that they retained structural integrity despite their removal from chromosomes. This was especially striking since most of the spindles appeared to have been arrested for some time, as evidenced by the fact that AIR-2 had reloaded onto the separated chromosomes, presumably in preparation for RC assembly in meiosis II (Fig. 3.2A, arrowhead). Therefore, RC disassembly is not initiated concurrently with anaphase onset, but rather sometime after, and this process either requires MEL-28/PP1 function or relies on events after this point in early anaphase. Given our hypothesis that SUMO removal from the RCs promotes RC disassembly, we next assessed SUMO localization following *mel-28(RNAi)* and found that it was robustly associated with the stabilized RCs (Fig. 3.2B). Therefore, we went on to ask whether SUMO plays a role in maintaining RC structural integrity after their release from chromosomes.

To ask this question, we created spindles with both SUMOylated and non-SUMOylated RCs, so that we could compare their stability in anaphase. To do this, we used a strain in which the SUMO E3 ligase GEI-17 was linked to an auxin-inducible degron tag[45]. This strain was previously used to demonstrate that depletion of GEI-17 for extended periods of time (4+ hour auxin incubation) completely prevented RC formation. However, we found that a shorter, 30-minute, auxin incubation resulted in both properly formed RCs (marked by both SUMO and AIR-2) and also RCs lacking SUMO (marked only by AIR-2) during prometaphase and metaphase (not shown, characterized by Nikita Divekar); this experiment also confirmed

that SUMOylation is not required for AIR-2 localization to the chromosomes, as shown previously[45] although we did notice an observable reduction in AIR-2 on unSUMOylated rings. Under this condition, we observed

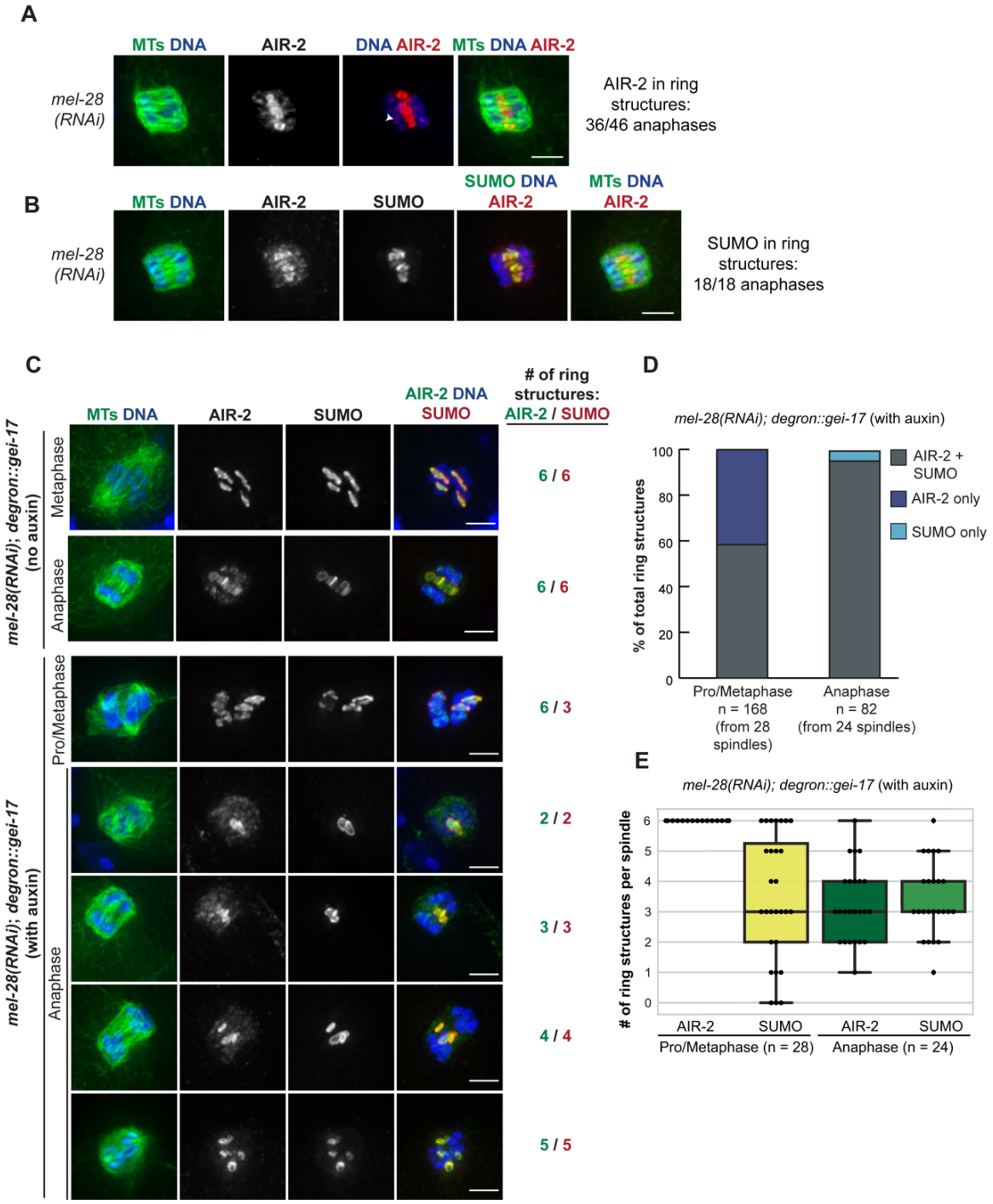

**Figure 3.2 (previous page) SUMO associates with stabilized anaphase RCs**
(A) *mel-28(RNAi)* anaphase spindle, stained for DNA (blue), tubulin (green), and AIR-2 (red); AIR-2 remained RC-associated (36/46 anaphases observed) and RCs remained intact even though the spindles appear to have been in anaphase for some time, as suggested by AIR-2 reloading onto chromosomes in preparation for MII (arrowhead). (B) Localization of SUMO (green, column 4), compared to AIR-2 (red), DNA (blue), and tubulin (green, columns 1 and 5) after *mel-28(RNAi)*. SUMO colocalized with AIR-2 on RCs in 18/18 spindles. (C) Spindles stained for DNA (blue), tubulin (green, column 1), AIR-2 (green, column 4), and SUMO (red). Top two rows show *mel-28(RNAi)* in the *degron::gei-17* strain without auxin. Six RCs marked by both AIR-2 and SUMO are present in both metaphase and anaphase. The bottom five rows show *mel-28* RNAi in the *degron::gei-17* strain after 30-minute incubation with auxin. This condition produces metaphase spindles with six RCs (shown by AIR-2 staining), of which a varying number are SUMOylated. In anaphase, the stabilized RCs always contained SUMO. (D) Quantification of part A. Percent of total RCs observed in pro/metaphase or anaphase that had either both AIR-2 and SUMO present, only AIR-2 present, or only SUMO present. (E) Quantification of part C (using the same data set as part D). Number of AIR-2 stained RCs per spindle versus the number of SUMOylated RCs during pro/metaphase or anaphase. Box represents first quartile, median, and third quartile. Lines extend to data points within 1.5 interquartile range. Note that in D and E we only quantified anaphase spindles where we could distinguish at least one intact AIR-2-marked RC, excluding spindles that progressed past the *mel-28(RNAi)* arrest point due to incomplete depletion. Note that in D and E we only quantified anaphase spindles where we could distinguish at least one intact AIR-2-marked RC, excluding spindles that progressed past the *mel-28(RNAi)* arrest point due to incomplete depletion. Bar = 2.5μm.

spindles with a range of zero to all six RCs being marked by SUMO, demonstrating that this depletion timepoint likely represents a “tipping point”, where in some oocytes the level of GEI-17 depletion either prevented the formation or maintenance of SUMOylated RCs, while in other oocytes RC formation and/or maintenance was more mildly affected. Therefore, we sought to use this condition to determine if SUMO was required to maintain RC stability in anaphase.

To more easily assess the stability of these SUMOylated and nonSUMOylated RCs after their removal from the chromosomes in anaphase, we combined the short GEI-17 depletion with *mel-28(RNAi)* so that we would obtain a larger population of early anaphase spindles; AIR-2 normally relocalizes to microtubules shortly after anaphase onset, making this stage difficult to capture. Using this combined strategy, we found that SUMO has a role in early anaphase RC stabilization. First, while we observed some metaphase RCs marked by both SUMO and AIR-2 and others that contained only AIR-2, in anaphase we never observed RCs that did not contain SUMO (Fig. 3.2 C, D), suggesting that AIR-2 RCs lacking SUMO do not maintain a ring-like structure once they are released from the chromosomes. Moreover, we observed

an average of approximately three SUMO-marked RCs per spindle in metaphase and a similar average in early anaphase (Fig. 3.2E), again suggesting that RCs containing SUMO prior to anaphase onset are the only complexes that subsequently maintain their stability. We obtained similar results when we analyzed GEI-17-depleted spindles in the absence of *mel-28(RNAi)* (data not shown, work by Nikita Divekar), demonstrating that the stabilization of SUMO-associated anaphase RCs was not dependent upon the *mel-28(RNAi)* early anaphase arrest condition.

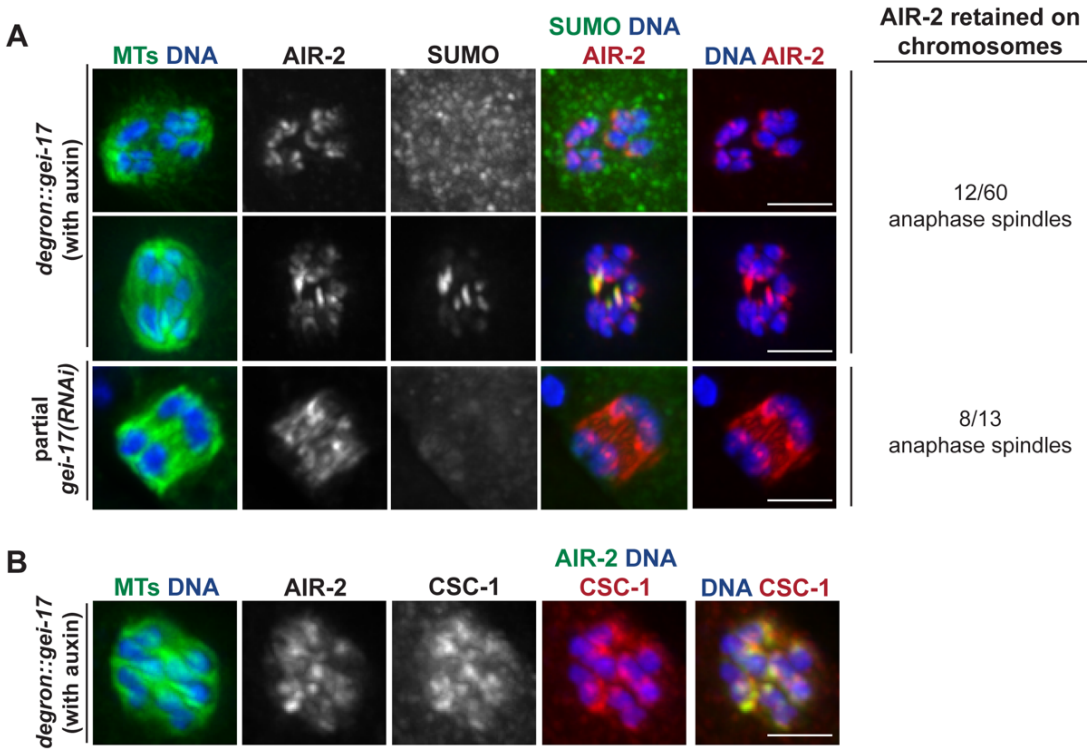


**Figure 3.3 GEI-17-dependent SUMOylation regulates AIR-2 release from chromosomes**
(A) AIR-2 release from chromosomes is GEI-17 dependent. In both the *degron::gei-17* strain after a 30-minute auxin incubation and in a control strain (EU1067) after 24-hour *gei-17* RNAi, AIR-2 sometimes remained on inner surfaces of segregating chromosomes (quantification shown on right). This behavior did not depend on the presence of SUMO. (B) CSC-1 release from chromosomes is also GEI-17 dependent. After 30-minute auxin incubation, CSC-1 is colocalized with AIR-2 on inner surfaces of chromosomes. Bar = 2.5μm.

### 3.D GEI-17-dependent SUMOylation regulates AIR-2 release from chromosomes

During our analysis of GEI-17 depleted oocytes, we also made a surprising observation concerning AIR-2 release from chromosomes. After auxin-induced GEI-17 depletion, AIR-2 was retained on chromosomes in a significant number of anaphase spindles (12/60), remaining associated with the inside surfaces of separating chromosomes (a phenomenon never observed in wild-type anaphase); we also noticed this phenotype following 24-hour *gei-17(RNAi)* (8/13 anaphases) (Fig. 3.3A). We went on to test whether other CPC components also exhibit this retention on chromosomes after GEI-17 depletion, and we found that CSC-1 also remains chromosome-associated in anaphase with AIR-2 (Fig. 3.3B). This finding is exciting because it suggests a new role for SUMOylation in CPC release from chromosomes at the metaphase to anaphase transition, and it illustrates the dynamic and complex nature of this modification during meiotic progression.

### 3.E The SUMO protease ULP-1 is required for RC disassembly and anaphase progression

Given our evidence that SUMOylation promotes RC stability, we next hypothesized that SUMO removal triggers RC disassembly. In *C. elegans*, there are four SUMO proteases, ULP-1, 2, 4 and 5, which function to remove SUMO from target proteins. Therefore, we depleted each of these proteins to assess whether any are required for RC disassembly.

First, we assessed ULP-4, since this protease was shown to regulate AIR-2 behavior in mitosis[133]. Interestingly, although we did not observe localization of ULP-4 to the RC in either metaphase or anaphase, we observed RC assembly defects following *ulp-4(RNAi*) (Fig. 3.4A, B). Although AIR-2 and SUMO were targeted to the structures, they were not properly connected to the chromosomes, often appearing stretched (Fig. 3.4A, arrow) and sometimes seeming connected to RCs on other chromosomes (Fig. 3.4A, arrowhead). During anaphase, there were varying phenotypes; some spindles looked normal, while others had RC disassembly defects (Fig. 3.4A, row 3) or lacked SUMO altogether (Fig. 3.4A, row 4). While these findings demonstrate that ULP-4 deSUMOylation activity is required for some aspect of RC assembly and raise the possibility that it is also required for RC disassembly, the metaphase defects caused by ULP-4 depletion made it difficult to assign an anaphase-specific role for this protease.

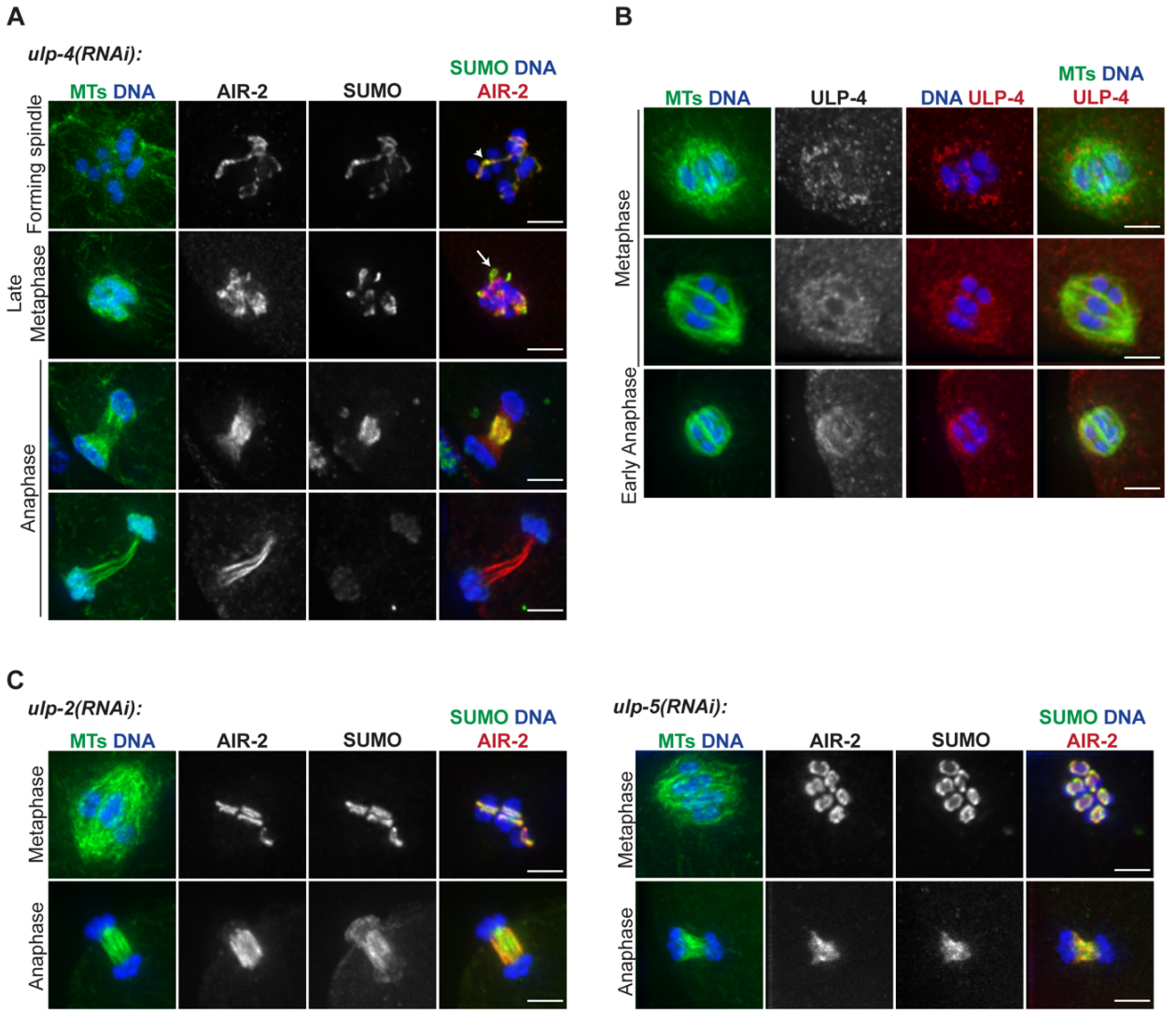


**Figure 3.4 Characterization of the SUMO proteases ULP-2, ULP-4, and ULP-5**
(A, C) Examples of metaphase and anaphase spindles after *ulp-2*, *ulp-4*, or *ulp-5(RNAi)*. Spindles stained for DNA (blue), tubulin (green, column 1), SUMO (green, column 4) and AIR-2 (red). While ULP-2 and ULP-5 do not have observable RC defects, *ulp-4(RNAi)* causes RC defects during prometaphase, with these structures appearing stretched away from the chromosomes, and some anaphase defects, ranging from pooled SUMO/AIR-2, to spindles lacking RC-associated SUMO. ULP-2 depletion usually caused more SUMO signal on late anaphase chromosomes. (B) Localization of ULP-4 is diffuse across the spindle, sometimes colocalized with microtubules or appearing kinetochore-like. Spindles stained for DNA (blue), tubulin (green), and ULP-4 (red). Row 2 is a projection of 3 z-slices. Bar = 2.5μm.

Therefore, we turned our attention to the other proteases. Depletion of ULP-2 or ULP-5 did not have noticeable effects on either metaphase RC morphology, AIR-2 anaphase behavior, or RC disassembly (Fig. 3.4C), so we did not characterize them further. Following full *ulp-1(RNAi)*, we found that most spindles lacked SUMO (Fig. 3.5B, row 1, Fig. 3.6A), consistent with a general role for ULP-1-family proteases in processing SUMO into a conjugatable form. However, in some cases we observed accumulations of persisting AIR-2 and SUMO structures in the center of the spindle in late anaphase (Fig. 3.5B, row 2), suggesting that in the cases where SUMO achieved RC conjugation, RC disassembly was aberrant.

Since this result potentially implicated ULP-1 in RC disassembly, we went on to partially deplete ULP-1, using 24-48 hour feeding RNAi, rationalizing that partial ULP-1 function would promote enough SUMO processing to allow us to more specifically assess a role for ULP-1 in anaphase (Figure 3.5D). As predicted, a majority of spindles following 24-48 hour *ulp-1(RNAi)* contained six SUMOylated RCs, and, consistent with our full depletion results, we observed instances of defective RC disassembly, with persisting AIR-2 and SUMO structures in the center of the anaphase spindle (Fig. 3.5C, row 2). Consistent with the idea this is defective RC disassembly, we found that other RC proteins, such as BUB-1 and UBC-9(E2) were also localized to these persisting RC structures (Fig. 3.7A). We also observed a small percentage of severely aberrant structures, in which chromosomes had segregated very far without extruding a polar body and SUMO and AIR-2 were faintly left behind at the center of what had been the spindle (Fig. 3.5C, row 3); we observed this same “unfinished meiosis” phenotype occasionally in our full depletion experiments (Fig. 3.5B, row 3). These results demonstrate that ULP-1 is required for RC disassembly, AIR-2 relocalization to the microtubules, and completion of the meiotic divisions. Additionally, we found that ULP-1 constructs of varying lengths can deSUMOylate both AIR-2 and KLP-19 *in vitro* (Fig. 3.8), two proteins previously hypothesized to be SUMOylated during RC assembly. Although *in vivo* ULP-1 may have different or additional substrates, this result is at least suggestive that ULP-1 promotes RC disassembly by removing SUMO from an RC component or components.

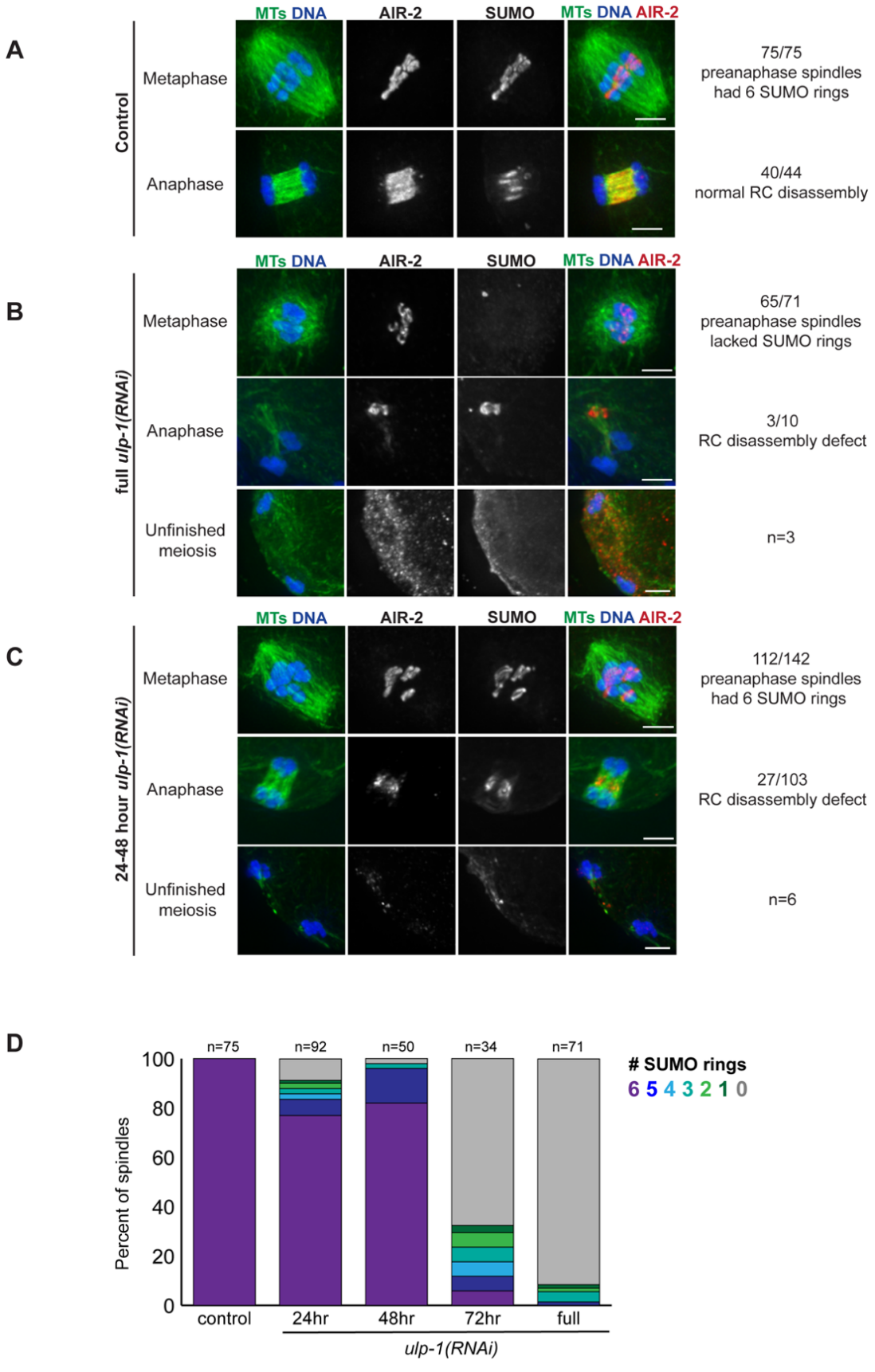
A
MTs DNA
AIR-2
SUMO
MTs DNA AIR-2
Control
Metaphase
Anaphase
75/75
preanaphase spindles
had 6 SUMO rings
40/44
normal RC disassembly
B
full ulp-1(RNAi)
Metaphase
Anaphase
Unfinished
meiosis
65/71
preanaphase spindles
lacked SUMO rings
3/10
RC disassembly defect
n=3
C
24-48 hour ulp-1(RNAi)
Metaphase
Anaphase
Unfinished
meiosis
112/142
preanaphase spindles
had 6 SUMO rings
27/103
RC disassembly defect
n=6
D
n=75
n=92
n=50
n=34
n=71
100
80
60
40
20
0
Percent of spindles
control
24hr
48hr
72hr
full
ulp-1(RNAi)
# SUMO rings
6 5 4 3 2 1 0

**Figure 3.5 (previous page) The SUMO protease ULP-1 is required for RC disassembly**
(A-C) Spindles stained for DNA (blue), tubulin (green), SUMO (not shown in merge) and AIR-2 (red) following control, full *ulp-1(RNAi),* or 24-48 hour *ulp-1(RNAi)*. (A) In 75/75 control pre-anaphase spindles, SUMO and AIR-2 stain six RCs. In 40/44 anaphase spindles, RC disassembly was normal. (B) Following full *ulp-1(RNAi),* SUMO was not observed on the RCs in 65/71 pre-anaphase spindles (top). Of the 10 anaphase spindles that contained SUMO, three of the spindles had RC disassembly defects (middle). In addition, we observed three spindles that had a failed meiosis phenotype (bottom). (C) Following 24-48 hour *ulp-1(RNAi)*, SUMO was observed on all six RCs in 112/142 pre-anaphase spindles (top). Of the 103 anaphase spindles that contained SUMO, 27 of the spindles had RC disassembly defects (middle). We also observed six spindles with a failed meiosis phenotype (bottom). Bar = 2.5μm. (D) Stacked bar graph illustrating the percent of SUMO rings in control spindles versus full (5 days), 24, 48, and 72 hours of feeding RNAi.

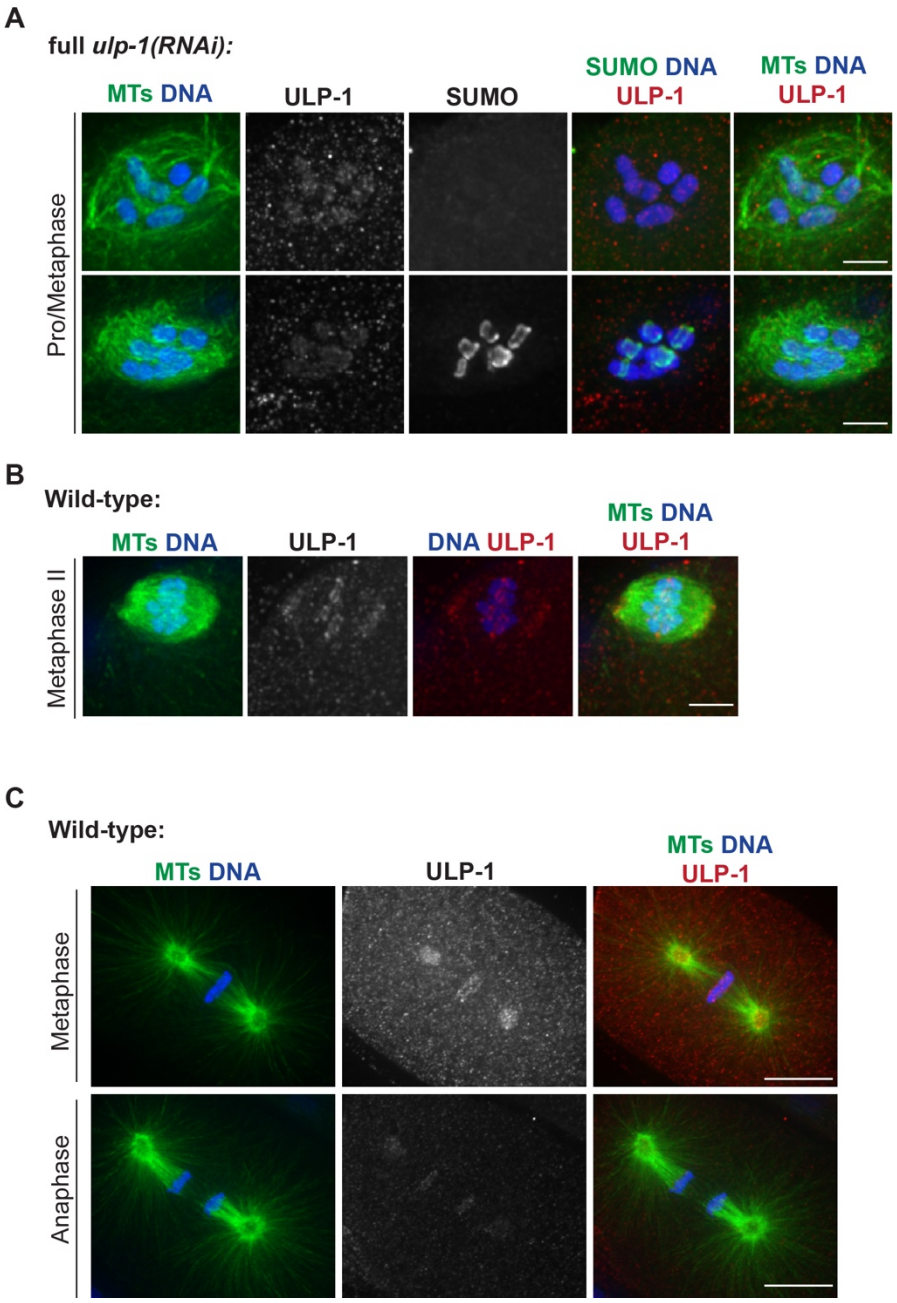


**Figure 3.6 ULP-1 antibody specificity and ULP-1 Meiosis II and Mitosis localization**
(A) Spindles stained for ULP-1 (red), SUMO (green, column 4), DNA (blue), tubulin (green, columns 1 and 5) after 5-day (long-term) ulp-1(RNAi). Long-term ulp-1(RNAi) usually prevents SUMOylation of the RCs (top), but in the rare case that the RCs are SUMOylated and formed (bottom), the ULP-1 antibody does not recognize the RCs, confirming the specificity of its localization. (B) ULP-1 localizes to the RCs and the spindle poles during metaphase II. The chromosomal localization of ULP-1 observed during meiosis I is not present. Bar = 2.5μm. (C) Mitotic spindles stained for ULP-1 (red), DNA (blue), and tubulin (green). ULP-1 localizes to metaphase chromosomes/kinetochores and this localization decreases in anaphase. Bar = 5μm.

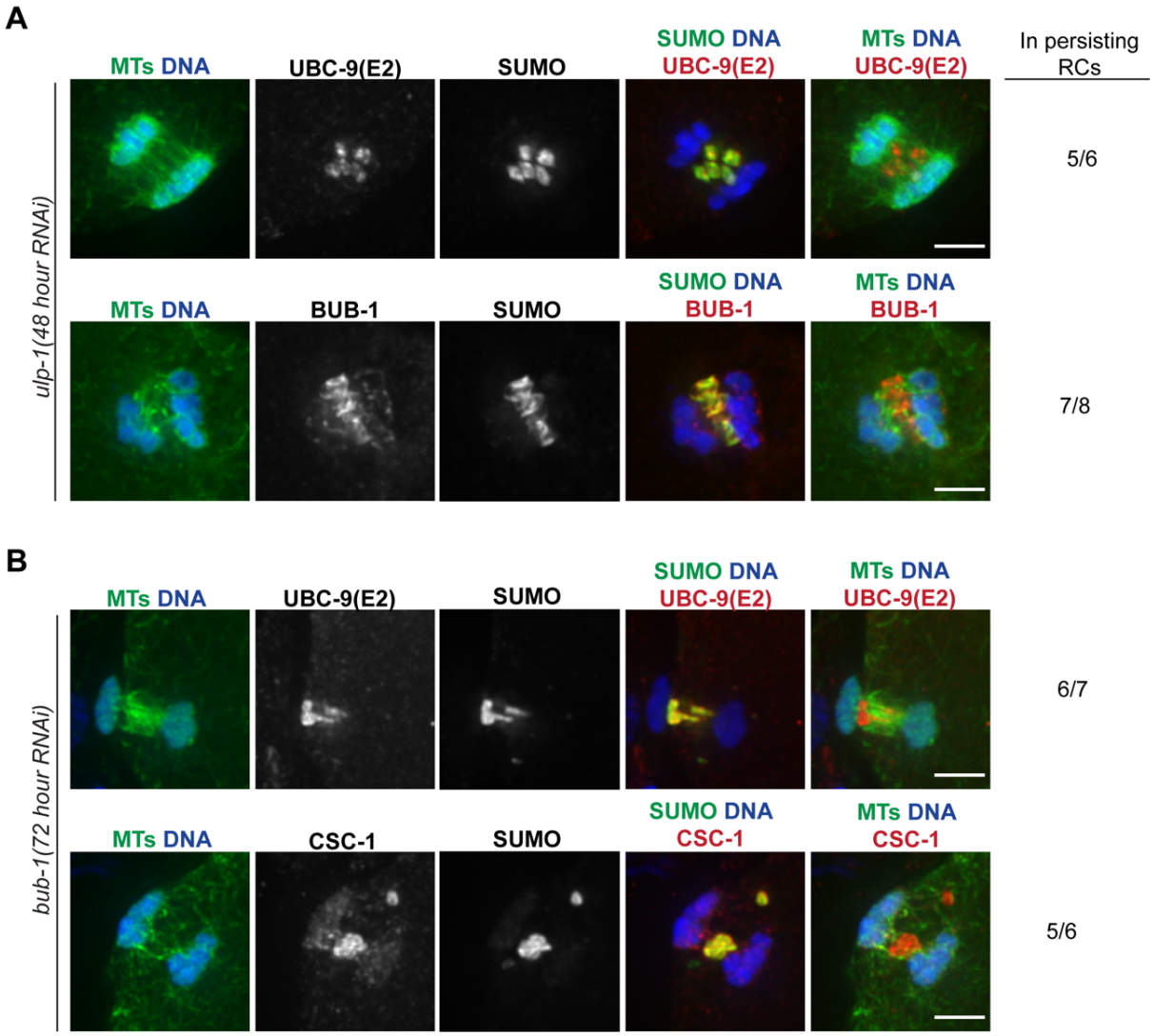


**Figure 3.7 Other RC components colocalize with persisting SUMO and AIR-2 structures**
(A) Spindles stained for UBC-9 (red, top row) or BUB-1 (red, bottom row), SUMO (green, column 4), DNA (blue), tubulin (green, columns 1 and 5) after 48-hour *ulp-1(RNAi)*. Quantification of colocalization with SUMO persisting structures shown on right. (B) Spindles stained for UBC-9 (red, top row) or CSC-1 (red, bottom row), SUMO (green, column 4), DNA (blue), tubulin (green, columns 1 and 5) after 72-hour *bub-1(RNAi)*. Quantification of colocalization with SUMO persisting structures shown on right. Bar = 2.5μm.

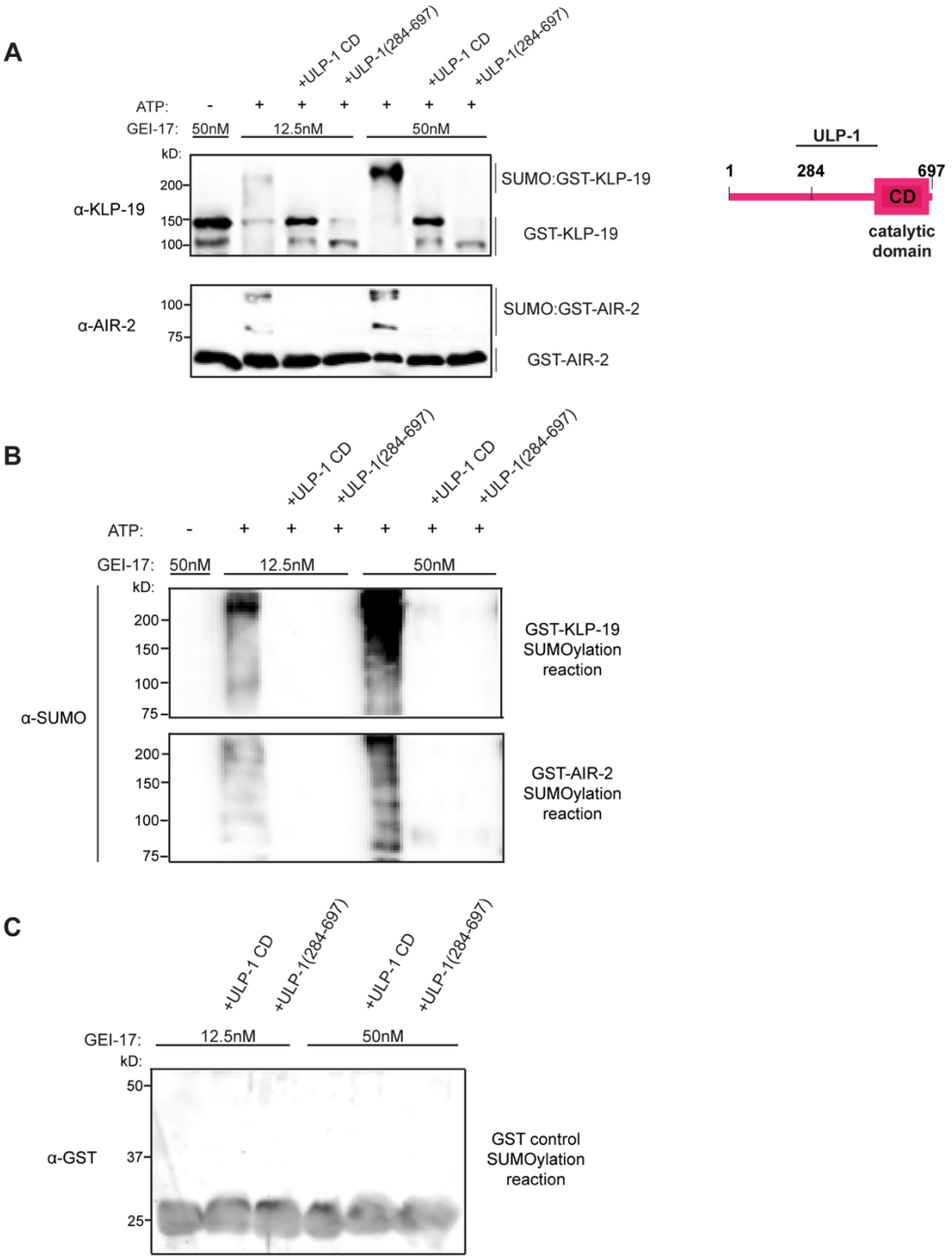


**Figure 3.8 ULP-1 can deSUMOylate RC components AIR-2 and KLP-19 *in vitro***
(A) GST-KLP-19 and GST-AIR-2 can be SUMOylated *in vitro*, and the SUMO modifications are removed when ULP-1 catalytic domain (CD) or ULP-1 (aa284-697) is added after the 4-hour SUMOylation reaction. Western blots using anti-KLP-19 and anti-AIR-2 antibodies. ULP-1 protein sequence schematic shown on right. (B) Western blots using anti-SMO-1 antibody. GST-KLP-19 (top) and GST-AIR-2 (bottom) SUMOylation and deSUMOylation reactions from Part A. SUMO signal is absent after incubation with ULP-1CD and ULP-1 (aa284-697). (C) Western blot using anti-GST antibody shows that GST is not SUMOylated after SUMOylation and deSUMOylation reactions.

**3.F BUB-1 targets ULP-1 to the RC to promote disassembly**

Given our evidence that ULP-1 plays a role in RC disassembly, we next assessed its localization. We found that ULP-1 localizes to the nuclear envelope during diakinesis and then becomes RC-associated after NEBD (Fig. 3.9A, row 1-2). We also observed a chromosomal population in MI, but the staining was not fully removed after *ulp-1(RNAi)*, suggesting that it could be nonspecific (Fig 3.6A). ULP-1 has a similar localization pattern during MII, with additional localization to spindle poles during metaphase II (Fig. 3.6B). In both MI and MII, ULP-1 is absent from RCs during mid anaphase, at the stage when AIR-2 has relocalized to the microtubules and the RCs have flattened and are disassembling (Fig. 3.9A, row 5-6). These results suggest that ULP-1 is targeted to the RC, where it could perform deSUMOylation event(s) in early anaphase to trigger disassembly. Further supporting this idea, when we induce meiotic errors that delay RC disassembly, ULP-1 remains associated with stabilized RCs well into mid anaphase, potentially poised to later trigger the disassembly process (Fig. 3.9A, row 7).

Next, we sought to understand how ULP-1 is targeted to the RC. In a previous study, we assessed AIR-2 anaphase behavior in a range of depletion conditions, to characterize the response of oocytes to errors. Under most of these conditions, AIR-2 relocalization to microtubules was delayed but not prevented. However, in the course of that analysis we found that depletion of RC component BUB-1 caused a severe defect in AIR-2 relocalization to microtubules, with pools of AIR-2 in the center of the anaphase spindle (Fig. 3.9B), suggesting that BUB-1 is more directly involved in RC disassembly. Therefore, we investigated a possible connection between BUB-1 and ULP-1 and found BUB-1 is required for proper ULP-1 localization; following partial *bub-1(RNAi),* ULP-1 is no longer enriched on the RCs (Fig. 3.9C). Under these conditions, SUMO colocalizes with AIR-2 in persisting structures at the center of late anaphase spindles during MI, and these RC accumulations are also observed in the vicinity of the spindle if the oocyte is able to progress to MII (Fig. 3.9D), similar to what we observed upon ULP-1 depletion (Fig. 3.5B, C). These SUMO/AIR-2 structures also contained other RC proteins, such as CSC-1 and UBC-9(E2) (Fig. 3.7B), suggesting that preventing ULP-1 localization to the RCs prevents SUMO removal from the RCs, consequently inhibiting RC disassembly during anaphase.

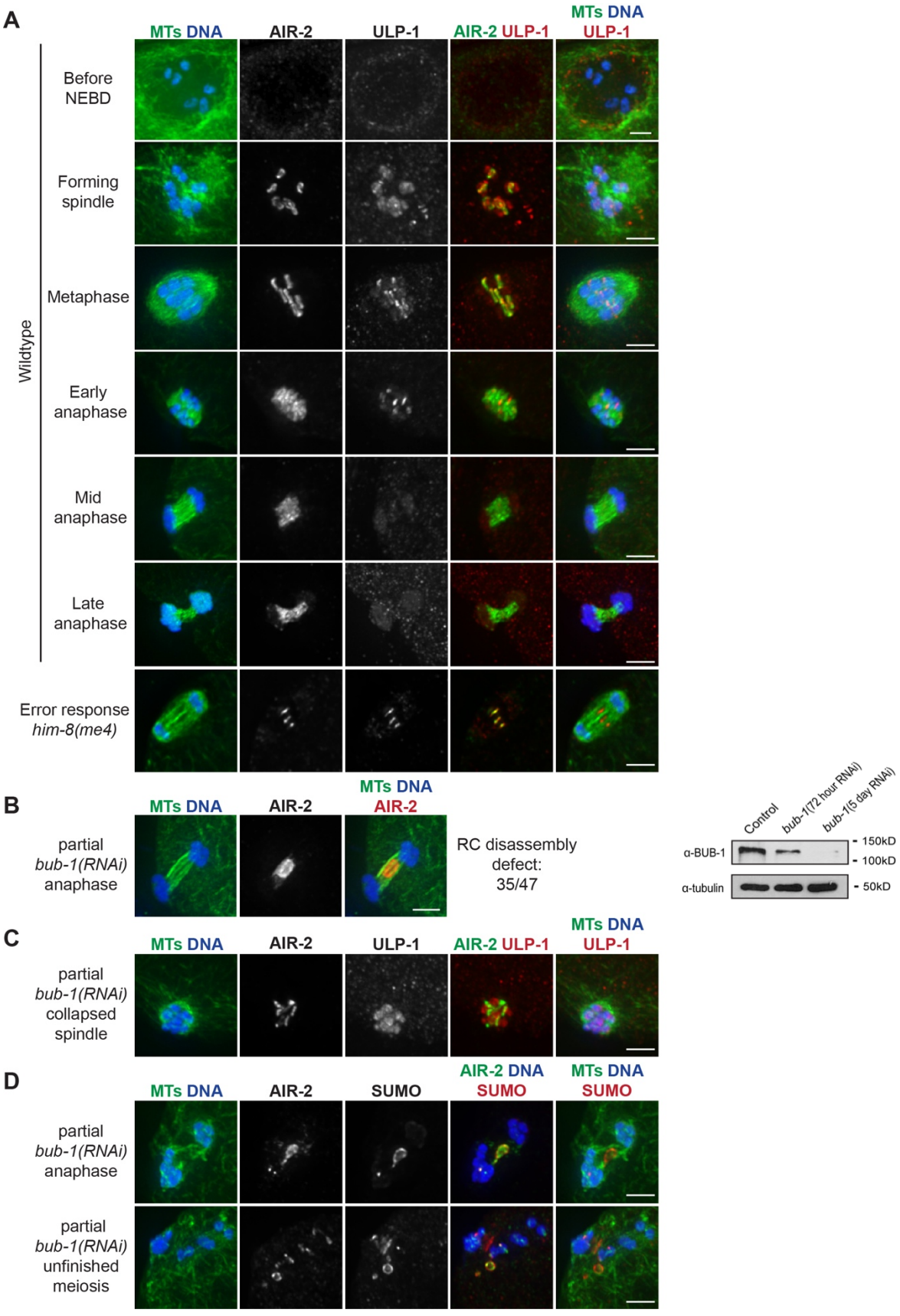
A
MTs DNA
AIR-2
ULP-1
AIR-2 ULP-1
MTs DNA
ULP-1
Wildtype
Before NEBD
Forming spindle
Metaphase
Early anaphase
Mid anaphase
Late anaphase
Error response
him-8(me4)
B
MTs DNA
AIR-2
MTs DNA
AIR-2
partial bub-1(RNAi) anaphase
RC disassembly defect: 35/47
Control
bub-1(72 hour RNAi)
bub-1(5 day RNAi)
α-BUB-1
α-tubulin
150kD
100kD
50kD
C
MTs DNA
AIR-2
ULP-1
AIR-2 ULP-1
MTs DNA
ULP-1
partial bub-1(RNAi) collapsed spindle
D
MTs DNA
AIR-2
SUMO
AIR-2 DNA
SUMO
MTs DNA
SUMO
partial bub-1(RNAi) anaphase
partial bub-1(RNAi) unfinished meiosis

**Figure 3.9 (previous page) BUB-1 targets ULP-1 to the RC to promote disassembly**
(A) ULP-1 (red) localization from diakinesis through late anaphase in wild-type oocytes (rows 1-6), compared to AIR-2 (green, column 4), DNA (blue), and tubulin (green, columns 1 and 5). ULP-1 begins to concentrate on the RC during spindle formation and then leaves the RC in mid anaphase. Row 7 shows ULP-1 and AIR-2 remaining associated with the RCs when disassembly is delayed in the *him-8(me4)* mutant. (B) (Right) Anaphase spindle showing AIR-2 (red) relocalization defect (quantification on right) after partial *bub-1(RNAi)*. (Left) Western blot showing BUB-1 depletion level after 72-hour and 5-day (full) *bub-1(RNAi)*. (C) Collapsed spindle following partial *bub-1(RNAi)* stained for ULP-1 (red), compared to DNA (blue), tubulin (green, columns 1 and 5), and AIR-2 (green, column 4). ULP-1 localizes to chromosomes but is not RC-associated. (D) Partial *bub-1(RNAi)* spindles in late anaphase I (row 1) and prometaphase II (row 2) spindles, stained for SUMO (red), compared to DNA (blue), tubulin (green, columns 1 and 5), and AIR-2 (green, column 4). Defects in RC disassembly lead to pools of SUMO and AIR-2. Bar = 2.5μm.

During this analysis, we noted that our *bub-1(RNAi)* conditions resulted in a more severe phenotype than our *ulp-1(RNAi)* conditions; we observed AIR-2 pools in 26% of 24-48 hour *ulp-1(RNAi)* anaphase spindles (Fig. 3.5C), compared to 75% of partial *bub-1(RNAi)* anaphase spindles, and AIR-2 was also completely excluded from microtubules following partial *bub-1(RNAi)*. We speculate that the ULP-1 partial depletion conditions may allow for a small amount of active ULP-1 on the RCs. However, this difference could also indicate that BUB-1 might additionally be involved in AIR-2 regulation independent of ULP-1. Taken together, these results support the hypothesis that ULP-1 is targeted to the RCs by BUB-1, where it removes SUMO modifications in anaphase, facilitating RC disassembly.

### 3.G ULP-1 has a role on RCs independent of SUMO maturation and RC disassembly

The finding that ULP-1 is present on RCs well before they disassemble led us to ask if ULP-1 affects RCs prior to anaphase, independent of its role in SUMO maturation. To investigate this, we obtained a worm strain which expresses GFP::AIR-2 as well as mCherry::SUMO(GG), a conjugatable form of SUMO. In theory, if we deplete ULP-1 in these worms, they should still have the mature, mCherry::SUMO to use for RC assembly and maintenance, and ULP-1 depletion should not affect SUMO availability for RC assembly. Interestingly, after 48-hour *ulp-1(RNAi)* and ethanol fixation to preserve the mCherry::SUMO(GG) signal, we noticed that 30/62 spindles had less than six mCherry::SUMO(GG) rings

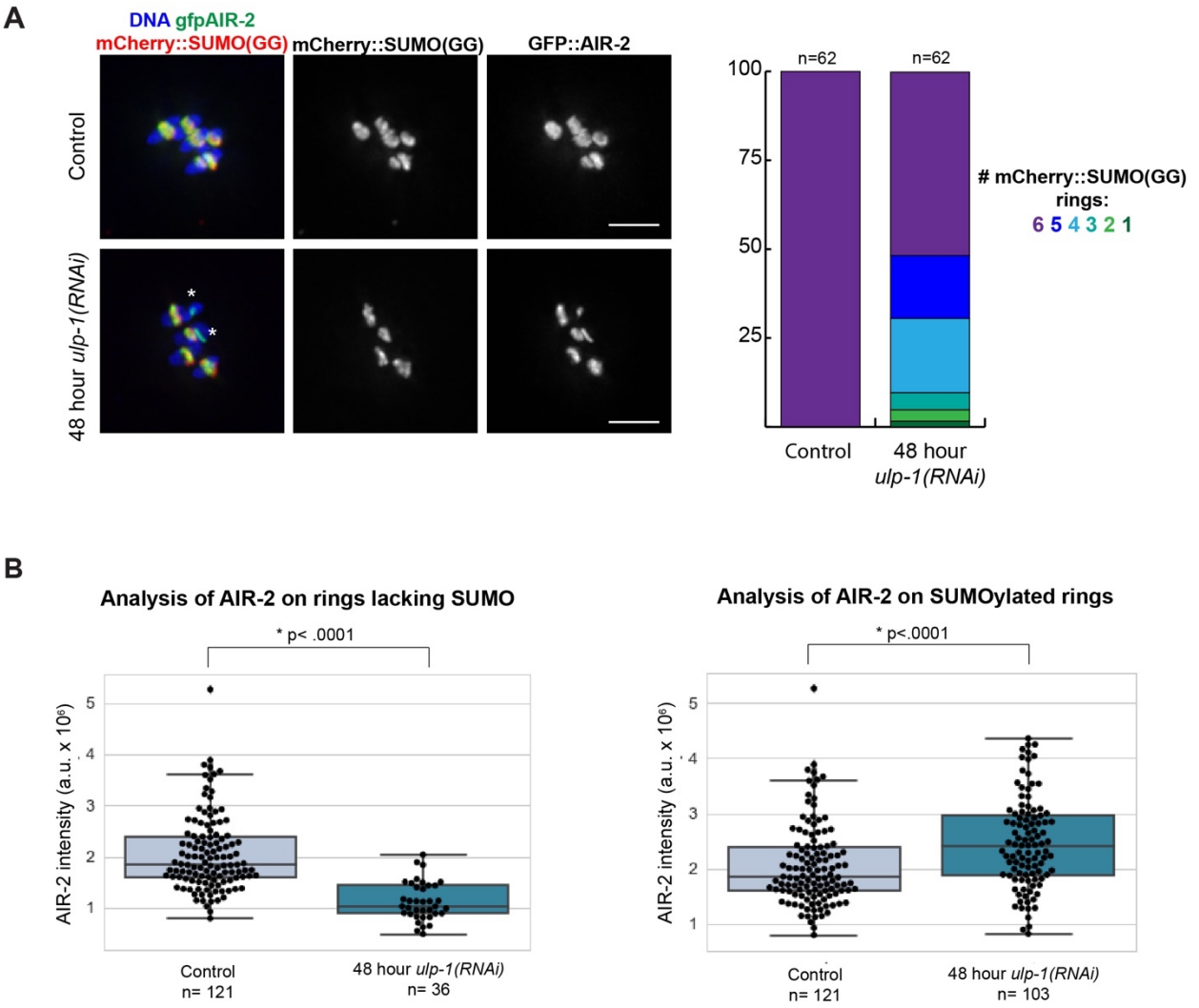


**Figure 3.10 ULP-1 has a role on RCs independent of SUMO maturation and RC disassembly**
(A) Ethanol fixed images showing control versus 48-hour *ulp-1* (RNAi) metaphase chromosomes from worms expressing GFP::AIR-2 and mCherry::SUMO(GG). ULP-1 depletion results in unSUMOylated rings as shown by the asterisks. Percent of mCherry::SUMO(GG) rings shown in stacked bar graph on the right. B) Box plots showing AIR-2 intensity per RC during metaphase after control or 48-hour *ulp-1(RNAi)* on unSUMOylated and SUMOylated rings; data points represent individual RCs. Box represents first quartile, median, and third quartile. Lines extend to data points within 1.5 interquartile range. Asterisks represent significant difference (two-tailed t test; *, $p < 0.004$). Bar = 2.5μm.

present (Fig. 3.10A). In contrast, all spindles contained six AIR-2 rings. The fact that there were some bivalents lacking the mCherry::SUMO(GG) signal tells us that ULP-1 has a pre-anaphase role outside of maturing SUMO and making it available for RC conjugation. This data suggests that RC-localized ULP-1 may contribute to the recruitment or maintenance of SUMOylated RC proteins.

During this analysis, we also noticed that AIR-2 levels were affected by ULP-1 depletion. After 48-hour *ulp-1* (RNAi), we observed an increase in the amount of AIR-2 present on SUMOylated RCs (Fig. 3.10B). Conversely, the RCs that lacked SUMO showed a significant decrease in the amount of AIR-2 fluorescence intensity as compared to control spindle RCs (Fig. 3.10B). This data illustrates that despite the fact that AIR-2 initially localizes to RCs before and independent of SUMO, the progressive recruitment and maintenance of AIR-2 may be dependent on ULP-1 and the SUMOylation state of the RC.

**3.H ULP-1 protease is active prior to anaphase**

Given that ULP-1 appears to have a role on metaphase spindles, we wanted to assess whether the protease is active during that stage. We hypothesized that if ULP-1 is active prior to anaphase, it could be competing for substrate with the E2/E3 enzymes in order to obtain a specific level of SUMOylation on the RCs. We predicted that if ULP-1 is competing for substrate with the E2/E3 enzymes, then depletion of ULP-1 would increase the amount of SUMOylation on RCs, which would be reflected by increased fluorescence. To test this hypothesis, we first needed to find a timepoint where the AIR-2 fluorescence intensity was not perturbed, and RC structure was more or less normal. We found that 44-hour *ulp-1* (RNAi) achieved this; 15/16 spindles contained 6 SUMOylated RCs and GFP::AIR-2 intensity was similar to the control. Upon 44-hour ULP-1 depletion, the ratio of mCherry::SUMO(GG) to GFP::AIR-2 fluorescence intensity on individual RCs in metaphase spindles increased relative to control spindles due to a significant increase in the SUMO intensity (Fig. 3.11). Taken together these results suggest that ULP-1 not only plays a role in SUMO maturation, but also has an important role on RCs prior to anaphase where it may compete for substrate with the E2/E3 enzymes.

We also tested the other three ULPs and found that the SUMO intensity did not significantly change after ULP-4 and ULP-5 depletion (Fig. 3.12B, C). However, ULP-2 depletion increased SUMO intensity (Fig. 3.12A), suggesting that while this protease does not appear to be required for overall RC assembly (Fig. 3.4C), it may more subtly regulate aspects of RC organization or function. We noticed a visual increase

in the amount of SUMO on late anaphase chromosomes after *ulp-2* (RNAi), and this may reflect an overall shift in the regulation of SUMO (Fig. 3.4C).

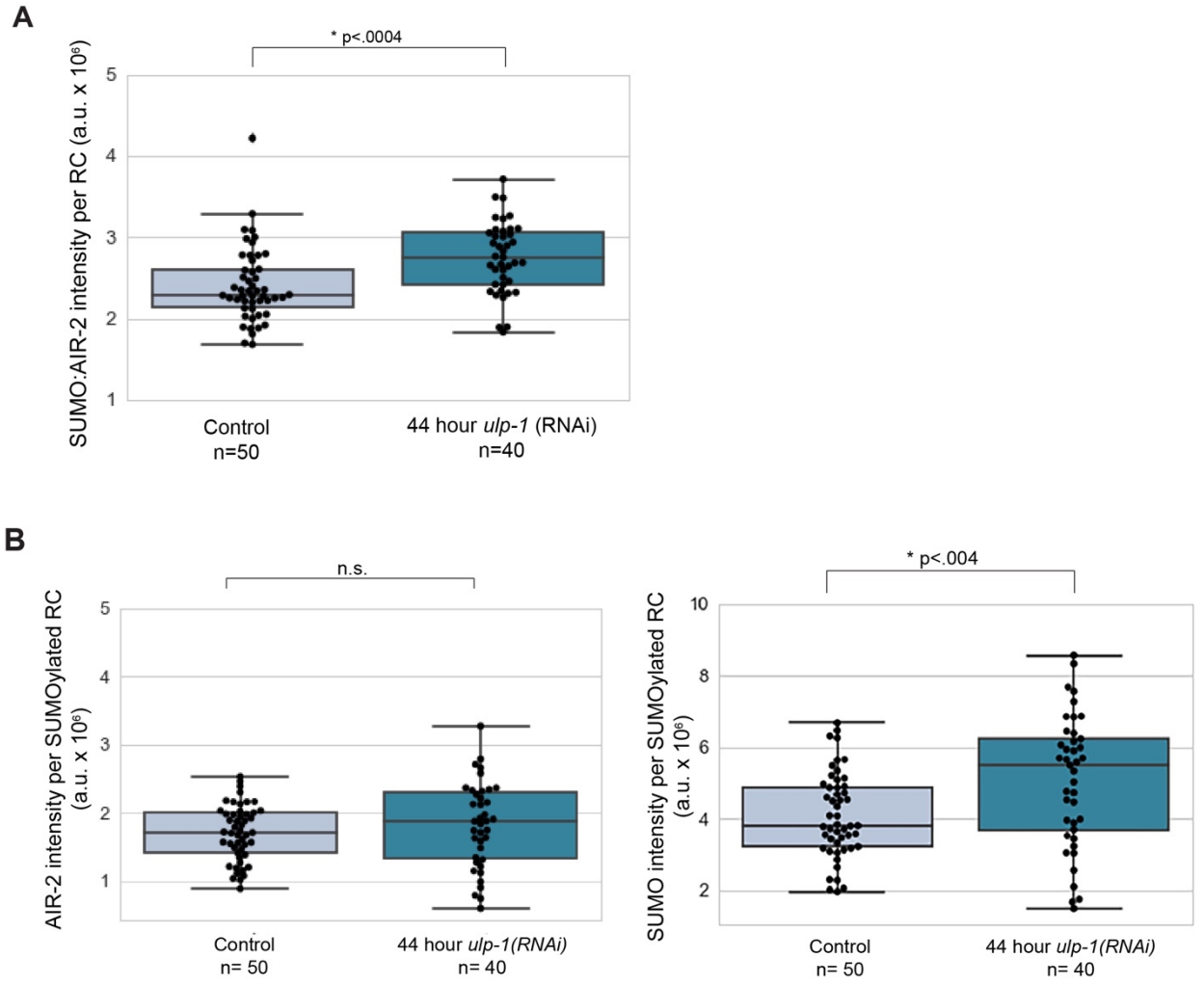


**Figure 3.11 SUMO intensity on RCs increases following *ulp-1* (RNAi)**
(A-B) Box plots showing the mCherry::SUMO(GG) to GFP::AIR-2 ratio per RC, GFP::AIR-2 intensity per RC, or mCherry::SUMO(GG) only intensity per RC during metaphase in SMW23 after vector control or 44-hour *ulp-1* (RNAi); data points represent individual RCs. Box represents first quartile, median, and third quartile. Lines extend to data points within 1.5 interquartile range. Asterisks represent significant difference, n.s. = not significant (two-tailed t test).

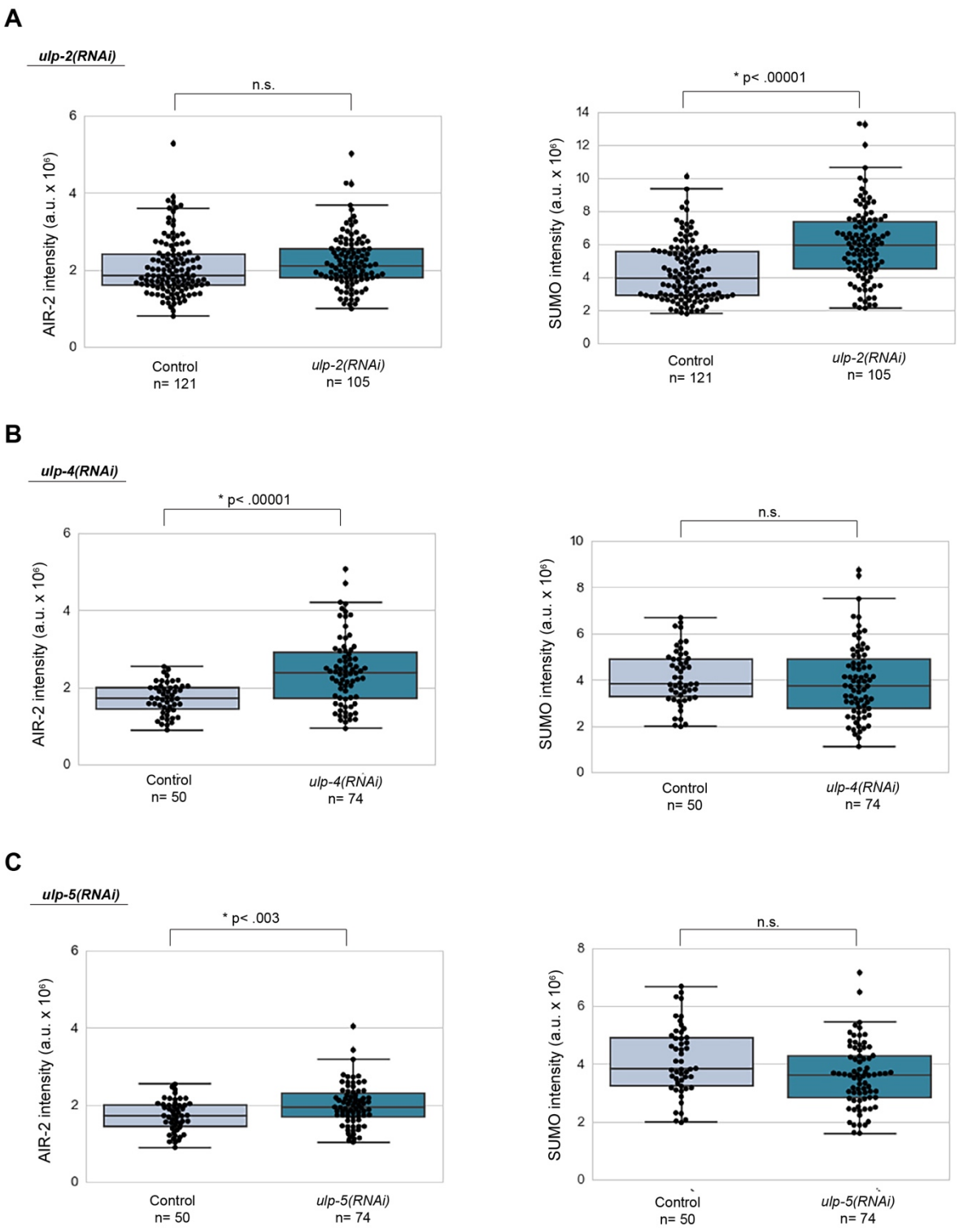


**Figure 3.12 SUMO and AIR-2 intensity on RCs following ULP depletions**
(A-B) Box plots showing GFP::AIR-2 or mCherry::SUMO(GG) intensity per RC during metaphase in SMW23 after vector control or *ulp-2, ulp-4,* or *ulp-5* (RNAi); data points represent individual RCs. Box represents first quartile, median, and third quartile. Lines extend to data points within 1.5 interquartile range. Asterisks represent significant difference, n.s. = not significant (two-tailed t test).

### 3.I E2/E3 enzymes leave RCs before ULP-1 protease

We next hypothesized that since ULP-1 is active before anaphase and seems to compete for substrate with the E2/E3 enzymes, that the removal of the E2/E3 enzymes in early anaphase would enable ULP-1 to remove SUMO modifications that trigger RC disassembly. Supporting this idea, we found that UBC-9 leaves the RCs before ULP-1 in early anaphase (GEI-17 also leaves the RCs during this time (Fig. 3.1C), but we could not directly compare its localization to ULP-1 for technical reasons). When we co-stained early anaphase spindles with antibodies against ULP-1 and UBC-9, we found spindles distributed equally into two categories: 1) spindles where both UBC-9 and ULP-1 were present on all six RCs or 2) spindles where there was significantly more ULP-1 than UBC-9; we never observed spindles with only UBC-9 present (Fig. 3.13A). These results support the view that prior to anaphase, RC SUMOylation is maintained by a balance between UBC-9/GEI-17 and ULP-1 presence. Then, removal of UBC-9 and GEI-17 from the RCs in early anaphase could enable ULP-1 to deSUMOylate RC components and trigger disassembly.

We further hypothesized that if UBC-9 and GEI-17 were retained on RCs past early anaphase, the RCs would maintain their ring-like structures. To test this, we assessed whether these enzymes are retained on error-response spindles, where in response to various meiotic errors and short temperature stresses, the oocyte delays RC disassembly and AIR-2 relocalization to the microtubules through mid to late anaphase (discussed in Chapter 2[46]). Under these conditions, we found that the persisting RCs were strongly marked by SUMO, UBC-9, and GEI-17 (Fig. 3.13B), the latter two of which are normally absent from the RCs during this stage (Fig. 3.1C). This suggests that UBC-9 and GEI-17 are actively maintained on the RCs during an error response to achieve a SUMOylation state that promotes RC stability.

### 3.J Conclusions and discussion

In summary, our findings support a model in which dynamic remodeling of SUMO modifications drives a series of essential events during the meiotic divisions (Fig. 3.14). First, SUMO is required for building the RC[45]. SUMOylation events driven by UBC-9 and GEI-17 aid in RC assembly, enabling the targeting of other components to the structures. Our studies have further revealed that ULP-1 protease,

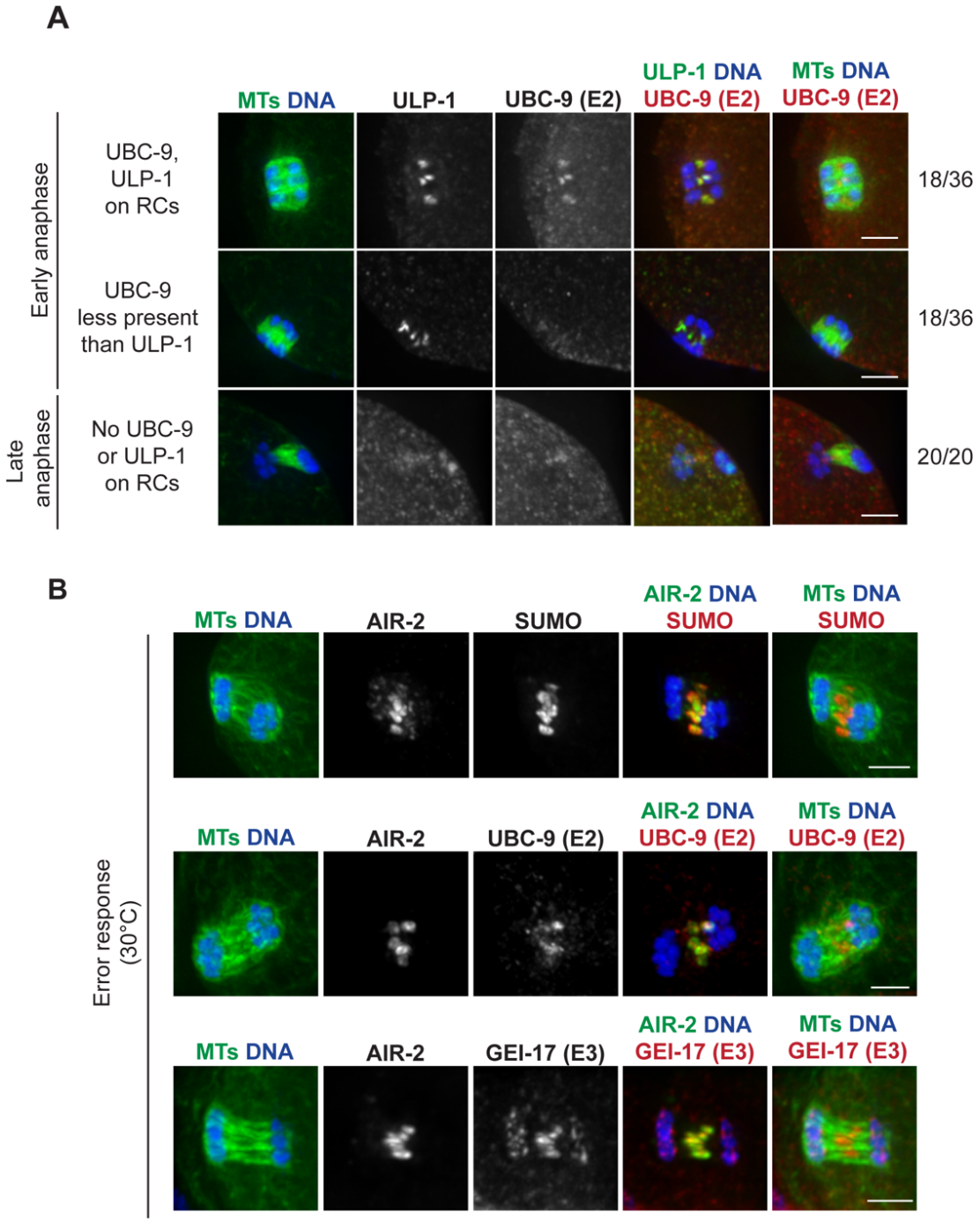


**Figure 3.13 E2/E3 enzymes leave RCs before ULP-1 protease**
(A) Comparison of UBC-9 (red) to the SUMO protease ULP-1 (green in column 4), with DNA (blue) and tubulin (green, columns 1 and 5). In 50% of early anaphase spindles, UBC-9 and ULP-1 are localized to the RCs (row 1), but in the other 50%, UBC-9 is either not present or less present that ULP-1 (row 2), suggesting that conjugating enzymes leave the RCs first. As anaphase progresses, both proteins are absent from the RCs (row 3). Quantifications shown on right. (B) When RC disassembly is delayed (shown is a 30˚C incubation that induces an error response), SUMO, UBC-9, and GEI-17 remain RC associated. Anaphase spindles stained with SUMO (red, top row), UBC-9 (red, second row), or GEI-17 (red, third row) and AIR-2 (green, column 4), DNA (blue), and tubulin (green, columns 1 and 5). Bar = 2.5μm.

which localizes to the RCs during assembly, also plays an important role in recruitment and/or maintenance of SUMOylated RC proteins independent of its role in SUMO maturation. Furthermore, we have demonstrated the importance of SUMO in promoting RC stability during anaphase once RCs are released from chromosomes. We hypothesize that in metaphase, SUMO is not required for components like the CPC to maintain a ring-like shape, since the chromosomes likely act as scaffolds at this stage. However, we found that SUMOylation is essential for maintaining the structural integrity of the RCs after they are released from the chromosomes, suggesting that it could act as a "glue" that provides structural support to the complex. This stabilization is important because it facilitates chromosome segregation. During early anaphase, chromosomes move towards spindle poles through open microtubule channels. Our previous work (Chapter 2[46]) suggested that the RCs act as physical wedges within the microtubule channels, keeping them wide to allow chromosome movements during Anaphase A and also during an error response. Thus, maintaining the stability and ring-like structure of the RCs is likely important.

Our findings also demonstrate that RC disassembly in anaphase is an active process in which proteins are removed in a sequential manner from the RCs; we find that this process may rely on MEL-28 and/or PP1 function. Moreover, we have implicated deSUMOylation of RC component(s) as a major driving force. Prior to anaphase, ULP-1 and the E2/E3 enzymes seem to compete for substrate until at anaphase onset, removal of E2/E3 enzymes shifts this balance and allows ULP-1 to remove SUMO modifications that initiate the disassembly process. This allows for AIR-2 relocalization to microtubules and for the RCs to lose structural integrity, flattening then breaking down, which enables the channels to close. Importantly, proper regulation and coordination of these events is essential for meiotic progression; in conditions where ULP-1 is not targeted to the RCs, RC proteins end up in persisting structures at the center of the spindle during anaphase and prevent the proper completion of the meiotic divisions.

Our studies suggest that the disassembly process is not driven by removing SUMO entirely from the RC, since 1) the SUMO signal persists longer than ULP-1 and other RC proteins such as SEP-1 and 2) the flattening RCs still have a SUMO signal. Therefore, we propose that removal of a small population of SUMO modifications from RC components in early anaphase helps to disengage specific protein-protein interactions and allows the RC to disassemble. This could also involve deSUMOylation events that allow

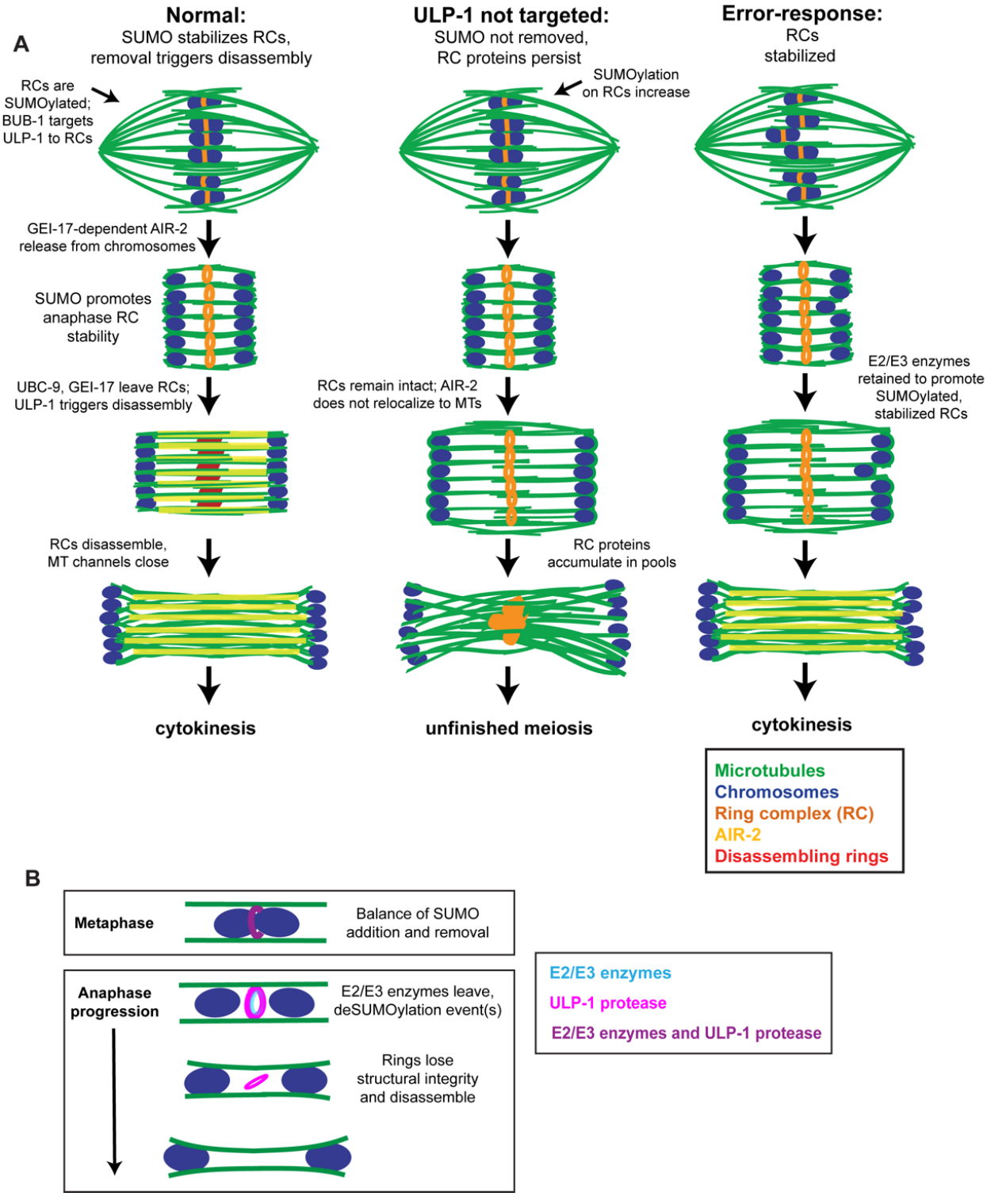
A
Normal:
SUMO stabilizes RCs,
removal triggers disassembly
ULP-1 not targeted:
SUMO not removed,
RC proteins persist
Error-response:
RCs
stabilized
RCs are
SUMOylated;
BUB-1 targets
ULP-1 to RCs
SUMOylation
on RCs increase
GEI-17-dependent AIR-2
release from chromosomes
SUMO promotes
anaphase RC
stability
E2/E3 enzymes
retained to promote
SUMOylated,
stabilized RCs
UBC-9, GEI-17 leave RCs;
ULP-1 triggers disassembly
RCs remain intact; AIR-2
does not relocalize to MTs
RCs disassemble,
MT channels close
RC proteins
accumulate in pools
cytokinesis
unfinished meiosis
cytokinesis
Microtubules
Chromosomes
Ring complex (RC)
AIR-2
Disassembling rings
B
Metaphase
Balance of SUMO
addition and removal
Anaphase
progression
E2/E3 enzymes leave,
deSUMOylation event(s)
Rings lose
structural integrity
and disassemble
E2/E3 enzymes
ULP-1 protease
E2/E3 enzymes and ULP-1 protease

**Figure 3.14 (previous page) Model for SUMO-mediated anaphase regulation**
(A) Model depicting DNA (blue), microtubules (green), the fully-assembled RCs with AIR-2 (orange), AIR-2 (yellow), and the disassembling RCs without AIR-2 (red). In normal oocyte meiosis (left column), the RCs are SUMOylated and the SUMO protease ULP-1 is targeted to the RCs by BUB-1. During anaphase, SUMO E2/E3 enzymes leave the RCs, allowing ULP-1 to remove SUMO modifications that trigger RC disassembly. When this happens, AIR-2 leaves the RCs and relocalizes to the microtubules and the RCs break down. Under experimental conditions in which ULP-1 cannot localize to the RC (middle column), the RCs remain in a SUMOylated state that prevents RC disassembly and AIR-2 relocalization and impedes completion of the meiotic divisions. In an error-response (right column), the oocyte retains the E2/E3 enzymes to delay RC disassembly and AIR-2 relocalization. Eventually though, RC disassembly proceeds and cytokinesis occurs. (B) ULP-1 (SUMO protease, magenta), UBC-9 (SUMO E2, blue), and GEI-17 (SUMO E3, blue) are on the RCs in metaphase where they compete for substrate. During early anaphase UBC-9 (E2) and GEI-17 (E3) leave the structures and ULP-1 deSUMOylation activity promotes RC disassembly. By mid anaphase, the RCs are breaking down (not shown in cartoon) and ULP-1 is absent from the complexes.

for Ubiquitin-mediated degradation. Since we have shown that AIR-2 and KLP-19 can be substrates of ULP-1 *in vitro*, it is possible that deSUMOylation of one of these proteins is the key event required for RC disassembly. However, since the RC is a SUMO-SIM network that has many known components, this process is likely more complex (Appendix B). Future studies building on this work will therefore be important to reveal principles underlying the dynamic remodeling of SUMO-SIM networks.

Our data also demonstrate that SUMO remodeling not only regulates RC assembly and disassembly but could serve to connect the RCs to the chromosomes. First, we found that depletion of the SUMO protease ULP-4 led to defective RC morphology; although ring structures still formed, they often appeared to stretch off the chromosomes and link together. This result suggests that ULP-4 is required to create a stable connection between the RCs and the chromosomes. Since ULP-4 depletion did not affect the SUMOylation level of the RCs and the protease did not appear to localize to the RCs, we think that it is unlikely that ULP-4 performs this function by regulating modifications on the RCs themselves. Alternatively, we hypothesize that because ULP-4 affected the level of AIR-2 on the bivalents, it's deSUMOylation activity instead promotes some other fundamental aspect of RC assembly. Notably, we also observed anaphase RC defects following ULP-4 depletion, raising the possibility that this protease is involved in RC disassembly alongside ULP-1. However, the metaphase RC defects that we observed made it impossible to convincingly assign an anaphase-specific role for ULP-4; future studies will therefore be important to better understand ULP-4's precise contributions to oocyte meiosis.

Dynamic SUMO regulation also appears to be important for RC release from chromosomes. After GEI-17 depletion, we frequently observed that AIR-2 remained attached to chromosomes during anaphase, suggesting that release of the chromosomal passenger complex (CPC) from chromosomes is dependent on GEI-17-mediated SUMOylation. But given that AIR-2 normally loads onto chromosomes in the absence of SUMO and GEI-17, these data suggest that the SUMOylation state of the RC is remodeled during metaphase to allow for CPC release. This could be a direct modification to the CPC to allow it to release from histones but given that SUMO does not spread to the microtubules at the same time as the CPC, in this scenario the modification would have to be quickly removed before microtubule binding in early anaphase. This idea is reminiscent of prior work demonstrating that Survivin (BIR-1), is ubiquitinated and deubiquitinated to promote centromere binding and release during mitosis in HeLa cells[152]. Regardless of the specific modification regulating CPC release, our results are exciting because they suggest that even after RC assembly, the SUMOylation state of the RCs continues to be modified in order to facilitate subsequent meiotic events.

This idea that SUMO modifications are being dynamically remodeled throughout prometaphase and metaphase is also supported by our analysis of SUMO proteases. Depletion of either ULP-1 or ULP-2 increases the fluorescence intensity of SUMO on the RCs, implicating these proteases in the cleavage of SUMO from RC substrates. These data provide further evidence that many enzymes are involved in the tight regulation of the SUMOylation states of RC proteins.

In recent years, it has become apparent that SUMO plays an important role in the regulation of meiotic and mitotic progression, as many SUMOylated cell division proteins have been identified, SUMO localizes to the spindle in many organisms, and disruption in global SUMOylation and/or specific SUMOylated substrates generally results in severe spindle and/or chromosome segregation defects[111, 128]. Given its reversible nature, SUMOylation is now appreciated as a useful post-translational modification for regulating protein localization and function during dynamic cellular processes such as cell division. Our study reinforces and expands upon this view, demonstrating a new role for SUMO in regulating anaphase progression in *C. elegans* oocytes by mediating the assembly and disassembly of an important protein complex. Moreover, our work reveals novel insight into the complexity of how SUMO/SIM networks can be

regulated and remodeled, by targeting both SUMO E2/E3 enzymes and SUMO proteases to the protein complex to achieve fine-tuning and rapid changes in protein interactions.

In addition to further examining how competition between conjugating and deconjugating enzymes regulates the overall SUMOylation state of the RC, it will be interesting to investigate how these enzymes achieve substrate specificity. Since the RC appears to be built in discrete layers, one possibility is that access to substrates plays a key role in regulating substrate specificity. Additionally, phosphorylation states likely have a role in influencing protein targets, with the modification occurring on the enzyme itself and/or on the substrate RC proteins. Supporting this idea, 1) there are kinases in the RC (AIR-2, BUB-1) and 2) the phosphorylation state of many cell division proteins changes during the transition from metaphase to anaphase. Finally, many SUMO proteases have preferences for either mono-SUMOylation or various SUMO chain lengths, and this preference could act as another mode of regulation[92]. Our study establishes the RC as an ideal model for addressing these questions, as it represents a protein complex whose progressive remodeling is regulated by a balance of SUMOylation and deSUMOylation activity. Future studies expanding upon this work will therefore not only uncover mechanisms acting to ensure the faithful segregation of chromosomes during oocyte meiosis but will also shed light on principles underlying the regulation of SUMO during dynamic cellular processes.

# CHAPTER 4:

## Expanded studies of chromosome segregation in *C. elegans* oocytes reinforce a role for lateral microtubule bundles

The data presented in this chapter is being prepared for submission as part of an *eLife Research Advance*
All data shown is that of Amanda Roca.

**4.A Introduction**

In most types of cell division, microtubules form end-on attachments to kinetochores, and these connections facilitate both chromosome congression and segregation. In contrast, *C. elegans* oocytes assemble acentrosomal spindles in which bundles of microtubules run alongside chromosomes in prometaphase, forming lateral associations, and congression is thought to be mediated by plus-end-directed movement along these bundles to the metaphase plate[35]. Moreover, anaphase chromosome movements are kinetochore-independent; although kinetochores form cup-like structures around the chromosome ends during prometaphase[23], these kinetochores are removed from chromosomes in anaphase and experimental depletion of kinetochore proteins does not slow chromosome separation. In a previous publication we used super-resolution imaging to demonstrate that lateral chromosome-microtubule interactions are present during anaphase, creating "channels" in the spindle, suggesting that these interactions could serve to drive chromosome movements[39]. Experiments using both bipolar and monopolar spindles demonstrated that chromosomes are subjected to both plus and minus-end-directed forces prior to anaphase onset; the plus-end forces are generated by the RC complex prior to anaphase and depletion experiments suggested that chromosome-associated dynein provides a minus end force. At anaphase onset, the RCs dissociate from chromosomes and minus-end forces on the chromosomes drive segregation, representing a novel form of "Anaphase A-like" chromosome-to-pole movement[39].

More recent studies have questioned some aspects of our previous study, including whether lateral bundles run alongside chromosomes throughout the entire segregation process; these studies proposed that different types of chromosome-microtubule contacts facilitate this process: 1) microtubules on the poleward-facing surfaces of chromosomes creating a physical tether to the spindle poles throughout anaphase[38] or 2) microtubules polymerizing between two separating chromosome masses and pushing on their inside surfaces[153]. To address these models, we revisited our previous studies, providing additional evidence that lateral microtubule associations are an important feature of the *C. elegans* oocyte spindle during metaphase and anaphase, and therefore likely contribute to the segregation mechanism in these cells.

**4.B Lateral microtubule bundles represent a stabilized population of spindle microtubules**

During *C. elegans* spindle assembly, microtubules initially form a "cage-like" array adjacent to the disassembling nuclear envelope that is then rearranged to form a bipolar spindle[28]. At this early stage, we have observed a mix of laterally-associated microtubule bundles that run alongside the bivalents, as well as bundles at random angles in relation to the long axis of the bivalent (work by Keila Torre-Santiago). As prometaphase progresses, the microtubules appear to be predominately laterally-associated with bivalents and kinetochore end-on attachments are not apparent. We wanted to determine if these lateral associations with chromosomes are cold-stable interactions, potentially mimicking a cold-stable end-on kinetochore attachment.

In other cell types, end-on kinetochore-microtubule attachments represent the predominant way that chromosomes attach to the spindle, and these kinetochore-associated microtubules are more resistant to cold temperatures (i.e., are more stable) than other spindle microtubules. We therefore adapted this assay for use in *C. elegans* oocytes, to determine if the laterally-associated microtubule bundles are cold-stable. We dissected oocytes into cold buffer and then incubated on ice for varying times; we found that after a 10-minute cold treatment, there were significantly fewer microtubules in both mitotic and oocyte spindles (Figure 4.1A, B). This timepoint produced a range of microtubule destabilization, as some oocyte spindles still contained a substantial number of microtubules, while others had very few remaining (Figure 4.1B). Some of the cold-treated spindles looked bipolar, but the poles were often splayed and disorganized. Because not all spindles had this disorganized bipolar appearance, we hypothesize that we are observing spindles at a range of stages, including earlier prometaphase.

Importantly, we found that in cases where there were reduced microtubules, the remaining microtubules were predominantly in the vicinity of chromosomes, while cytoplasmic non-spindle associated microtubules were largely abolished (Figure 4.1A, zoom). Moreover, we observed laterally-associated microtubules in a majority of these spindles; although we assessed lateral chromosome-microtubule contacts in all cold-treated spindles, these lateral contacts were particularly clear in spindles where only a few bundles remained (Figure 4.1C, asterisks). Therefore, our results demonstrate that oocyte spindles have a stabilized population of microtubules despite the absence of end-on attachments and suggest that

lateral contacts with chromosomes could serve as an alternative, stable point of contact to aid in spindle assembly and chromosome congression.

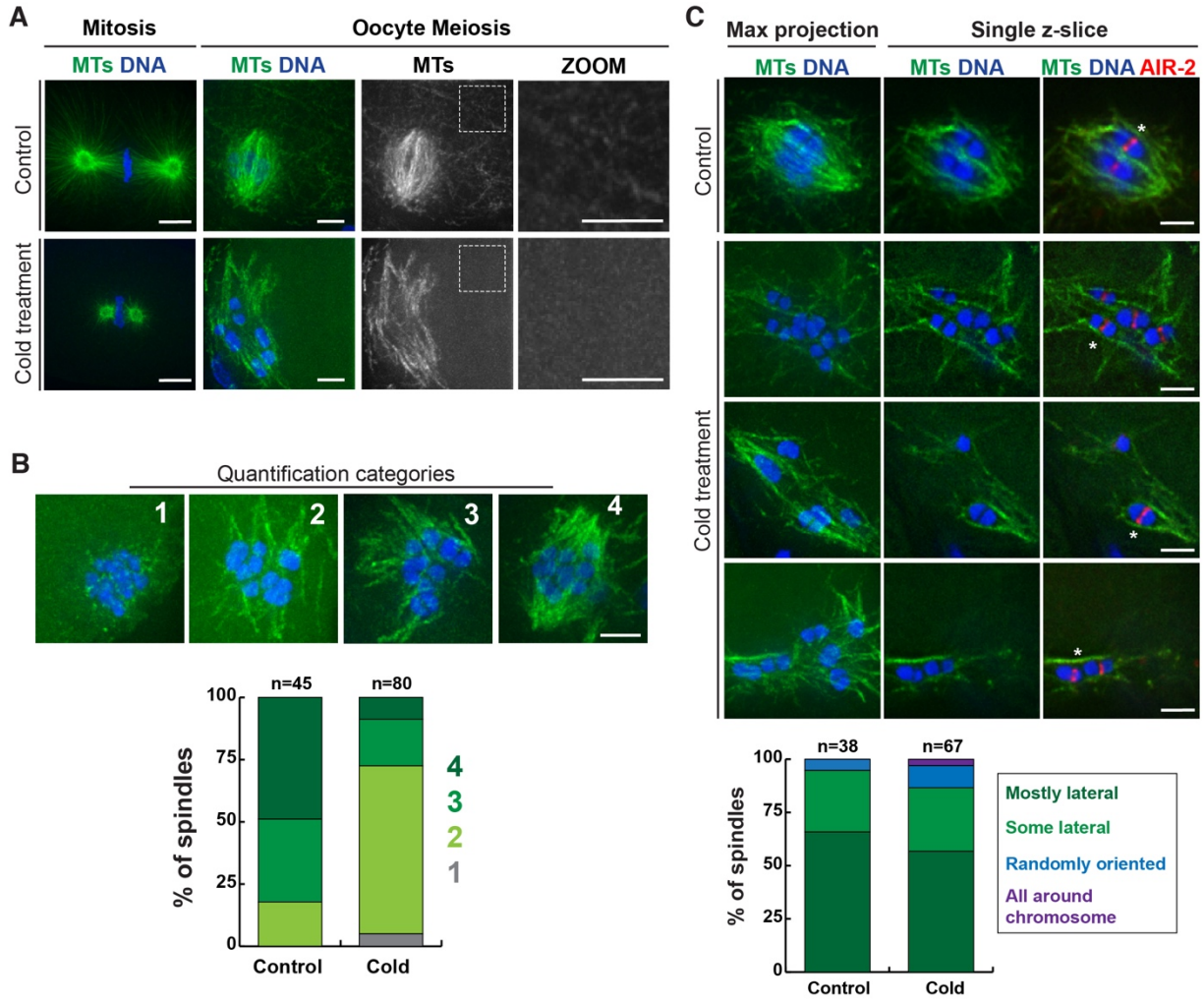


**Figure 4.1 Stabilized lateral microtubule bundles run alongside chromosomes prior to anaphase**
(A) Spindles stained for DNA (blue) and tubulin (green). Images show control versus cold-treated one-cell stage mitotic spindles and oocyte spindles. Zooms illustrate that the cytoplasmic pool of microtubules is decreased after cold treatment. Bar = 5μm for mitotic images, 2.5μm for meiotic images. (B) Oocyte spindles stained for DNA (blue) and tubulin (green). Images show a representative image for each category of microtubule density after cold treatment. All images taken were categorized by eye on a scale of 1-4 for microtubule density around chromosomes. Percent of spindles in each category quantified in graph below. Bar = 2.5μm. (C) Oocyte spindles stained for DNA (blue), tubulin (green), and AIR-2 (red). Images show lateral bundles within a control oocyte spindle as well as three examples of persisting lateral bundles in oocytes after cold treatment. Percent of spindles with lateral bundles in control versus cold-treated oocytes is quantified in the graph below. Maximum projections and single z-slices shown for each image. Bar = 2.5μm.

**4.C Lateral microtubule bundles run alongside chromosomes throughout anaphase**

Previous work from our lab has suggested that lateral microtubule bundles are important for chromosome segregation in *C. elegans* oocytes, but a subsequent study proposed that microtubule polymerization against the surface of a merged group of chromosomes facilitates chromosome segregation[153]. Laband *et al* proposed this after generating partial 3D reconstructions using electron tomography that did not reveal a significant population of microtubules running laterally alongside chromosomes in either mid or late anaphase (two spindles were analyzed, with chromosome segregation distances reminiscent of mid to late anaphase). This study reported two separable arrays of microtubules: 1) one array inside the separating chromosomes aligned along the long axis of the spindle, and 2) another on the poleward facing surface of the chromosomes. A notable feature of these reconstructions is that microtubules could not be detected between individual chromosomes of a segregating set, and instead the chromosomes appeared to merge into a single electron-dense mass, with the ends of some microtubules terminating on the inside surface; this led the authors to propose that pushing by these microtubules on the inside surfaces of closely-apposed chromosomes created the force to drive segregation. To address this controversy, we initiated a careful analysis of chromosome-microtubule contacts during anaphase.

First, we addressed the proposal that the chromosomes merge into two distinct masses. To do this, we established that chromosomes are individualized throughout anaphase and do not merge into two large masses. This is important because we hypothesize that lateral microtubule bundles remain associated with each chromosome throughout anaphase to act as an anchor so that chromosomes segregate when the spindle elongates during Anaphase B. Our published fixed imaging has always shown six, individualized chromosomes, but to illustrate this this is not merely a result of methanol fixation, we showed that in live imaging, chromosomes are distinguishable (work by Tim Mullen). Once that was established, we showed that a chromosome-associated protein, MEL-28, encircles each chromosome throughout anaphase, illustrating six, distinct structures, similar to what had been previously shown by another group[151]. In spindles that were oriented end-on, we also observed microtubule staining around each circle of MEL-28, demonstrating that lateral contacts are also present in mid and late anaphase (Fig. 4.2). Therefore, our

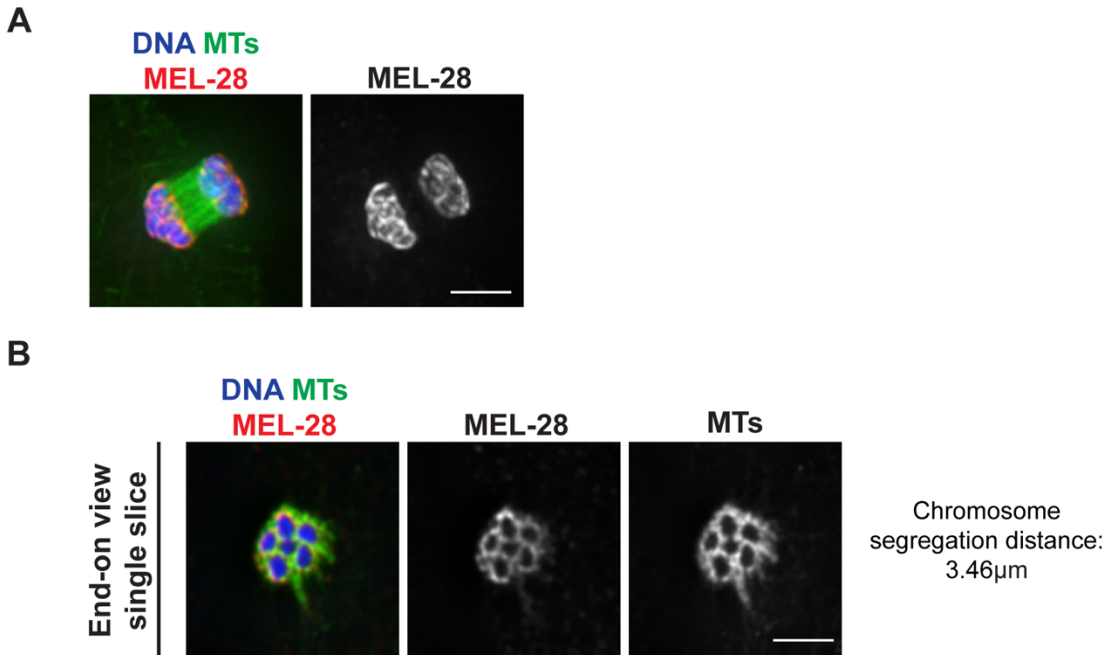


**Figure 4.2 MEL-28 encircles mid to late anaphase chromosomes**
Spindles stained for DNA (blue), tubulin (green), and GFP-MEL-28 (red). (A) Shows a mid-anaphase spindle with MEL-28 encircling individualized chromosomes. (B) Shows a different, end-on spindle illustrating both circles of MEL-28 and laterally associated microtubules. End-on spindle is an individual z-slice. Bar = 2.5µm.

studies demonstrate that chromosomes do not merge into a single mass, arguing against one important feature of the "pushing" model.

Next, we tested another aspect of the Laband model. Given that chromosomes do not merge into a single mass, in order for the microtubules to exert pushes forces, we would predict that there should be high microtubule density adjacent to the inside surface of each chromosome to provide the putative "pushing" force. However, our imaging shows that the primary population of microtubules during anaphase is laterally associated with the chromosome, running alongside approximately half of the length of the chromosome (Fig. 4.3A) We therefore imaged mid anaphase spindles and performed 5-pixel wide linescans through both the chromosomal region (near the inside surface) and the region adjacent to, but not touching, the inside surfaces of chromosomes. Linescans through the chromosomal region (Figure 4.3B, "region 1") showed an anti-correlation of tubulin and DNA intensity, further supporting the conclusion that lateral

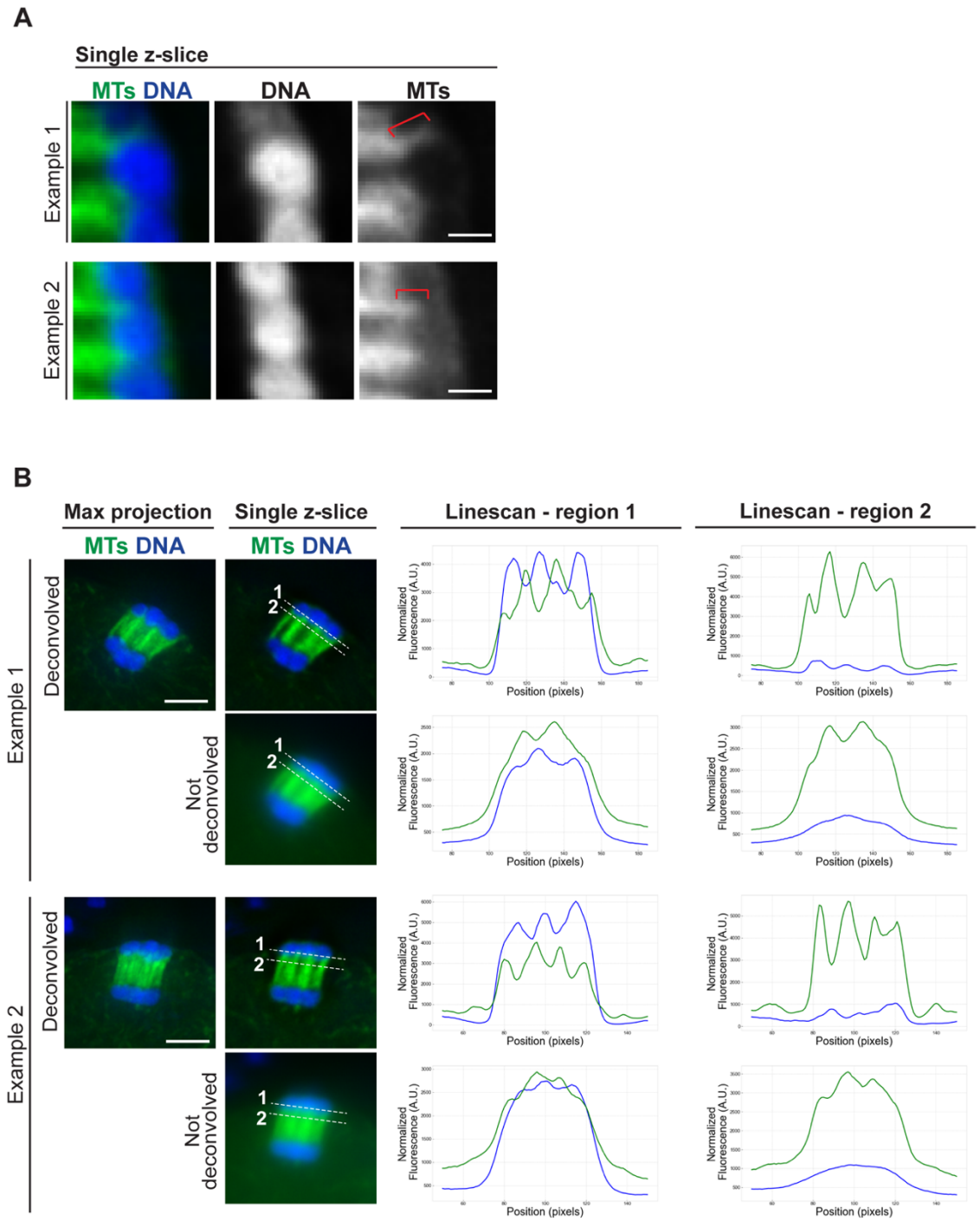


**Figure 4.3 Lateral chromosome-microtubule interactions persist until the end of anaphase**
(A-B) Wild-type anaphase spindles stained for DNA (blue) and tubulin (green). (A) Examples shown are single z-slices, illustrating the lateral microtubule association along the anaphase chromosome. Red brackets show examples of a lateral interaction. Bar = 0.625μm (B) Examples shown as a maximum projection (same as part A) and as a central z-slice. Linescans of microtubule and DNA fluorescence intensity were performed across the chromosome edge and just before the chromosome edge to illustrate that microtubules are primarily laterally associated with chromosomes, as they show opposite peaks. Linescans were also performed using the non-deconvolved images and show a similar trend. Bar = 2.5μm.

microtubule bundles run between individual chromosomes. Moreover, linescans adjacent to the chromosomal surface (Figure 4.3B, “region 2”) displayed the same alternating pattern of microtubule intensity, with low intensity adjacent to the chromosomal surface and high intensity between the chromosomes. To control for microtubule populations that might have been eliminated by the deconvolution process, we performed the same analysis on the original images and observed the same trend. This analysis suggests that lateral bundles running alongside chromosomes are the most prominent microtubule population at this stage, inconsistent with the “pushing on the inside surfaces of chromosomes” model.

**4.D Lateral microtubule bundles are stabilized during anaphase**

Building on these findings, we next used the cold stable assay to assess whether these anaphase lateral bundles represent a stable population of microtubules. Following a 10-minute cold treatment, we observed two major populations of anaphase spindles; spindles at the metaphase to anaphase transition that had clear “end-on” contacts (Fig. 4.4) and mid to late anaphase spindles (Fig. 4.5) with obvious lateral bundles contacting chromosomes.

Upon cold treatment, spindles at the metaphase to anaphase transition/very early anaphase had clear end-on contacts near the kinetochore (Fig. 4.4A). We hypothesize that at this stage, when the spindle shrinks so that pole microtubules come in proximity of the chromosomes, microtubules make transient end-on attachments to kinetochores. These attachments persist in early anaphase but are not present after kinetochores disassemble by the end of early anaphase. We went on to test whether this population of cold-stable microtubules is kinetochore-dependent and found that upon *knl-1(RNAi)* and cold-treatment, spindles at the metaphase to anaphase transition/very early anaphase (these stages are difficult to distinguish so we grouped them together) made up a lesser percentage of the total distribution of stages and images (Fig. 4.4B). Additionally, we found that in images at this stage, the “end-on” microtubule population was greatly reduced upon *knl-1(RNAi)* with and without cold treatment (Fig. 4.4C-E, arrows). Our data suggests that kinetochores make cold-stable, end-on attachments during the metaphase to anaphase transition, despite the lack of end-on attachments prior to this stage.

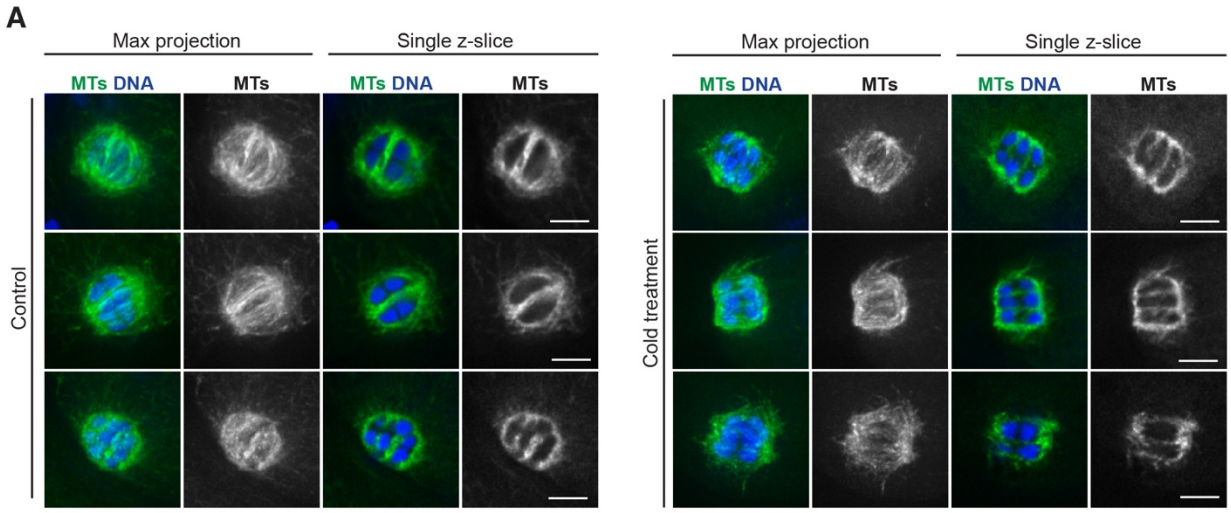
A
Max projection
Single z-slice
Max projection
Single z-slice
MTs DNA
MTs
MTs DNA
MTs
MTs DNA
MTs
MTs DNA
MTs
Control
Cold treatment

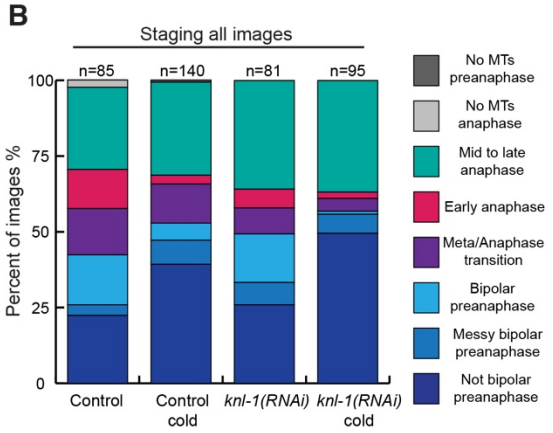
B
Staging all images
n=85
n=140
n=81
n=95
100
75
50
25
0
Percent of images %
Control
Control cold
knl-1(RNAi)
knl-1(RNAi) cold
No MTs preanaphase
No MTs anaphase
Mid to late anaphase
Early anaphase
Meta/Anaphase transition
Bipolar preanaphase
Messy bipolar preanaphase
Not bipolar preanaphase

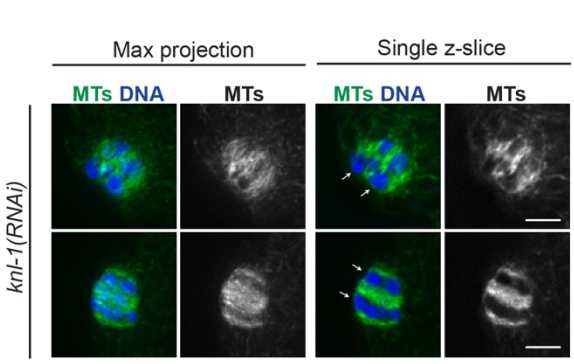
D
Max projection
Single z-slice
MTs DNA
MTs
MTs DNA
MTs
knl-1(RNAi)

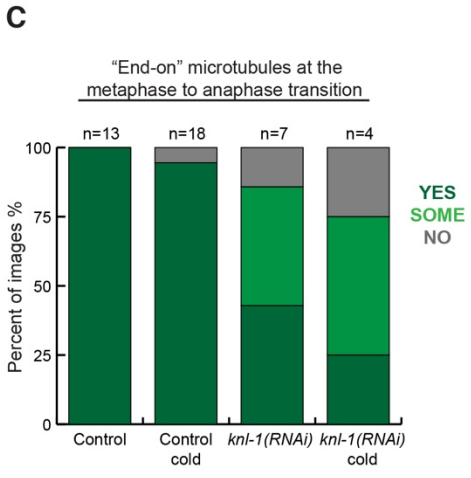
C
"End-on" microtubules at the metaphase to anaphase transition
n=13
n=18
n=7
n=4
100
75
50
25
0
Percent of images %
Control
Control cold
knl-1(RNAi)
knl-1(RNAi) cold
YES
SOME
NO

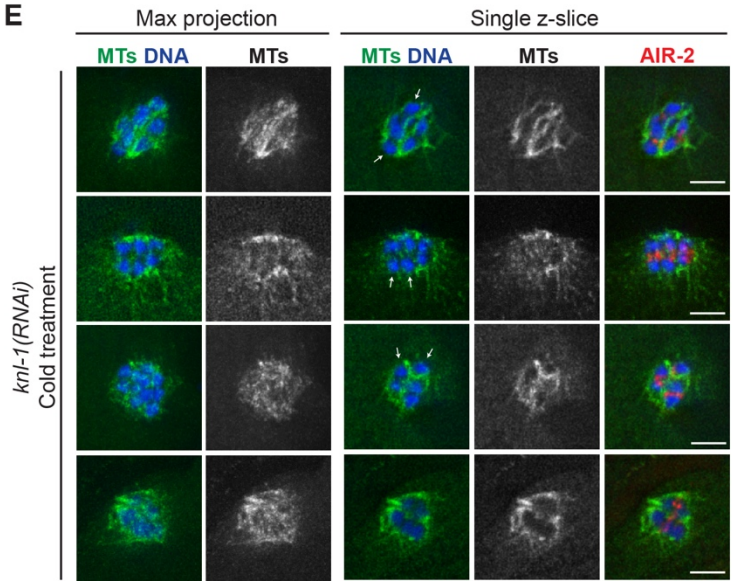
E
Max projection
Single z-slice
MTs DNA
MTs
MTs DNA
MTs
AIR-2
knl-1(RNAi)
Cold treatment

**<u>Figure 4.4 (previous page)</u> End-on microtubule interactions at the metaphase to anaphase transition are cold stable and depend on the kinetochore**
(A)Spindles at the metaphase to anaphase transition stained for DNA (blue) and tubulin (green) after 10 minute control or cold treatment. (B) Graph shows, for each condition, the percent of total images with spindles at the corresponding stage. (C) Graph shows, for each condition, the percentage of spindles at the metaphase to anaphase transition that contain "end-on" chromosome-microtubule contacts. (D) Two examples of spindles at the metaphase to anaphase transition after *knl-1(RNAi)*, stained for DNA (blue) and tubulin (green). Arrows mark chromosome ends with reduced microtubule contacts. (E) The only four examples of spindles at the metaphase to anaphase transition after *knl-1(RNAi)* and 10 minute cold-treatment, stained for DNA (blue), tubulin (green), and AIR-2 (red). Arrows mark chromosome ends with reduced microtubule contacts. Bar = 2.5μm.

Upon cold-treatment, mid to late anaphase spindles had prominent microtubule bundles that ran laterally alongside the chromosomes (Figure 4.5A), demonstrating that these microtubules are stabilized in anaphase and additionally, chromosome-lateral microtubule contacts are cold-stable (95% of anaphase spindles showed clear lateral contacts). We also noticed that these lateral bundles appeared more clearly defined as the microtubule intensity within the channels decreased somewhat following cold treatment (Figure 4.5A). This finding suggests that there could be a less prominent, potentially more dynamic, population of microtubules within the channels that is not cold-resistant.

Given this finding, we decided to assess the localization of factors that have been proposed to contribute to anaphase chromosome separation, to determine whether they are localized to the lateral bundles or to the less stable microtubule population that may be residing between them. First, we examined the CLASP-family protein CLS-2, since this protein has been proposed to stimulate microtubule polymerization in anaphase in both meiosis and mitosis. Although CLS-2 was previously shown to be localized within the anaphase spindle, our imaging clarified that this protein was enriched within the microtubule channels (Figure 4.5B). In addition, following cold treatment CLS-2 was no longer present within the channels and instead became enriched on the cold-resistant lateral microtubule bundles. Together, these findings raise the possibility that CLS-2 may be interacting with an unstable population of microtubules within the channels; therefore, upon depolymerization of these microtubules, this localization is lost. The fact that CLS-2 became prominent on the lateral bundles under these conditions could either mean that CLS-2 is also normally present at low levels in this location, but that this staining is obscured by the much brighter "channel" localization, or it could represent relocalization of CLS-2 to the lateral bundles,

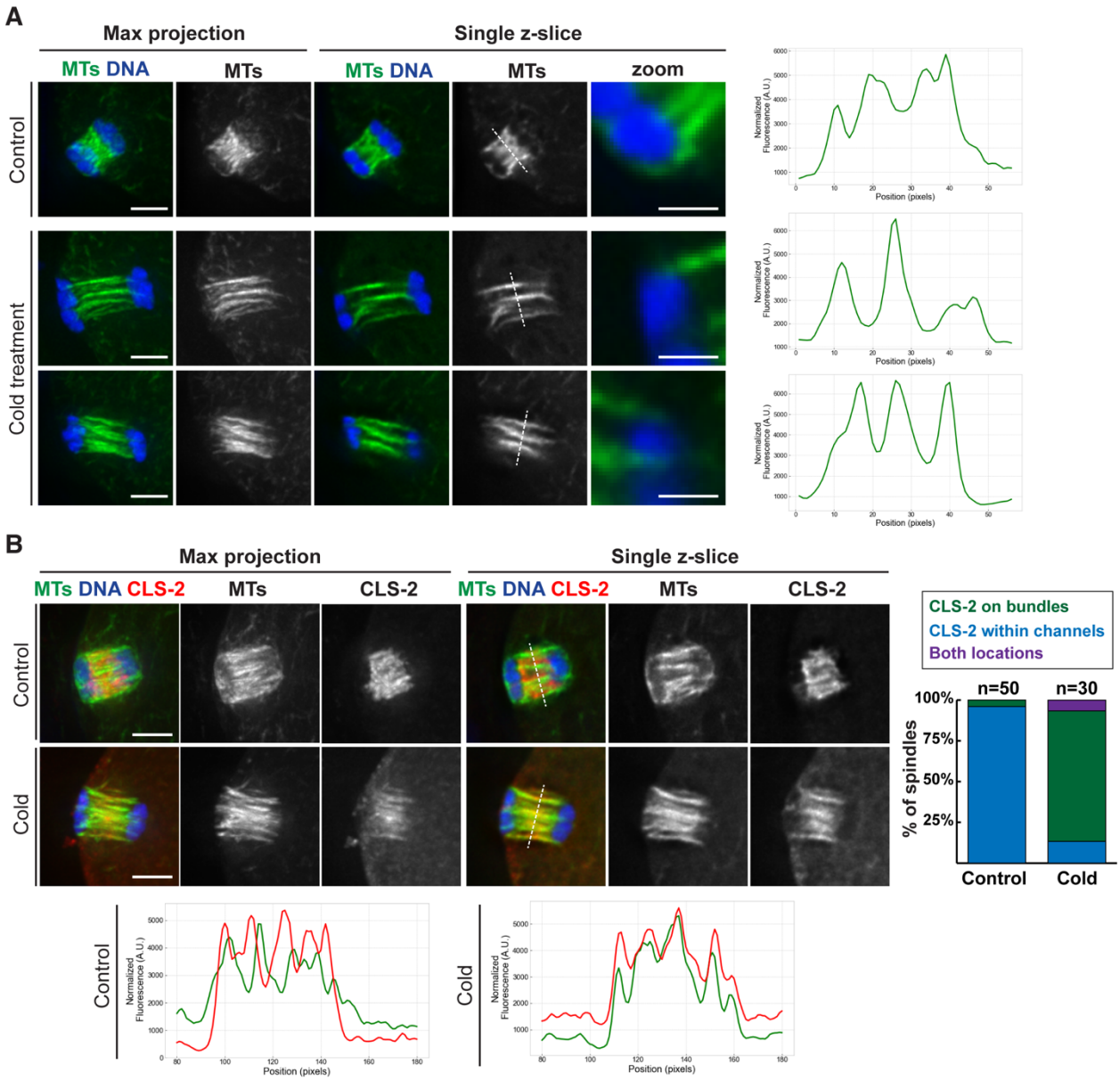


**Figure 4.5 Lateral microtubule bundles represent a stabilized population of anaphase spindle microtubules**

(A) Control versus cold-treated anaphase spindles stained for DNA (blue) and tubulin (green). Zooms illustrate lateral interactions between microtubule bundles and chromosomes. Linescans show the microtubule fluorescence intensity across the center of the spindle of a single z-slice to illustrate the decreased intensity within channels after cold treatment. Bar = 2.5μm for full spindles, and 1μm for zooms. (B) Control versus cold-treated anaphase spindles stained for DNA (blue), tubulin (green), and CLS-2 (red). Maximum projection and single z-slice shown to illustrate the change in localization of CLS-2 from within channels to on microtubule bundles after cold treatment. Quantification of CLS-2 localization before and after cold treatment shown in the graph on the right. Linescans show the microtubule and CLS-2 fluorescence intensity across the center of the spindle of a single z-slice and illustrates the change in localization of CLS-2 between control and cold-treated oocytes. Bar = 2.5μm

in the absence of the labile channel microtubules. Regardless of which of these interpretations is correct, our data demonstrate that CLS-2 is normally enriched within the channels, rather than on the lateral bundles.

Importantly, others in the lab have shown that anaphase midzone proteins that bundle and stabilize microtubules, such as SPD-1, localize to lateral microtubule bundles under control and cold treatment conditions (work of Tim Mullen). These findings suggest that, while CLS-2 may help nucleate an unstable array of microtubules that could in theory provide some force to push on the inside surfaces of chromosomes, the predominant stabilized microtubule array within the anaphase spindle is composed of lateral bundles that run alongside chromosomes.

**4.E Conclusions and discussion**

Taken together, our results reinforce our original proposal that lateral microtubule bundles facilitate this unusual mode of kinetochore-independent chromosome segregation. Lateral bundles are present and stabilized prior to anaphase (Figure 4.1), and these chromosome-microtubule contacts remain in place throughout segregation (Figure 4.3). We propose that first, chromosomes exhibit Anaphase A-like chromosome-to-pole movement along lateral microtubule bundles that appear to form microtubule-poor "channels". Then once the chromosomes reach the poles, they make stable attachments to lateral bundles that are organized by factors such as SPD-1. Next the spindle elongates for "Anaphase B" and this drives the chromosomes further apart, representing the majority of chromosome movement (Figure 4.6A). Importantly, the data presented here demonstrate that lateral chromosome-microtubule associations are in place during this second phase of segregation (Figure 4.3), and that these bundles are stable and cold-resistant at this stage (Figure 4.5).

Notably, our data contradict a model proposing that "microtubule pushing" on the inside surfaces of separating chromosomes provides the force for segregation[153]. This alternate model was supported by 3D reconstructions of anaphase spindles generated using electron tomography, where lateral microtubule interactions were not observed and instead there was a microtubule array that appeared to terminate near the inside surfaces of separating chromosomes. Although it is possible that such a configuration exists once

the chromosomes move out past the ends of the channels in late anaphase/telophase, our demonstration that lateral associations are present during mid anaphase (Figure 4.3) contradicts the view that a switch to an end-on "pushing" configuration drives Anaphase B segregation. One puzzling feature of these reconstructions that may explain our different conclusions is that the chromosomes in their 3D reconstructions at each pole appeared to fuse into one electron-dense mass at each pole, with few microtubules penetrating that region and no significant population of microtubules running between them. In contrast, our imaging demonstrates that this is not the case chromosomes do not merge together and instead microtubules run alongside and create spaces between them (Figure 4.2, 4.3). Therefore, we speculate that these lateral microtubule populations were not resolvable in the electron-dense chromosomal regions when the tomographic reconstructions were generated. This idea is also supported by the intriguing observation that these 3D reconstructions show areas of both high and low microtubule density within the anaphase spindles (visible when they are rotated). We speculate that the high-density regions represent the lateral bundles and that the low-density regions represent the "channels" in between and that, if it had been possible to distinguish individual chromosomes, the lateral bundles would be seen running at least partway alongside them (Fig. 4.6B). This interpretation also makes sense in the context of the specialized meiotic divisions of the oocyte, where there are two sequential rounds of chromosome segregation (MI and MII). Since the chromosomes do not decondense between these two divisions, it is difficult to imagine that it would be advantageous for the oocyte to merge chromosomes together to create a stable "pushing" surface, only to have to immediately de-entangle them in preparation for the second round of division.

The same group also performed functional studies to support the microtubule pushing model[153]. In particular, chromosome segregation halted when the authors ablated microtubules in the center of the spindle, leading them to propose that this blocked the ability of the central array to push on the inside surfaces of chromosomes. In contrast, microtubule ablation on the poleward sides of the chromosomes did not impact segregation. However, our model is also consistent with these findings, as ablation of microtubules in the center of the spindle would block elongation of the lateral bundles, which would halt

Anaphase B segregation. Moreover, our model (Figure 4.6) does not rely on poleward microtubules, but rather emphasize the contribution of lateral associations.

Going forward, it will be important to further probe the mechanisms by which these bundles facilitate segregation. The first outstanding question is what drives Anaphase A chromosome-to-pole movement.

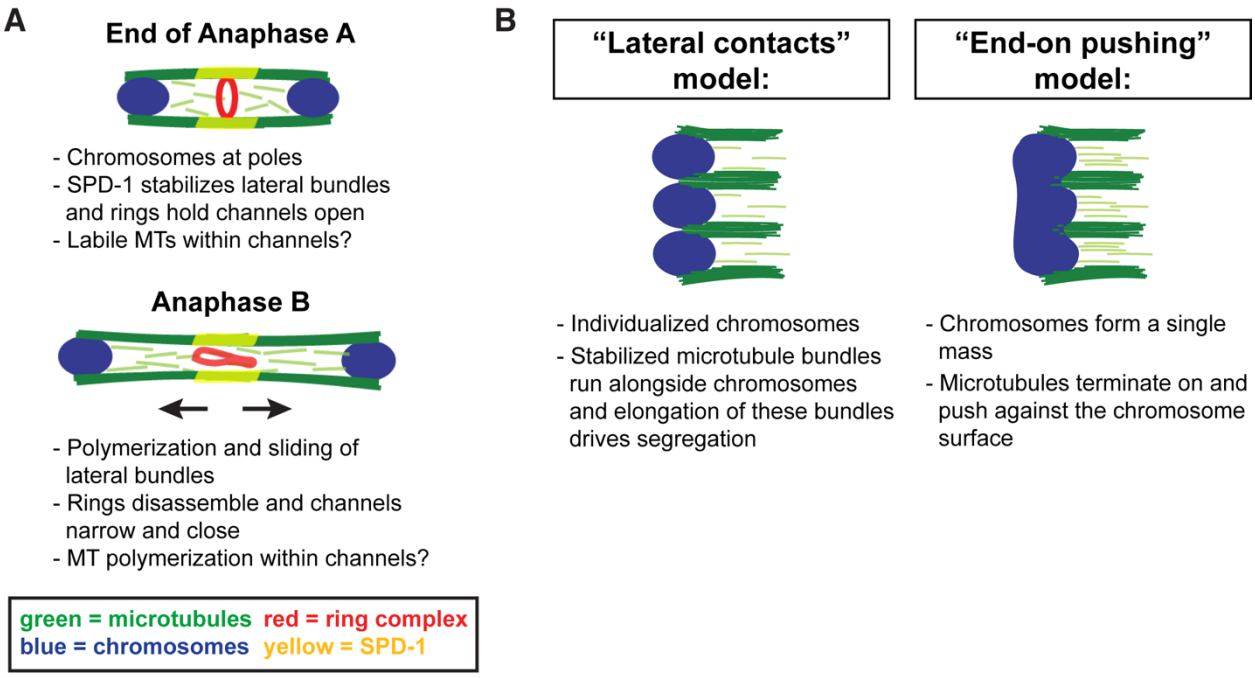


**Figure 4.6 Model for lateral microtubule-mediated chromosomes segregation**
(A) Microtubules (green), chromosomes (blue), RCs (red) and SPD-1 (yellow). At the start of anaphase, the RC is released from chromosomes, releasing plus-end directed forces from the chromosomes and enabling them to move poleward along laterally-associated microtubules ("Anaphase A"); during this time there may also be a more minor population of microtubules within the channels and SPD-1 and other factors stabilize the lateral bundles. After chromosomes reach the spindle poles, polymerization and sliding of the lateral bundles drives Anaphase B spindle elongation. (B) Diagrams aimed at reconciling our findings with those of Laband *et al*[153] who proposed that microtubule pushing drives chromosome segregation in oocytes. Our data suggest that chromosomes are individualized in anaphase, with microtubules running alongside and between individual chromosomes (the "Lateral contacts" model, a single slice through the spindle is diagrammed on the left). In this diagram, the dark green represents microtubules in the stabilized lateral bundles, and the light green represents the labile microtubules that may be present within the channels. In contrast, Laband and colleagues proposed that a population of microtubule terminates on the chromosome surface (the "Microtubule pushing" model). In their 3D EM reconstructions, the chromosomes appeared to merge into a single chromosome mass. This feature of the reconstruction may make it difficult to resolve the lateral contacts that we observe between microtubules and individual chromosomes, making it appear as if the lateral bundles terminate on and push against the chromosome surface (diagrammed on the right).

Our lab previously proposed a lateral-bundle mediated mode of chromosome segregation where dynein was hypothesized to be a possible contributor, by providing minus-end directed forces to move chromosomes along the lateral bundles.[39] This was based on functional studies using temperature sensitive strains that resulted in segregation defects as well as localization studies with what appeared to be a population of dynein on chromosomes. However, we now appreciate that dynein is not concentrated on chromosomes and is instead on the spindle pole microtubules during anaphase (Fig. 4.7); these locations are close together and therefore were difficult to distinguish in the original study. Thus, dynein is unlikely to be a major driver of segregation, although it is still possible that a minor chromosomal population could contribute to the short-range movements that occur during Anaphase A. A second potential mechanism involves a contribution from end-on attachments; since we found that microtubules that associate with the poleward surfaces of chromosomes at the metaphase-to-anaphase transition are cold-stable and depend on the kinetochore (Figure 4.4). Although kinetochore depletion does not affect the chromosome segregation rate[27], kinetochores may contribute to Anaphase A, which accounts for only a small percent of total segregation distance. Finally, Anaphase B could in principle be driven by maintaining lateral chromosome-microtubule contacts near the minus ends of the microtubules and then elongating the lateral bundles. This idea is similar in concept to a model proposing that chromosomes become tethered to a crosslinked network of microtubules and pole proteins, which keeps the chromosomes connected to the poles as the spindle elongates. However, since we did not find evidence for a stabilized population of “pole” microtubules near the ends of chromosomes in mid to late anaphase during our cold stable assay (Figure 4.5), we think that chromosomes are more likely to be associated with the lateral bundles.

We have shown that SPD-1 and the minus-end-directed kinesins KLP-15/16 act redundantly to bundle anaphase spindle microtubules and that when these factors are depleted chromosome segregation fails[32]. Given that these factors localize to the lateral bundles (Figure 4C), they likely play an important role in stabilizing these bundles to enable Anaphase B spindle elongation. Additionally, since the doublecortin family protein ZYG-8, a protein that promotes microtubule polymerization, has been shown to be required for Anaphase B chromosome separation[38], we predict that ZYG-8 facilitates elongation of the lateral bundles. Finally, since CLS-2 depletion impairs chromosome segregation and since the lateral bundles

have been proposed to be a tiled array of shorter microtubules stitched together by bundling factors, it is possible that CLS-2 promotes the assembly of microtubules within the channels that are then incorporated into the lateral bundles to help them elongate[27, 153]. In summary, our results support a model where lateral microtubule bundles are a crucial feature of the segregation mechanism during both Anaphase A and B (Figure 4.6). Future studies further elucidating their precise contributions will therefore increase our understanding of chromosome segregation during this important specialized form of cell division.

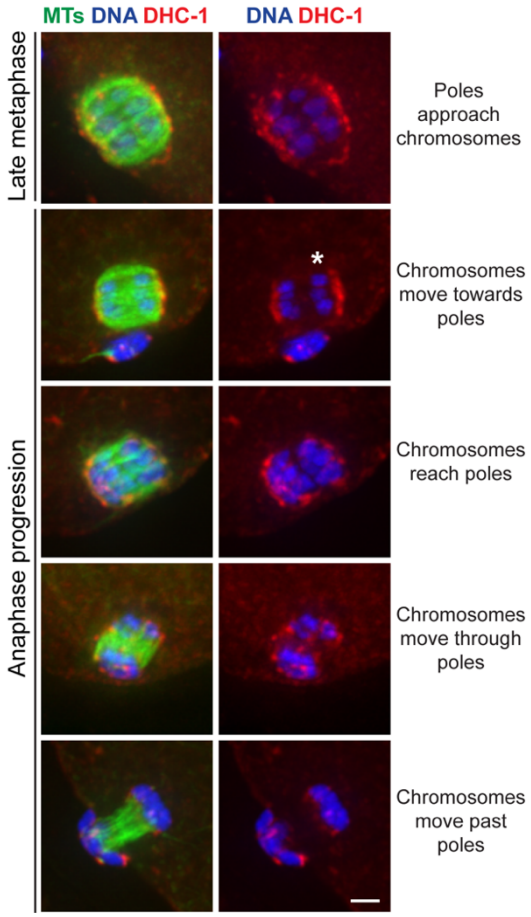


**Figure 4.7 Dynein is localized to pole microtubules until mid anaphase**
Spindles stained for DNA (blue), tubulin (green), and DHC-1 (red). In late metaphase the spindle shrinks so that poles are in close proximity to the chromosomes. Then chromosomes move towards the poles, enter the pole region, and finally move past the majority of the pole staining. During most of these phases, dynein localizes near the outside surfaces of separating chromosomes, in the vicinity of spindle poles. When poles and chromosomes are not adjacent (asterisk), dynein clearly displays greater pole enrichment. Bar = 2μm.

# CHAPTER 5:

## Final conclusions and future directions

**5.A Summary of findings**

It is remarkable that evolution has come up with such elegant and distinct ways to use an established set of regulatory and cell division proteins, and I believe that we have learned an immense amount by studying the fundamental cell biology involved in *C. elegans* meiosis. Our studies have revealed novel forms of error-detection, protein complex regulation, and spindle organization, and illustrate the value in studying organisms that utilize unique cell biology mechanisms. Taken together, this body of work contributes to the general understanding of how mitotic and meiotic processes are executed and regulated.

In Chapter 2, we revealed a novel form of pre-anaphase error-detection in the *C. elegans* oocyte that requires the kinetochore despite a lack of canonical end-on kinetochore attachments during metaphase. This error-sensing mechanism delays many aspects of normal anaphase progression, including RC disassembly, kinetochore disassembly, and microtubule reorganization. We believe that this reflects an effort to keep Anaphase A chromosome segregation mechanisms on while Anaphase B mechanisms, namely spindle elongation, proceeds. This may allow lagging chromosomes a better chance of reaching a spindle pole to either be retained or extruded into a polar body. This work encourages further study of novel error detection methods in cells in which SAC does not play an obvious role.

In Chapter 3, we showed that SUMOylation, deSUMOylation, and the enzymes involved in the SUMO pathway play important roles throughout many stages of *C. elegans* oocyte meiosis, including RC assembly, maintenance, and adhesion to chromosomes during prometaphase, RC release from chromatin at anaphase onset, RC chromatin-independent stability in early anaphase, and finally, RC disassembly during mid anaphase. This work illustrates that SUMO modification is a useful strategy in assembling, rearranging, and disassembling an intricate protein complex, which in the case of the RC occurs twice within a span of 30 minutes. Our findings illuminate the importance of studying this post-translational modification in dynamic cellular processes such as cell division.

In Chapter 4, we revisited the existence of lateral microtubule bundles and demonstrated that they are in fact a cold-stable population. This means that during metaphase and anaphase chromosomes form stable interactions with lateral bundles, and this is potentially a key interaction for chromosome segregation. We propose that because anaphase chromosome-microtubule contacts are cold-stable, elongation of

lateral microtubule bundles drives chromosome segregation by pushing chromosomes outward. Intriguingly, we also found that at the metaphase to anaphase transition, when the spindle shrinks and the pole microtubules come in contact with kinetochores, these microtubules are cold-stable and this depends on the kinetochore. This suggests that this transition may involve canonical end-on kinetochore attachments, and this shapes our hypothesis for how error-detection may be sensed at this stage.

In conclusion, we have revealed new insights into mechanisms aiding in meiotic anaphase progression. Our data suggest that this rapid cell division is extremely complex and involves many changing protein-protein interactions, but the oocyte has elegant strategies in place to accomplish these. Further studies are necessary to determine the mechanistic details of how the oocyte carries out error-sensing, RC regulation, and chromosome segregation.

### 5.B Future Directions

These findings invoke three major follow-up questions. First, how are errors sensed and how is that signal propagated to the spindle? Second, what proteins are involved in chromosome segregation during Anaphase A, Anaphase B, and the switch between these two stages? And finally, which specific proteins in the RC are SUMOylated and how are these modifications regulated?

#### 5.B.1 Error-sensing during oocyte meiosis

The error-detection mechanism operating in *C. elegans* oocytes only senses errors occurring prior to anaphase, requires the kinetochore to do this, and can sense univalents which lack RCs (Chapter 2). We also know that the spindle shrinks at the very end of metaphase, the microtubule-kinetochore contacts made at this stage are cold-stable and depend on the kinetochore (Chapter 4), and the bivalent and kinetochore transiently stretch at this time[38]. Finally, we know that when the kinetochores are retained throughout mid anaphase during an error-response, so are the microtubules that appear to make end-on attachments (Chapter 2). Thus, I hypothesize that the cell senses errors through tension across the bivalent via transient end-on kinetochore attachments that appear to occur at the metaphase to anaphase transition. Although we do not know whether the kinetochores are required for the sensing or the propagation of the

signal, our data is consistent with a role in either.

To begin to test a kinetochore-tension-mediated response, we must first establish that a kinetochore-microtubule attachment is in fact occurring at the metaphase to anaphase transition. Because Aurora B is known to phosphorylate kinetochore proteins to inhibit microtubule binding, it would be interesting to see if those same sites are phosphorylated up until the end of metaphase to prevent end-on attachments until that point. We could use phospho-specific antibodies to test whether these marks are present throughout prometaphase, correlated with the absence of end-on attachments, and then present during the transition to anaphase, representing a functional change in the kinetochore. We could also implement experiments in which the kinetochore is present, but is not able to make attachments, potentially through mutation of key sites in NDC-80. Using these kinetochore mutants or depletions, we could perform a cold stable assay to test whether microtubules on chromosome ends are still present at the metaphase to anaphase transition in the absence of functional kinetochores after cold treatment, as well as whether the error response still occurs without functional kinetochores. We could also film the worms (expressing fluorescently tagged DNA) to measure whether the observed “bivalent stretch” still occurs at this transition without kinetochores. Finally, end-on kinetochore attachments could be further confirmed by detailed analysis of microtubules at the metaphase to anaphase transition using electron tomography. This established method would allow us to film oocytes until they reach metaphase, then quickly transfer them to be frozen for electron tomography and analysis of microtubule attachments at chromosome ends[154]. It would also be important to consider throughout all of these experiments that kinetochores may be using lateral attachments to sense proper tension across the bivalent. When bivalents reach the center of the metaphase spindle, the kinetochores could sense tension due to the fact that they have reached the overlap zone, where microtubules emanating from each pole now make contact with the lateral part of the kinetochore. Some of the previously mentioned experiments should distinguish between the two models. For example, the inhibitory phosphorylation marks on the kinetochore would probably not be present or would not change. Additionally, if lateral associations mediate tension-sensing we could use the cold stable assay to see if lateral contacts in late metaphase change upon kinetochore depletion.

During the error-detection mechanism, the kinetochore must relay the information to generate a global response. This means that all bivalents, RCs, kinetochores, and microtubule structures are affected, suggesting that an error signal could be relayed through some cytoplasmic-cycling factor that transiently interacts with the kinetochore at anaphase onset (similar to MAD-2) or responds to an intrinsic change that occurs upon proper tension. While pursuing the analysis in Chapter 2, we did not test MAD-2's involvement in this response, as reagents were not available at the time and we were under time pressure to resubmit my revised manuscript for publication, so we focused on other SAC components. However, this may be a useful starting point for future projects. Although if involved, it would function entirely different from canonical SAC, as MAD-1 and MAD-3 are not required for the error-response. To investigate this, we would generate a strain with fluorescently labeled MAD-2 and microtubules so that we could film the localization and dynamics of MAD-2 in the presence and absence of an error response. Because an error-response seems to occur in less than 50% of the oocytes, we would also need to include a fluorescently labeled AIR-2 to distinguish an error-response from normal anaphase. (An error response would be denoted by a delay in AIR-2 relocalization to the anaphase microtubules.) This would be a useful strategy for investigating any potentially cycling, chromatin-associated protein involved in the error-response.

In the *C. elegans* meiosis field we have just bits and pieces of information on the cell cycle regulators and the kinases and phosphatases antagonizing one another in the system. I think that a large screen investigating these types of proteins would be highly valuable in order to determine what proteins are involved in error-detection. This would involve depletion of candidate proteins within a strain expressing fluorescently labeled AIR-2 and microtubules so that we could visualize a delay (or lack thereof) by assessing the timing of AIR-2 relocalization across spindle microtubules in anaphase spindles. We could induce an error-response by using a 30°C heated stage on the microscope (five minutes is sufficient) and quickly screening through the anesthetized worms to find depletion conditions where AIR-2 relocalization is normal. That would suggest that the depleted candidate protein is necessary for the error-response. This screen should include proteins that are already thought to be involved in meiotic progression, such as CDK-1 and the three Cyclin B isoforms, kinases like BUB-1 that localize to both the kinetochore and the RC and could potentially mediate the communication between these structures, and phosphatases such as PLK-1

and PP1, already known to be involved in anaphase progression. The error signal could also be propagated to a chromatin-associated factor; therefore, it would be useful to screen through chromatin-associated proteins. Because many of these proteins are important for various aspects of development and meiotic entry, partial RNAi or small molecular inhibitors may be more useful than full knockdown. Once the candidate list has been narrowed down, further analysis using CRISPR-generated mutant and auxin-inducible degron strains will be essential to analyze meiosis specific roles in error-detection.

**5.B.2 The error-response and chromosome segregation mechanisms**

The error-response induces many changes to normal anaphase progression, including a delay in kinetochore disassembly, RC disassembly, and microtubule channel collapse. We propose that the cell responds to error by keeping Anaphase A mechanisms on while Anaphase B spindle elongation occurs. Therefore, another aspect of investigation will be uncovering the mechanism by which the cell prevents Anaphase A from turning off. We know that PP1 becomes enriched on chromosomes during early anaphase and that its depletion (via MEL-28 depletion) causes an Anaphase A arrest. This suggests that PP1 promotes the switch to Anaphase B. Therefore, it will be important to screen through the extensive, validated lists of PP1 substrates for meiotic candidates; there are at least 100 known substrates in mammals[155, 156]. If PP1 dephosphorylation activates a spindle elongation factor during anaphase, then depletion of PP1's substrate should result in a similar phenotype as PP1 depletion - an early anaphase arrest. This will be easily identifiable in a live imaging screen where GFP:tubulin/GFP:histone worms are anesthetized and imaged on an 8-well slide. Normally, early anaphase I is a hard stage to catch, so an early anaphase arrest will be obvious.

We also know that ZYG-8 is essential for spindle elongation during anaphase in the oocyte, so this would be a useful starting point as a protein regulated by PP1. But first it will be important to determine ZYG-8 localization during anaphase, as PP1 is enriched on chromosomes and ZYG-8 seems to elongate spindle microtubules. I hypothesize that ZYG-8 will be exclusively localized to lateral bundles, like SPD-1 and centralspindlin (this will be an important piece of evidence that elongation of these bundles in particular is what drives segregation), and that this localization may be influenced by PP1 dephosphorylation. Thus,

we should test whether ZYG-8 is able to localize to microtubules after PP1 (or MEL-28) depletion. We will also have to consider how PP1 and ZYG-8 come in contact with one another; FRAP of GFP:PP1 could help us determine the dynamics of PP1 and whether cycling off the chromosomes is possible. In any case, it will be useful to investigate the relationship between PP1 and ZYG-8; I hypothesize that PP1 may activate ZYG-8 through dephosphorylation. Recombinant *C. elegans* PP1 is commercially available so the direct interaction with ZYG-8 could be easily tested *in vitro* first before pursuing any CRISPR-generated mutations. (We could also look into an interaction between recombinant PP1 and CLS-2, which I have already made and is also thought to be involved in microtubule polymerization during spindle elongation[27, 153].) Even if PP1 does not directly dephosphorylate ZYG-8 or CLS-2, the immense amount of literature on PP1 substrates should lead us to the protein directly involved in the switch between Anaphase A and Anaphase B. Once we have identified factors regulating the switch from Anaphase A to Anaphase B we can formally test whether the error-response signals to these factors and how the whole process is regulated.

During the error-response, Anaphase A mechanisms appear to stay “on” rather than being “turned off” for spindle elongation, but we don’t know what these mechanisms are. We do know that minus-end forces are important for segregation[39] and that kinetochores do not appear to contribute[27]. However, when the “kinetochore-independent chromosome segregation” study was performed it was not known that there were two distinct stages and rates of chromosomes segregation[27], and the relatively short period of Anaphase A may have been overlooked. Therefore, it would be useful to screen through candidates including kinetochore components and proteins involved in microtubule minus-end movements, to see if they are involved in Anaphase A segregation. We can deplete these candidates in a ZYG-8 depletion background and use fixed or live imaging to screen for segregation defects. If we deplete a protein essential for Anaphase A segregation and we’ve blocked spindle elongation by ZYG-8 depletion, the chromosomes should not segregate at all and the phenotype will be quite obvious. Of course, more subtle defects will need to be filmed in order to obtain the rate of segregation during the early stages of anaphase.

It will also be important to investigate Anaphase B mechanisms of segregation. We now appreciate that the centralspindlin complex, KLP-15/16, and SPD-1 stabilize lateral bundles[32] while ZYG-8 and

potentially CLS-2 polymerize lateral bundles to drive segregation[38, 153]. We do not know, however, how chromosomes are anchored to lateral bundles. This is an interesting question because at this point in anaphase, the kinetochores and the RCs are not present on chromosomes. Therefore, we need to look at other chromosome-associated proteins that persist through anaphase. These include the chromosomal populations of KLP-19 and MCAK (Appendix A and [30]), the katanin proteins MEI-1/2[31], and nuclear pore proteins that localize to chromosomes after NEBD[151]. This should be fairly easy to identify now that we have established a cold stable assay. If the "anchor protein" is depleted, we should not observe lateral microtubule bundles contacting chromosomes after a ten-minute cold treatment. If we can successfully identify which chromatin associated factor binds lateral microtubules, then we can test our hypothesis that the chromosomes are simply anchored to the ends of elongating lateral bundles and that is what drives chromosome segregation during Anaphase B.

Finally, many of these questions may be answered if we look at the ubiquitination pathway during meiosis. In addition to phosphorylation state changes, many transitions during mitosis involve ubiquitin-mediated degradation of proteins. In our system, transitions from metaphase to anaphase, switches between segregation mechanisms, and protein complex disassembly processes likely involve this as well. Preliminary experiments from Nikita Divekar show that this mark is faintly localized to the RCs prior to anaphase, so this is definitely an area worth exploring.

Taken together, our analysis of anaphase progression in *C. elegans* oocytes has opened up many further areas of investigation. The next steps involve creating lists of candidate proteins that may contribute to the error-sensing or propagating mechanism as well as Anaphase A and B segregation and regulation mechanisms. These candidate lists should include kinetochore/centromeric proteins, any known chromatin-associated protein, all cell-cycle regulators, and all mitotic/meiotic kinases and phosphatases. We need to identify the key players involved before more complicated questions can be pursued. It will also be particularly interesting to take what we've learned from *C. elegans* and apply to it questions in other systems. For example, it is clear from the literature that mammalian oocytes have distinct features of spindle organization and checkpoint mechanisms from mammalian mitotic cells and therefore, it is worth investigating whether these oocytes use mechanisms similar to *C. elegans*. We have already learned that

spindle assembly mechanisms appear similar between human oocytes and *C. elegans* oocytes, both of which not only lack centrioles, but also lack MTOCs (microtubule organizing centers)[28, 157]. We also know that mouse oocytes establish lateral microtubule bundles before kinetochore attachments are made in metaphase and after they are released in anaphase (unpublished data from Carissa Heath), suggesting that these microtubules may be functionally relevant, similar to *C. elegans* lateral bundles. Finally, although mammalian oocytes appear to use the spindle assembly checkpoint proteins in a more canonical fashion as compared to *C. elegans* oocytes, studies have shown that mammalian oocytes are more reliant on these proteins in a wildtype setting as compared to mammalian mitotic cells[73, 76]. This is reminiscent of our results in Chapter 2 in which depletion of SAC proteins induced an "error response". For these reasons, it is important that we continue to investigate seemingly unique features of *C. elegans* oocyte meiosis.

**5.B.3 SUMO-mediated RC regulation**

Another important point of future investigation will be determining the exact substrates in the RC that are SUMOylated and which specific deSUMOylation event or events drives RC disassembly. As a starting point, we should compare a list of predicted meiotic SUMO substrates to the mass spectrometry screens that have identified hundreds of SUMO-conjugated proteins in *C. elegans*[101]. We can also generate hypotheses from the SUMOylation assays I have already performed (Chapter 3 and Appendix B). Once we have a candidate list, one way to determine meiotic SUMO substrates is through more careful imaging techniques, by directly comparing candidates to SUMO using super-resolution microscopy to see if they overlap or using Proximity Ligation Assays to determine whether the two proteins are within 30-40nm of one another. Western Blotting may also be useful strategy in order to deplete SUMO or SUMO enzymes and probe for RC proteins to see if there are changes in molecular weight. Furthermore, it would be very interesting to use the auxin-inducible degron tag on SUMO itself. Then, we could rapidly degrade the modification while it is covalently linked to SUMO substrates, presumably causing those proteins to be degraded as well. The resulting phenotype may lead us to a particular meiotic protein, or alternatively, we can use imaging techniques to screen through RC proteins and look for an absence in signal upon SUMO degradation. Finally, CRISPR will be a powerful technique in understanding how SUMO modifications and

interactions influence RC proteins by simply mutating predicted (or validated by mass spectrometry) SUMO consensus motifs or SIMs. Of course, once we begin to understand more about SUMOylation in the oocyte, we can then ask the ultimate question of how SUMO-mediated regulation is specifically linked to the error-sensing mechanism.

Another area of investigation will be the understanding how these marks are regulated, i.e. how substrate specificity by the conjugating and deconjugating enzymes is achieved. We speculate that there is a link between AIR-2 or BUB-1 activity and the SUMO pathway. Because phosphorylation is known to regulate SUMOylation[90-92], we hypothesize that these kinases may phosphorylate RC components or the enzymes themselves to promote or prevent SUMOylation or deSUMOylation. Alternatively, SUMOylation may regulate kinase activity or the substrate's ability to be phosphorylated. We can begin to test this by combining the SUMOylation and deSUMOylation *in vitro* assays that I have already established in the lab with AIR-2 and BUB-1 kinase assays. We can use mass spectrometry to identify the modified residues and use CRISPR to generate phosphomimetic or non-phosphorylatable strains to see how this affects the SUMO signal on the RC and SUMO-dependent aspects of meiotic progression.

The SUMOylation field is relatively new, but it has become increasingly obvious that cycles of SUMOylation and deSUMOylation play a significant role in dynamic cellular processes and regulating protein complexes across all eukaryotes. The next stage of discovery will be piecing together identified SUMO substrates with the function of the modification and vice versa. It will be particularly beneficial for scientists to be mindful of SUMO research in fields completely different from their own because we can gain insight into how SUMOylation is regulated by studying any cell type or organism. It will also be important for Ubiquitin/SUMO chemists and cell biologists to communicate with one another to create novel techniques for characterizing these sometimes extremely transient modifications. In summary, SUMO-mediated cell division is an exciting new field, and there is much to be explored and discovered.

**5.C Final remarks**

We have made considerable progress in understanding the fundamental principles underlying cell division since Walther Flemming first peered into his microscope to observe the elegant process of mitosis

[158]. We have reached a point where scientists are digging deep into the mechanistic details of protein-protein interactions, comparing and contrasting protein relationships between organisms and cell types, and attempting to understand how these very particular details affect the overall process of spindle assembly, chromosome congression, and segregation. And this complements the work of other researchers, who focus on understanding systems in which these processes do not function in a canonical fashion. Beyond the pure sake of knowledge, both approaches are extremely valuable and have contributed extensively to clinical research efforts in cancer treatment and female fertility.

Although we have identified what appears to be most of the key players in cell division and we understand generally how they contribute to the system as a whole, as Albert Einstein once warned us, the more we learn the more we realize how much we don't know. In the coming decades, I think that cell biologists will start to piece together exactly what interactions, conformational changes, and modifications at the individual protein level allow for the intricacies of cell division. These investigations will help to answer key questions about cancer cell division and female meiosis. Namely, how do these cell types sense error? Why is error-detection so ineffective in cancer cells and oocytes? Why is chromosome segregation so inherently error-prone in these cells? And finally, how do SUMO modifications influence all of this?

Beyond scientific curiosity, our science is generally done in the name of human health, and I think it is extremely important that we continue to look beyond the "more important" mammalian systems. Given that *C. elegans* generally contain all of the same players as humans, I am optimistic that studies like mine will inspire scientists to think outside of the box and generate novel hypotheses for solving medically relevant problems.

# CHAPTER 6:

# Materials and Methods

**Antibody Purification Protocol**

BIR-1, CSC-1, KLP-19 (stalk and motor domain constructs), MCAK(neck-head), and CLS-2 antibodies were purified using the following protocol.

Protein-Affigel Coupling: Thaw 10mLs of resuspended Affigel and add it to the vacuum filter set-up. Wash with 50mLs of 100% cold ETOH, then 50mLs of 50% cold ETOH, then 50mLs of cold dH20. Add 5mLs of 5% ethylene diamine (dissolved in dH20) and place Affigel into a conical and incubate at room temperature for 15 minutes. Place Affigel back into the filter set-up and wash with 100mLs of cold dH20, then 50mLs of cold 0.1M NaPi pH 7.8, then in the dark, resuspend Affigel in 10mLs of cold 0.1M NaPi pH 7.8. Add 35mg 1AA-NHS dissolved in DMSO to the tube and incubate at room temperature for 10 minutes. Add contents of the conical back into the filter set-up and wash with 400mLs of cold 0.1M NaPi pH 7.8. Resuspend in cold 0.1M NaPi pH 7.8 to make a 50% slurry and add ~7mg of protein to the Affigel. Cover the conical in aluminum foil and rotate at 4C overnight. On day 2, place Affigel back into the filter set-up and wash Affigel in the following order: 50mLs of 0.1M $NaHCO_3$, 50mLs of 1M $Na_2CO_3$, 50mLs of dH20, 50mLs of 0.2M Glycine pH 2.0, 50mLs of 150mM NaCl, 50mLs of 1x TBS, 50mLs of 6M Guanidine-HCl (dissolved in TBS). Resuspend gel into 10mLs of TBS+0.1%$NaN_3$ in a 15mL conical and store at 4C.

Affinity Purification: Equilibrate the column containing the Affigel by washing with 20mLs of 1x TBS. Dilute 10mLs of serum 1:1 in TBS. Filter diluted serum using a 0.2um syringe filter into a clean 50mL falcon tube and keep on ice. Pass filtered serum over the column 3 times. Wash column with 25mLs of 1x TBS, then with 25mLs of 20mM Tris-HCl pH 7.4, 0.5M NaCl, 0.2% Triton-X100, then again with 25mLs of 1x TBS. Set up 20 1.5mL of eppendorf tubes each containing 50ul 2M Tris-HCl pH 8.5. Pass 10mLs of 0.2M Glycine-HCl pH 2.0, 150mM NaCl over column and collect 0.5 mL factions. Wash column with 25mLs of 1X TBS and pass 10mLs of 1X TBS+ 1.0% azide. Dialyze antibody overnight in cold, sterile-filtered TBS.

**Auxin-inducible degron experiments**

Auxin was diluted in M9 to 1mM from a 400mM stock solution on the day of the experiment. Worms were picked into a drop of 1mM auxin (or M9 for control experiments) and incubated in a humidity chamber at

15°C for 20, 30, or 45 minutes. Worms were then cut and prepared for immunofluorescence as described above.

**Cold stable assay**

Experiments were done in N2 and EU1067 worms. Worms were picked into a drop of either 15°C (control) or ice cold (cold treatment) buffer (both M9 and L15 egg media were used) on poly-l-lysine slides and then cut to release oocytes. Slides were then incubated at either 15°C (control) in a humidity chamber or directly on ice (cold treatment) for 10 minutes. Slides were then prepared for immunofluorescence as described above.

**Determining anaphase stages**

This analysis was primarily performed for Figure 2.2 as well as any further investigation requiring anaphase staging. We analyzed 246 anaphase spindles noting whether AIR-2 was relocalized across the microtubules or concentrated in RCs (colocalized with another RC marker and within open microtubule channels). We then measured the chromosome segregation distance for all anaphase spindles and looked for the chromosome distance at which AIR-2 had relocalized to the microtubules in most spindles. The 246 spindles analyzed includes both anaphase I and II spindles, as well as both N2 worms and EU1067, as the trends for chromosome distance and AIR-2 behavior were indistinguishable between these groups. We defined 2.5μm as roughly the transition from early to mid anaphase: the segregation distance at which AIR-2 should be relocalized in most wild-type spindles. All images labeled as mid anaphase, as well as all spindles quantified in Figure 2.1C, Figure 2.3D, Figure 2.5C, and Figure 2.7B have a chromosome distance of at least 2.5μm. The spindle lengths at late anaphase were variable, so rather than using a specific chromosome distance, this stage was defined by the microtubules being severely collapsed and the chromosomes being significantly past the poles. Late anaphase spindles were excluded from all quantifications in Figure 2.1C, Figure 2.3D, Figure 2.5C, and Figure 2.7B.

**Image analysis for chromosome segregation distances**

Imaris 3D Imaging Software (Bitplane) was used for chromosome distance and spindle width measurements. To calculate chromosome distances, the "Surfaces" tool was first used to determine the volume of each grouping of separating chromosomes, and then to assign the center of the volume for each set. The distance between these two center points was then measured as the chromosome segregation distance. For some conditions with severe chromosome segregation defects (e.g. the *zim-1* mutant or centralspindlin RNAi in MII), we could not accurately determine chromosome distance measurements for all spindles, since it was difficult to assign the chromosomes to two distinct groups. Therefore, these spindles were excluded from our analysis in Chapter 2. Note that this may result in an under-representation of the percentage of spindles with AIR-2 in RCs (data presented in Figures 2.1 and 2.3) for some of the mutant conditions, since AIR-2 was often RC-associated in these severely defective spindles.

**Image analysis for spindle width**

Imaris 3D Imaging Software (Bitplane) was used to determine spindle width measurements shown in Figure 2.4. Images were viewed in the slice gallery, and a line was drawn across the width of the microtubule signal at the center of the spindle. This was done for 3 z-slices within each spindle, and the line lengths were averaged to obtain a spindle width measurement.

**Immunofluorescence**

Immunofluorescence was performed as previously described[25]. by picking worms into a drop of M9 buffer on poly-L-lysine slides and then cutting them with a needle to release oocytes. A coverslip was placed on top, the slide was frozen in liquid nitrogen for 5-10 minutes, and then the coverslip was quickly removed. Embryos were fixed for 40-45 minutes in -20°C methanol, rehydrated in PBS (2x, 5-minute wash), and blocked in AbDil (PBS plus 4% BSA, 0.1% Triton X-100, 0.02% Sodium azide) for 30 minutes to an hour at room temperature. Primary antibodies were diluted in AbDil and incubated either on the bench for 1-2 hours or overnight at 4°C. Secondary antibodies were diluted in AbDil and incubated for 1-2 hours at room temperature. Hoechst 33342 (Invitrogen) was diluted 1:1000 in PBST (PBS + 0.1% Triton X-100) and

incubated for 10-15 minutes at room temperature. Slides were washed with PBST between antibody incubations and mounted in 0.5% p-phenylenediamine in 90% glycerol, 20mM Tris, pH 8.8 and sealed with nail polish.

**Immunofluorescence antibodies**

rabbit anti-AIR-2 (1:1000; gift from Jill Schumacher)

rat anti-AIR-2 (1:1000) *

rabbit anti-BIR-1 (1:500)**

rabbit anti-BUB-1 (1:1500)**

rabbit anti-CLS-2 (1:2000)**

rabbit anti-CSC-1 (1:800)**

rabbit anti-GEI-17 (1:600; gift from Ronald Hay)

mouse anti-GFP (1:200; Abcam)

rabbit anti-KLP-19motor (1:900)**

rabbit ant-KLP-19stalk (1:2500)**

rabbit anti-KNL-3 (1:3800; gift from Arshad Desai)

rabbit anti-MCAK (NH) 1:200**

rabbit anti-MDF-1 (1:3000; a gift from Risa Kitagawa)

mouse anti-MPM-2 (1:500; Millipore)

rabbit anti-SEP-1 (1:350; gift from Andy Golden)

mouse anti-SUMO (1:500; gift from Ronald Hay)

mouse anti-α-tubulin-FITC (1:500; Sigma)

sheep anti-UBC-9 (1:800; gift from Ronald Hay)

rabbit anti-ULP-1 (1:350; gift from Ronald Hay)

rabbit anti-ULP-4 (1:300 or 1:1500; gift from Ronald Hay)

Alexa-fluor 488, 555 and 647- conjugated secondary antibodies (1:500; Invitrogen)

*Rat anti-AIR-2 was generated by Covance using the C-terminal peptide sequence KIRAEKQQKIEKEASLRNH (synthesized by the Peptide Synthesis Core Facility at Northwestern University).

** Proteins were made recombinantly in house. Antibodies were generated by Covance in rabbits. Serum was affinity purified (protocol above).

**Microscopy**

All imaging was performed on a DeltaVision Core deconvolution microscope with a 100x objective (NA = 1.4) (Applied Precision). This microscope is housed in the Northwestern Biological Imaging Facility supported by the NU Office for Research. Slides were imaged at room temperature and image stacks were obtained at 0.2μm z-steps and deconvolved (ratio method, 15 cycles) using SoftWoRx (Applied Precision). All images in this study were displayed as full maximum intensity projections of data stacks encompassing the entire spindle structure unless otherwise noted. Although sometimes the displayed maximum projection image does not accurately show the number of RCs/chromosomes present since structures from different z-stacks can appear to merge, for our RC quantifications we analyzed the entire z-stack, examining RC staining separately (in grayscale) and also together (as a merge) in order to accurately count and make claims about these structures.

**Protein Purification**

His-tagged SMO-1, UBC-9, and GEI-17 were purified using previously published methods [135] except that after Ni resin purification the proteins were loaded onto a size-exclusion column (AKTA prime plus, HiLoad 16/600 Superdex 200pg), and the protein was collected and concentrated. ULP-1 catalytic domain ("ULP-1 CD", aa 470-697) and a longer fragment of ULP-1 (aa 284-697) were made by cloning the corresponding nucleotide sequence into a 6x his-tagged modified pET vector. The two proteins were purified following previously published methods for the ULP-4 catalytic domain[133].

GST-AIR-2, GST-BIR-1, GST-CSC-1, GST-CLS-2, GST-MCAK(neck-head domain), GST-KLP-19 (amino acids 371-1084), and GST were made using the pGEX-6P-1 vector, and by transforming into BL21

DE3 pLysS Escherichia coli cells. Cultures were induced with 0.2mM-1mM IPTG and grown overnight at 16-20°C. After harvesting, cells were resuspended in a buffer containing protease inhibitors and 1x PBS, 10mM EGTA, 10mM EDTA, 1mM PMSF, 0.1% Tween, and 250mM NaCl, lysed by sonication, centrifuged for 40 minutes at 11,000K, and the supernatant was rotated with GST resin for 1.5-2 hours. The proteins were purified using a batch method, by rotating for 10-minutes in 1X PBS, 250mM NaCl, 0.1% Tween 20, 1mM PMSF, and 1mM DTT and spinning resin down at 2100rpm. Resin was washed 3x using a buffer containing 1x PBS, 250mM NaCl, 1mM DTT, 1mM PMSF, and 0.1% Tween. Protein was eluted using a buffer containing 50mM Tris pH 8.1, 10mM reduced glutathione, and 75mM KCl and concentrated.

**Quantification of cold stable images**

Preanaphase spindle images were categorized by eye into four groups based on microtubule density surrounding the chromosomes. Group 1 represents images with few to no microtubules. Group 2 represents images with some microtubules. Group 3 represents images with just less than wild-type microtubules. Group 4 represents images with wild-type microtubules. Images were also categorized by whether chromosomes had lateral microtubule contacts. “Mostly lateral” means that 4 or more chromosomes had clear lateral contacts. “Some lateral” means that between 2-3 chromosomes had clear lateral contacts. “Randomly oriented” means that lateral bundles were not clear for any number of chromosomes. “All around chromosomes” means that short microtubules appeared fuzzy but in contact with all sides of the chromosomes.

**RNAi**

Feeding RNAi was performed as previously described[159]. Individual RNAi clones were picked from a feeding library and grown overnight at 37°C in LB with 100µg/ml ampicillin. Overnight cultures were spun down, plated on NGM (nematode growth media) plates containing 100µg/ml ampicillin and 1mM IPTG, and dried overnight. Worms were synchronized by bleaching gravid adults and hatching isolated eggs overnight without food. For full RNAi (*klp-19, capg-1, ani-1, aspm-1, mdf-1, san-1, ulp-1, ulp-2, ulp-4, ulp-5, mel-28* and all double depletions), synchronized L1s were plated on RNAi plates and grown to adulthood at 15° for

4-5 days. When full RNAi prevented proper germline formation or global SUMOylation, partial RNAi was performed (*knl-1, knl-3, cyk-4, zen-4, bub-1, ulp-1, and gei-17*). For these depletions, worms were grown until the L2-L4 stage on regular NGM/OP50 plates and then transferred to the RNAi plate 24-72 hours before preparing for immunofluorescence.

**Statistical methods**

For all p-values reported, all data points for a given condition were compared with the control data points using a two-tailed t test. Data distribution was assumed to be normal, but this was not formally tested.

**Strains**

Throughout this dissertation "wild-type" refers to conditions tested in both N2 and EU1067 worms. "Control" refers to the RNAi vector control in the corresponding worm strain. All strains used are listed below.

**BN426:** (bq5[GFP::mel-28]) III

**CA1215:** dhc-1(ie28[dhc-1::degron::GFP]) I, ieSi38 [sun-1p::TIR1::mRuby::sun-1 3'UTR + Cbr-unc-119(+)]IV

**CA151:** *him-8(me4) IV*

**CA324:** *zim-1(tm1813) IV*

**EU1067:** unc-119(ed3) ruIs32[unc-119(+) pie-1promoter::GFP::H2B] III; ruIs57[unc-119(+) pie-1promoter::GFP::tubulin]

**FGP8:** unc-119(ed3) ruIs32[unc-119(+) pie-1promoter::GFP::H2B] III; fgpIs20[pFGP79; pie-1promoter::mCherry::smo-1(GG) unc-119(+)]

**FGP29:** gei-17(fgp1[GFP::FLAG::degron::loxP::gei17]) I; ieSi38[sun-1promoter::TIR1::mRuby::sun-1 3'UTR + Cbr-unc-119(+)] IV

**FM13:** *mei-2(ct98) I*; *ruIs57 [pAZ147: pie-1$^{promoter}$::tubulin::GFP; unc-119 (+)]; itIs37 [unc-119(+) pie-1$^{promoter}$::mCherry::H2B]; him-8(e1489) IV*

**N2**

**RB1391:** *san-1(ok1580) I*

**SA141:** tjIs8 [pie-1p::GFP::ebp-1 + unc-119(+)]

**SMW6:** strain EU1067 crossed with strain CA151 resulting in: *unc-119(ed3) ruIs32 [unc-119(+) pie-1$^{promoter}$::GFP::H2B] III; ruIs57 [unc-119(+) pie-1$^{promoter}$::GFP::tubulin]; him-8(me4) IV*

**SMW23:** fgpls [(pFGP79) pie-1p::mcherry::smo-1(GG) + unc-119(+)]; ojls50 [pie-1p::GFP::air-2 + unc-119(+)]

**VC2773:** *bub-3(ok3437) II*

**SUMO intensity experiments**

SMW23 worms were grown at 15°C for optimal RNAi efficiency but transferred to 25°C 16 hours prior to the experiment for optimal mCherry::SUMO(GG) expression. SMW23 worms were picked into a 10µl drop of 15°C M9 on a slide, and then the M9 was wicked away. A 10µl drop of 100% ethanol was placed on the worms, the drop was evaporated, and this was repeated twice. The slide was mounted using a solution of 50% diluted Hoechst (1:1000 in M9) and 50% mounting media (0.5% p-phenylenediamine in 90% glycerol, 20mM Tris, pH 8.8). Slides were imaged within 48 hours of preparation. Every repetition had its own control performed and imaged at the same time. Only MI images were collected. Images were deconvolved, and a sum projection was made from 11 slices encompassing an entire ring structure. One to three ring structures (individual sum projections) were used per image, with the limitation being that a single ring had to be completely separable from others. A 22x20 pixel box was drawn around an area encompassing the AIR-2 or SUMO ring, and the mCherry::SUMO(GG) and GFP::AIR-2 intensity of that area was recorded. The final SUMO and AIR-2 intensity values were then calculated by subtracting a 22x20 square of background SUMO or AIR-2 intensity from the ring SUMO or AIR-2 intensity.

**SUMOylation and deSUMOylation assays**

SUMOylation reactions in Figure 3.8 were performed using 2mM ATP, 5µg his-SMO-1, 200nM his-UBC-9, 12.5 or 50nM his-GEI-17, and 100ng of SAE1/SAE2 (Boston Biochem). 1µg of substrate protein

(GST, GST-AIR-2, or GST-KLP-19) was used for each reaction. First, the SUMOylation reactions were performed in 50mM TrisHCl pH7.5 containing 5mM DTT, 5mM MgCl2, and incubated for 4 hours at 37°C. Then, deSUMOylation assays were performed by adding 1.0μM his-ULP-1 CD or his-ULP-1(aa284-697) directly to the SUMOylation reaction that had incubated for 4 hours. We incubated the deSUMOylation reaction at 37°C for an additional hour. SUMOylation reactions in Appendix B were performed using 2mM ATP, 5μg his-SMO-1, 100nM, 500nM, or 1uM his-UBC-9, and 100ng of SAE1/SAE2 (Boston Biochem). No GEI-17 was added. 1μg of substrate protein (GST, GST-AIR-2, or GST-KLP-19) was used for each reaction. Reactions were incubated for 4 hours in 50mM TrisHCl pH7.5 containing 5mM DTT, 5mM MgCl2, at 37°C. Then, deSUMOylation assays were performed by adding 1.0μM his-ULP-1 CD directly to the SUMOylation reaction incubated at 37°C for 6.5 hours. The following antibody concentrations were used for Western blotting: mouse anti-SMO-1 (1:10,000), rat anti-AIR-2 (1:5000), and rabbit anti-GST (1:200) (Santa Cruz), rabbit anti-KLP-19 (stalk) (1:5000), rabbit anti-CSC-1 (1:5000), rabbit anti-BIR-1 (1:5000), rabbit anti-MCAK(NH) (1:5000), rabbit anti-CLS-2 (1:10000), HRP anti-mouse secondary (1:5000), HRP anti-rabbit secondary (1:5000).

**Temperature experiments for error response**

EU1067 worms were picked into a drop of M9 pre-incubated at specific temperatures (4°C, 25°C, or 30°C), then incubated for 4-5 minutes at the corresponding temperature, and prepared for immunofluorescence. The total time of incubation in M9 at a given temperature was approximately 10-15 minutes due to the picking and cutting steps. Note that this assay is also sensitive to the temperature of the room, as we have noticed a moderate increase in the number of control spindles with AIR-2 remaining in RCs on days where the ambient temperature is higher. To ensure that this day-to-day variation did not significantly affect our conclusions, we controlled for temperature as closely as we could, and we made sure that each of our quantified conditions incorporated slides generated on multiple days.

**Worm lysate western blots**

Ninety adult worms were picked onto empty plates, washed, and spun down in cold M9 twice. The M9 was reduced to approximately 20uL, 20uL of 2x SDS sample buffer was added to the worms, and the worms were boiled for 10 minutes. The 40uL of lysate was run in a single lane. Westerns were probed with the following antibodies: rabbit anti-BUB-1(1:10000), mouse anti-tubulin (1:5000, loading control), HRP anti-mouse secondary (1:5000), HRP anti-rabbit secondary (1:5000)

# CHAPTER 7:

# References

1. Ohkura, H. Meiosis: an overview of key differences from mitosis. *Cold Spring Harb Perspect Biol* **7** (2015).
2. Nogales, E. An electron microscopy journey in the study of microtubule structure and dynamics. *Protein Sci* **24**, 1912-1919 (2015).
3. Akhmanova, A. & Steinmetz, M.O. Control of microtubule organization and dynamics: two ends in the limelight. *Nat Rev Mol Cell Biol* **16**, 711-726 (2015).
4. Bornens, M. The centrosome in cells and organisms. *Science* **335**, 422-426 (2012).
5. Marston, A.L. & Amon, A. Meiosis: cell-cycle controls shuffle and deal. *Nat Rev Mol Cell Biol* **5**, 983-997 (2004).
6. Cheeseman, I.M. The kinetochore. *Cold Spring Harb Perspect Biol* **6**, a015826 (2014).
7. Burrack, L.S. & Berman, J. Flexibility of centromere and kinetochore structures. *Trends Genet* **28**, 204-212 (2012).
8. Szollosi, D., Calarco, P. & Donahue, R.P. Absence of centrioles in the first and second meiotic spindles of mouse oocytes. *J Cell Sci* **11**, 521-541 (1972).
9. Hunt, P.A. & Hassold, T.J. Sex matters in meiosis. *Science* **296**, 2181-2183 (2002).
10. Bennabi, I., Terret, M.E. & Verlhac, M.H. Meiotic spindle assembly and chromosome segregation in oocytes. *J Cell Biol* **215**, 611-619 (2016).
11. Hassold, T. & Hunt, P. To err (meiotically) is human: the genesis of human aneuploidy. *Nat Rev Genet* **2**, 280-291 (2001).
12. Lagirand-Cantaloube, J. *et al.* Loss of Centromere Cohesion in Aneuploid Human Oocytes Correlates with Decreased Kinetochore Localization of the Sac Proteins Bub1 and Bubr1. *Sci Rep* **7**, 44001 (2017).
13. Herbert, M., Kalleas, D., Cooney, D., Lamb, M. & Lister, L. Meiosis and maternal aging: insights from aneuploid oocytes and trisomy births. *Cold Spring Harb Perspect Biol* **7**, a017970 (2015).
14. Chiang, T., Duncan, F.E., Schindler, K., Schultz, R.M. & Lampson, M.A. Evidence that weakened centromere cohesion is a leading cause of age-related aneuploidy in oocytes. *Curr Biol* **20**, 1522-1528 (2010).

15. Liu, L. & Keefe, D.L. Defective cohesin is associated with age-dependent misaligned chromosomes in oocytes. *Reprod Biomed Online* **16**, 103-112 (2008).

16. Lister, L.M. *et al.* Age-related meiotic segregation errors in mammalian oocytes are preceded by depletion of cohesin and Sgo2. *Curr Biol* **20**, 1511-1521 (2010).

17. Hillers, K.J. & Villeneuve, A.M. Chromosome-wide control of meiotic crossing over in C. elegans. *Curr Biol* **13**, 1641-1647 (2003).

18. Schvarzstein, M., Wignall, S.M. & Villeneuve, A.M. Coordinating cohesion, co-orientation, and congression during meiosis: lessons from holocentric chromosomes. *Genes Dev* **24**, 219-228 (2010).

19. Ferrandiz, N. *et al.* Spatiotemporal regulation of Aurora B recruitment ensures release of cohesion during C. elegans oocyte meiosis. *Nat Commun* **9**, 834 (2018).

20. Severson, A.F. & Meyer, B.J. Divergent kleisin subunits of cohesin specify mechanisms to tether and release meiotic chromosomes. *Elife* **3**, e03467 (2014).

21. Rogers, E., Bishop, J.D., Waddle, J.A., Schumacher, J.M. & Lin, R. The aurora kinase AIR-2 functions in the release of chromosome cohesion in Caenorhabditis elegans meiosis. *J Cell Biol* **157**, 219-229 (2002).

22. Steiner, F.A. & Henikoff, S. Holocentromeres are dispersed point centromeres localized at transcription factor hotspots. *Elife* **3**, e02025 (2014).

23. Monen, J., Maddox, P.S., Hyndman, F., Oegema, K. & Desai, A. Differential role of CENP-A in the segregation of holocentric C. elegans chromosomes during meiosis and mitosis. *Nat Cell Biol* **7**, 1248-1255 (2005).

24. Desai, A. *et al.* KNL-1 directs assembly of the microtubule-binding interface of the kinetochore in C. elegans. *Genes Dev* **17**, 2421-2435 (2003).

25. Oegema, K., Desai, A., Rybina, S., Kirkham, M. & Hyman, A.A. Functional analysis of kinetochore assembly in Caenorhabditis elegans. *J Cell Biol* **153**, 1209-1226 (2001).

26. Cheeseman, I.M. *et al.* A conserved protein network controls assembly of the outer kinetochore and its ability to sustain tension. *Genes Dev* **18**, 2255-2268 (2004).

27. Dumont, J., Oegema, K. & Desai, A. A kinetochore-independent mechanism drives anaphase chromosome separation during acentrosomal meiosis. *Nat Cell Biol* **12**, 894-901 (2010).

28. Wolff, I.D., Tran, M.V., Mullen, T.J., Villeneuve, A.M. & Wignall, S.M. Assembly of Caenorhabditis elegans acentrosomal spindles occurs without evident microtubule-organizing centers and requires microtubule sorting by KLP-18/kinesin-12 and MESP-1. *Mol Biol Cell* **27**, 3122-3131 (2016).

29. Askjaer, P., Galy, V., Hannak, E. & Mattaj, I.W. Ran GTPase cycle and importins alpha and beta are essential for spindle formation and nuclear envelope assembly in living Caenorhabditis elegans embryos. *Mol Biol Cell* **13**, 4355-4370 (2002).

30. Connolly, A.A., Sugioka, K., Chuang, C.H., Lowry, J.B. & Bowerman, B. KLP-7 acts through the Ndc80 complex to limit pole number in C. elegans oocyte meiotic spindle assembly. *J Cell Biol* **210**, 917-932 (2015).

31. Srayko, M., Buster, D.W., Bazirgan, O.A., McNally, F.J. & Mains, P.E. MEI-1/MEI-2 katanin-like microtubule severing activity is required for Caenorhabditis elegans meiosis. *Genes Dev* **14**, 1072-1084 (2000).

32. Mullen, T.J. & Wignall, S.M. Interplay between microtubule bundling and sorting factors ensures acentriolar spindle stability during C. elegans oocyte meiosis. *PLoS Genet* **13**, e1006986 (2017).

33. Yang, H.Y., Mains, P.E. & McNally, F.J. Kinesin-1 mediates translocation of the meiotic spindle to the oocyte cortex through KCA-1, a novel cargo adapter. *J Cell Biol* **169**, 447-457 (2005).

34. Sumiyoshi, E., Fukata, Y., Namai, S. & Sugimoto, A. Caenorhabditis elegans Aurora A kinase is required for the formation of spindle microtubules in female meiosis. *Mol Biol Cell* **26**, 4187-4196 (2015).

35. Wignall, S.M. & Villeneuve, A.M. Lateral microtubule bundles promote chromosome alignment during acentrosomal oocyte meiosis. *Nat Cell Biol* **11**, 839-844 (2009).

36. van der Voet, M. *et al.* NuMA-related LIN-5, ASPM-1, calmodulin and dynein promote meiotic spindle rotation independently of cortical LIN-5/GPR/Galpha. *Nat Cell Biol* **11**, 269-277 (2009).

37. Ellefson, M.L. & McNally, F.J. CDK-1 inhibits meiotic spindle shortening and dynein-dependent spindle rotation in C. elegans. *J Cell Biol* **193**, 1229-1244 (2011).

38. McNally, K.P., Panzica, M.T., Kim, T., Cortes, D.B. & McNally, F.J. A novel chromosome segregation mechanism during female meiosis. *Mol Biol Cell* **27**, 2576-2589 (2016).

39. Muscat, C.C., Torre-Santiago, K.M., Tran, M.V., Powers, J.A. & Wignall, S.M. Kinetochore-independent chromosome segregation driven by lateral microtubule bundles. *Elife* **4**, e06462 (2015).

40. Csankovszki, G. *et al.* Three distinct condensin complexes control C. elegans chromosome dynamics. *Curr Biol* **19**, 9-19 (2009).

41. Romano, A. *et al.* CSC-1: a subunit of the Aurora B kinase complex that binds to the survivin-like protein BIR-1 and the incenp-like protein ICP-1. *J Cell Biol* **161**, 229-236 (2003).

42. Schumacher, J.M., Golden, A. & Donovan, P.J. AIR-2: An Aurora/Ipl1-related protein kinase associated with chromosomes and midbody microtubules is required for polar body extrusion and cytokinesis in Caenorhabditis elegans embryos. *J Cell Biol* **143**, 1635-1646 (1998).

43. Speliotes, E.K., Uren, A., Vaux, D. & Horvitz, H.R. The survivin-like C. elegans BIR-1 protein acts with the Aurora-like kinase AIR-2 to affect chromosomes and the spindle midzone. *Mol Cell* **6**, 211-223 (2000).

44. de Carvalho, C.E. *et al.* LAB-1 antagonizes the Aurora B kinase in C. elegans. *Genes Dev* **22**, 2869-2885 (2008).

45. Pelisch, F. *et al.* A SUMO-Dependent Protein Network Regulates Chromosome Congression during Oocyte Meiosis. *Mol Cell* **65**, 66-77 (2017).

46. Davis-Roca, A.C., Muscat, C.C. & Wignall, S.M. Caenorhabditis elegans oocytes detect meiotic errors in the absence of canonical end-on kinetochore attachments. *J Cell Biol* **216**, 1243-1253 (2017).

47. Carmena, M., Wheelock, M., Funabiki, H. & Earnshaw, W.C. The chromosomal passenger complex (CPC): from easy rider to the godfather of mitosis. *Nat Rev Mol Cell Biol* **13**, 789-803 (2012).

48. Kelly, A.E. *et al.* Survivin reads phosphorylated histone H3 threonine 3 to activate the mitotic kinase Aurora B. *Science* **330**, 235-239 (2010).

49. Wang, F. *et al.* Histone H3 Thr-3 phosphorylation by Haspin positions Aurora B at centromeres in mitosis. *Science* **330**, 231-235 (2010).

50. Liu, X. *et al.* Chromatin protein HP1 interacts with the mitotic regulator borealin protein and specifies the centromere localization of the chromosomal passenger complex. *J Biol Chem* **289**, 20638-20649 (2014).

51. Bishop, J.D. & Schumacher, J.M. Phosphorylation of the carboxyl terminus of inner centromere protein (INCENP) by the Aurora B Kinase stimulates Aurora B kinase activity. *J Biol Chem* **277**, 27577-27580 (2002).

52. Mackay, A.M., Eckley, D.M., Chue, C. & Earnshaw, W.C. Molecular analysis of the INCENPs (inner centromere proteins): separate domains are required for association with microtubules during interphase and with the central spindle during anaphase. *J Cell Biol* **123**, 373-385 (1993).

53. Collette, K.S., Petty, E.L., Golenberg, N., Bembenek, J.N. & Csankovszki, G. Different roles for Aurora B in condensin targeting during mitosis and meiosis. *J Cell Sci* **124**, 3684-3694 (2011).

54. Cheeseman, I.M., Chappie, J.S., Wilson-Kubalek, E.M. & Desai, A. The conserved KMN network constitutes the core microtubule-binding site of the kinetochore. *Cell* **127**, 983-997 (2006).

55. Ciferri, C. *et al.* Implications for kinetochore-microtubule attachment from the structure of an engineered Ndc80 complex. *Cell* **133**, 427-439 (2008).

56. Knowlton, A.L., Lan, W. & Stukenberg, P.T. Aurora B is enriched at merotelic attachment sites, where it regulates MCAK. *Curr Biol* **16**, 1705-1710 (2006).

57. Welburn, J.P. *et al.* Aurora B phosphorylates spatially distinct targets to differentially regulate the kinetochore-microtubule interface. *Mol Cell* **38**, 383-392 (2010).

58. Guse, A., Mishima, M. & Glotzer, M. Phosphorylation of ZEN-4/MKLP1 by aurora B regulates completion of cytokinesis. *Curr Biol* **15**, 778-786 (2005).

59. Uehara, R. *et al.* Aurora B and Kif2A control microtubule length for assembly of a functional central spindle during anaphase. *J Cell Biol* **202**, 623-636 (2013).

60. Nunes Bastos, R. *et al.* Aurora B suppresses microtubule dynamics and limits central spindle size by locally activating KIF4A. *J Cell Biol* **202**, 605-621 (2013).

61. Zimniak, T. *et al.* Spatiotemporal regulation of Ipl1/Aurora activity by direct Cdk1 phosphorylation. *Curr Biol* **22**, 787-793 (2012).

62. Hummer, S. & Mayer, T.U. Cdk1 negatively regulates midzone localization of the mitotic kinesin Mklp2 and the chromosomal passenger complex. *Curr Biol* **19**, 607-612 (2009).

63. Kitagawa, M. *et al.* Cdk1 coordinates timely activation of MKlp2 kinesin with relocation of the chromosome passenger complex for cytokinesis. *Cell Rep* **7**, 166-179 (2014).

64. Cormier, A., Drubin, D.G. & Barnes, G. Phosphorylation regulates kinase and microtubule binding activities of the budding yeast chromosomal passenger complex in vitro. *J Biol Chem* **288**, 23203-23211 (2013).

65. Lara-Gonzalez, P., Westhorpe, F.G. & Taylor, S.S. The spindle assembly checkpoint. *Curr Biol* **22**, R966-980 (2012).

66. Musacchio, A. & Salmon, E.D. The spindle-assembly checkpoint in space and time. *Nat Rev Mol Cell Biol* **8**, 379-393 (2007).

67. De Antoni, A. *et al.* The Mad1/Mad2 complex as a template for Mad2 activation in the spindle assembly checkpoint. *Curr Biol* **15**, 214-225 (2005).

68. Cimini, D. *et al.* Merotelic kinetochore orientation is a major mechanism of aneuploidy in mitotic mammalian tissue cells. *J Cell Biol* **153**, 517-527 (2001).

69. Liu, D., Vader, G., Vromans, M.J., Lampson, M.A. & Lens, S.M. Sensing chromosome bi-orientation by spatial separation of aurora B kinase from kinetochore substrates. *Science* **323**, 1350-1353 (2009).

70. Akiyoshi, B. *et al.* Tension directly stabilizes reconstituted kinetochore-microtubule attachments. *Nature* **468**, 576-579 (2010).

71. Krenn, V. & Musacchio, A. The Aurora B Kinase in Chromosome Bi-Orientation and Spindle Checkpoint Signaling. *Front Oncol* **5**, 225 (2015).

72. Touati, S.A. *et al.* Mouse oocytes depend on BubR1 for proper chromosome segregation but not for prophase I arrest. *Nat Commun* **6**, 6946 (2015).

73. Shonn, M.A., McCarroll, R. & Murray, A.W. Requirement of the spindle checkpoint for proper chromosome segregation in budding yeast meiosis. *Science* **289**, 300-303 (2000).

74. Gilliland, W.D., Wayson, S.M. & Hawley, R.S. The meiotic defects of mutants in the Drosophila mps1 gene reveal a critical role of Mps1 in the segregation of achiasmate homologs. *Curr Biol* **15**, 672-677 (2005).

75. Marston, A.L. & Wassmann, K. Multiple Duties for Spindle Assembly Checkpoint Kinases in Meiosis. *Front Cell Dev Biol* **5**, 109 (2017).

76. Wassmann, K., Niault, T. & Maro, B. Metaphase I arrest upon activation of the Mad2-dependent spindle checkpoint in mouse oocytes. *Curr Biol* **13**, 1596-1608 (2003).

77. Kolano, A., Brunet, S., Silk, A.D., Cleveland, D.W. & Verlhac, M.H. Error-prone mammalian female meiosis from silencing the spindle assembly checkpoint without normal interkinetochore tension. *Proc Natl Acad Sci U S A* **109**, E1858-1867 (2012).

78. Galli, M. & Morgan, D.O. Cell Size Determines the Strength of the Spindle Assembly Checkpoint during Embryonic Development. *Dev Cell* **36**, 344-352 (2016).

79. Yoshida, S., Kaido, M. & Kitajima, T.S. Inherent Instability of Correct Kinetochore-Microtubule Attachments during Meiosis I in Oocytes. *Dev Cell* **33**, 589-602 (2015).

80. Norden, C. *et al.* The NoCut pathway links completion of cytokinesis to spindle midzone function to prevent chromosome breakage. *Cell* **125**, 85-98 (2006).

81. Mendoza, M. *et al.* A mechanism for chromosome segregation sensing by the NoCut checkpoint. *Nat Cell Biol* **11**, 477-483 (2009).

82. Steigemann, P. *et al.* Aurora B-mediated abscission checkpoint protects against tetraploidization. *Cell* **136**, 473-484 (2009).

83. Carlton, J.G., Caballe, A., Agromayor, M., Kloc, M. & Martin-Serrano, J. ESCRT-III governs the Aurora B-mediated abscission checkpoint through CHMP4C. *Science* **336**, 220-225 (2012).

84. Bembenek, J.N., Verbrugghe, K.J., Khanikar, J., Csankovszki, G. & Chan, R.C. Condensin and the spindle midzone prevent cytokinesis failure induced by chromatin bridges in C. elegans embryos. *Curr Biol* **23**, 937-946 (2013).

85. Biggins, S., Bhalla, N., Chang, A., Smith, D.L. & Murray, A.W. Genes involved in sister chromatid separation and segregation in the budding yeast Saccharomyces cerevisiae. *Genetics* **159**, 453-470 (2001).

86. Meluh, P.B. & Koshland, D. Evidence that the MIF2 gene of Saccharomyces cerevisiae encodes a centromere protein with homology to the mammalian centromere protein CENP-C. *Mol Biol Cell* **6**, 793-807 (1995).

87. Surana, P., Gowda, C.M., Tripathi, V., Broday, L. & Das, R. Structural and functional analysis of SMO-1, the SUMO homolog in Caenorhabditis elegans. *PLoS One* **12**, e0186622 (2017).

88. Li, S.J. & Hochstrasser, M. A new protease required for cell-cycle progression in yeast. *Nature* **398**, 246-251 (1999).

89. Johnson, E.S. Protein modification by SUMO. *Annu Rev Biochem* **73**, 355-382 (2004).

90. Zhao, Q. *et al.* GPS-SUMO: a tool for the prediction of sumoylation sites and SUMO-interaction motifs. *Nucleic Acids Res* **42**, W325-330 (2014).

91. Beauclair, G., Bridier-Nahmias, A., Zagury, J.F., Saib, A. & Zamborlini, A. JASSA: a comprehensive tool for prediction of SUMOylation sites and SIMs. *Bioinformatics* **31**, 3483-3491 (2015).

92. Hickey, C.M., Wilson, N.R. & Hochstrasser, M. Function and regulation of SUMO proteases. *Nat Rev Mol Cell Biol* **13**, 755-766 (2012).

93. Baldwin, M.L., Julius, J.A., Tang, X., Wang, Y. & Bachant, J. The yeast SUMO isopeptidase Smt4/Ulp2 and the polo kinase Cdc5 act in an opposing fashion to regulate sumoylation in mitosis and cohesion at centromeres. *Cell Cycle* **8**, 3406-3419 (2009).

94. Klein, U.R., Haindl, M., Nigg, E.A. & Muller, S. RanBP2 and SENP3 function in a mitotic SUMO2/3 conjugation-deconjugation cycle on Borealin. *Mol Biol Cell* **20**, 410-418 (2009).

95. Feligioni, M.M., Serena & Knock, Erin & Nadeem, Urooba & Arancio, Ottavio & E Fraser, Paul SUMO modulation of protein aggregation and degradation. *AIMS Molecular Science* **2**, 382-410 (2015).

96. Kerscher, O. SUMO junction-what's your function? New insights through SUMO-interacting motifs. *EMBO Rep* **8**, 550-555 (2007).

97. Prudden, J. *et al.* SUMO-targeted ubiquitin ligases in genome stability. *EMBO J* **26**, 4089-4101 (2007).

98. Mukhopadhyay, D., Arnaoutov, A. & Dasso, M. The SUMO protease SENP6 is essential for inner kinetochore assembly. *J Cell Biol* **188**, 681-692 (2010).

99. Fraser, A.G. *et al.* Functional genomic analysis of C. elegans chromosome I by systematic RNA interference. *Nature* **408**, 325-330 (2000).

100. Jones, D., Crowe, E., Stevens, T.A. & Candido, E.P. Functional and phylogenetic analysis of the ubiquitylation system in Caenorhabditis elegans: ubiquitin-conjugating enzymes, ubiquitin-activating enzymes, and ubiquitin-like proteins. *Genome Biol* **3**, RESEARCH0002 (2002).

101. Drabikowski, K. *et al.* Comprehensive list of SUMO targets in Caenorhabditis elegans and its implication for evolutionary conservation of SUMO signaling. *Sci Rep* **8**, 1139 (2018).

102. Roy Chowdhuri, S., Crum, T., Woollard, A., Aslam, S. & Okkema, P.G. The T-box factor TBX-2 and the SUMO conjugating enzyme UBC-9 are required for ABa-derived pharyngeal muscle in C. elegans. *Dev Biol* **295**, 664-677 (2006).

103. Broday, L. *et al.* The small ubiquitin-like modifier (SUMO) is required for gonadal and uterine-vulval morphogenesis in Caenorhabditis elegans. *Genes Dev* **18**, 2380-2391 (2004).

104. Lim, Y. *et al.* Sumoylation regulates ER stress response by modulating calreticulin gene expression in XBP-1-dependent mode in Caenorhabditis elegans. *Int J Biochem Cell Biol* **53**, 399-408 (2014).

105. Pferdehirt, R.R. & Meyer, B.J. SUMOylation is essential for sex-specific assembly and function of the Caenorhabditis elegans dosage compensation complex on X chromosomes. *Proc Natl Acad Sci U S A* **110**, E3810-3819 (2013).

106. Zhang, H. *et al.* SUMO modification is required for in vivo Hox gene regulation by the Caenorhabditis elegans Polycomb group protein SOP-2. *Nat Genet* **36**, 507-511 (2004).

107. Kaminsky, R. *et al.* SUMO regulates the assembly and function of a cytoplasmic intermediate filament protein in C. elegans. *Dev Cell* **17**, 724-735 (2009).

108. Tsur, A., Bening Abu-Shach, U. & Broday, L. ULP-2 SUMO Protease Regulates E-Cadherin Recruitment to Adherens Junctions. *Dev Cell* **35**, 63-77 (2015).

109. Li, Y. *et al.* SUMOylation of the small GTPase ARL-13 promotes ciliary targeting of sensory receptors. *J Cell Biol* **199**, 589-598 (2012).

110. Sapir, A. *et al.* Controlled sumoylation of the mevalonate pathway enzyme HMGS-1 regulates metabolism during aging. *Proc Natl Acad Sci U S A* **111**, E3880-3889 (2014).

111. Mukhopadhyay, D. & Dasso, M. The SUMO Pathway in Mitosis. *Adv Exp Med Biol* **963**, 171-184 (2017).

112. Almedawar, S., Colomina, N., Bermudez-Lopez, M., Pocino-Merino, I. & Torres-Rosell, J. A SUMO-dependent step during establishment of sister chromatid cohesion. *Curr Biol* **22**, 1576-1581 (2012).

113. D'Ambrosio, L.M. & Lavoie, B.D. Pds5 prevents the PolySUMO-dependent separation of sister chromatids. *Curr Biol* **24**, 361-371 (2014).

114. Wu, N. *et al.* Scc1 sumoylation by Mms21 promotes sister chromatid recombination through counteracting Wapl. *Genes Dev* **26**, 1473-1485 (2012).

115. Montpetit, B., Hazbun, T.R., Fields, S. & Hieter, P. Sumoylation of the budding yeast kinetochore protein Ndc10 is required for Ndc10 spindle localization and regulation of anaphase spindle elongation. *J Cell Biol* **174**, 653-663 (2006).

116. Chung, T.L. *et al.* In vitro modification of human centromere protein CENP-C fragments by small ubiquitin-like modifier (SUMO) protein: definitive identification of the modification sites by tandem mass spectrometry analysis of the isopeptides. *J Biol Chem* **279**, 39653-39662 (2004).

117. Zhang, X.D. *et al.* SUMO-2/3 modification and binding regulate the association of CENP-E with kinetochores and progression through mitosis. *Mol Cell* **29**, 729-741 (2008).

118. Yang, F., Chen, Y. & Dai, W. Sumoylation of Kif18A plays a role in regulating mitotic progression. *BMC Cancer* **15**, 197 (2015).

119. Cubenas-Potts, C. *et al.* Identification of SUMO-2/3-modified proteins associated with mitotic chromosomes. *Proteomics* **15**, 763-772 (2015).

120. Eifler, K. *et al.* SUMO targets the APC/C to regulate transition from metaphase to anaphase. *Nat Commun* **9**, 1119 (2018).

121. Lee, C.C., Li, B., Yu, H. & Matunis, M.J. Sumoylation promotes optimal APC/C Activation and Timely Anaphase. *Elife* **7** (2018).

122. Johnson, E.S. & Blobel, G. Cell cycle-regulated attachment of the ubiquitin-related protein SUMO to the yeast septins. *J Cell Biol* **147**, 981-994 (1999).

123. Martin, S.W. & Konopka, J.B. SUMO modification of septin-interacting proteins in Candida albicans. *J Biol Chem* **279**, 40861-40867 (2004).

124. Ribet, D. *et al.* SUMOylation of human septins is critical for septin filament bundling and cytokinesis. *J Cell Biol* **216**, 4041-4052 (2017).

125. Shih, H.P., Hales, K.G., Pringle, J.R. & Peifer, M. Identification of septin-interacting proteins and characterization of the Smt3/SUMO-conjugation system in Drosophila. *J Cell Sci* **115**, 1259-1271 (2002).

126. Ban, R., Nishida, T. & Urano, T. Mitotic kinase Aurora-B is regulated by SUMO-2/3 conjugation/deconjugation during mitosis. *Genes Cells* **16**, 652-669 (2011).

127. Yoshida, M.M., Ting, L., Gygi, S.P. & Azuma, Y. SUMOylation of DNA topoisomerase IIalpha regulates histone H3 kinase Haspin and H3 phosphorylation in mitosis. *J Cell Biol* **213**, 665-678 (2016).

128. Nottke, A.C., Kim, H.M. & Colaiacovo, M.P. Wrestling with Chromosomes: The Roles of SUMO During Meiosis. *Adv Exp Med Biol* **963**, 185-196 (2017).

129. Ding, Y., Kaido, M., Llano, E., Pendas, A.M. & Kitajima, T.S. The Post-anaphase SUMO Pathway Ensures the Maintenance of Centromeric Cohesion through Meiosis I-II Transition in Mammalian Oocytes. *Curr Biol* **28**, 1661-1669 e1664 (2018).

130. Huang, C.J., Wu, D., Khan, F.A. & Huo, L.J. The SUMO Protease SENP3 Orchestrates G2-M Transition and Spindle Assembly in Mouse Oocytes. *Sci Rep* **5**, 15600 (2015).

131. Wang, Z.B. *et al.* The SUMO pathway functions in mouse oocyte maturation. *Cell Cycle* **9**, 2640-2646 (2010).

132. Hooker, G.W. & Roeder, G.S. A Role for SUMO in meiotic chromosome synapsis. *Curr Biol* **16**, 1238-1243 (2006).

133. Pelisch, F. *et al.* Dynamic SUMO modification regulates mitotic chromosome assembly and cell cycle progression in Caenorhabditis elegans. *Nat Commun* **5**, 5485 (2014).

134. Reichman, R., Shi, Z., Malone, R. & Smolikove, S. Mitotic and Meiotic Functions for the SUMOylation Pathway in the Caenorhabditis elegans Germline. *Genetics* **208**, 1421-1441 (2018).

135. Pelisch, F. & Hay, R.T. Tools to Study SUMO Conjugation in Caenorhabditis elegans. *Methods Mol Biol* **1475**, 233-256 (2016).

136. Cheerambathur, D.K. & Desai, A. Linked in: formation and regulation of microtubule attachments during chromosome segregation. *Curr Opin Cell Biol* **26**, 113-122 (2014).

137. Etemad, B. & Kops, G.J. Attachment issues: kinetochore transformations and spindle checkpoint silencing. *Curr Opin Cell Biol* **39**, 101-108 (2016).

138. Phillips, C.M. *et al.* HIM-8 binds to the X chromosome pairing center and mediates chromosome-specific meiotic synapsis. *Cell* **123**, 1051-1063 (2005).

139. Phillips, C.M. & Dernburg, A.F. A family of zinc-finger proteins is required for chromosome-specific pairing and synapsis during meiosis in C. elegans. *Dev Cell* **11**, 817-829 (2006).

140. McNally, K., Audhya, A., Oegema, K. & McNally, F.J. Katanin controls mitotic and meiotic spindle length. *J Cell Biol* **175**, 881-891 (2006).

141. Jantsch-Plunger, V. *et al.* CYK-4: A Rho family gtpase activating protein (GAP) required for central spindle formation and cytokinesis. *J Cell Biol* **149**, 1391-1404 (2000).

142. Raich, W.B., Moran, A.N., Rothman, J.H. & Hardin, J. Cytokinesis and midzone microtubule organization in Caenorhabditis elegans require the kinesin-like protein ZEN-4. *Mol Biol Cell* **9**, 2037-2049 (1998).

143. Maddox, A.S., Habermann, B., Desai, A. & Oegema, K. Distinct roles for two C. elegans anillins in the gonad and early embryo. *Development* **132**, 2837-2848 (2005).

144. Brenner, S. The genetics of Caenorhabditis elegans. *Genetics* **77**, 71-94 (1974).

145. Hirsh, D., Oppenheim, D. & Klass, M. Development of the reproductive system of Caenorhabditis elegans. *Dev Biol* **49**, 200-219 (1976).

146. Encalada, S.E., Willis, J., Lyczak, R. & Bowerman, B. A spindle checkpoint functions during mitosis in the early Caenorhabditis elegans embryo. *Mol Biol Cell* **16**, 1056-1070 (2005).

147. Essex, A., Dammermann, A., Lewellyn, L., Oegema, K. & Desai, A. Systematic analysis in Caenorhabditis elegans reveals that the spindle checkpoint is composed of two largely independent branches. *Mol Biol Cell* **20**, 1252-1267 (2009).

148. Moyle, M.W. *et al.* A Bub1-Mad1 interaction targets the Mad1-Mad2 complex to unattached kinetochores to initiate the spindle checkpoint. *J Cell Biol* **204**, 647-657 (2014).

149. Davis, E.S. *et al.* Multiple subunits of the Caenorhabditis elegans anaphase-promoting complex are required for chromosome segregation during meiosis I. *Genetics* **160**, 805-813 (2002).

150. Golden, A. *et al.* Metaphase to anaphase (mat) transition-defective mutants in Caenorhabditis elegans. *J Cell Biol* **151**, 1469-1482 (2000).

151. Hattersley, N. & Desai, A. The nucleoporin MEL-28/ELYS: A PP1 scaffold during M-phase exit. *Cell Cycle* **16**, 489-490 (2017).

152. Vong, Q.P., Cao, K., Li, H.Y., Iglesias, P.A. & Zheng, Y. Chromosome alignment and segregation regulated by ubiquitination of survivin. *Science* **310**, 1499-1504 (2005).

153. Laband, K. *et al.* Chromosome segregation occurs by microtubule pushing in oocytes. *Nat Commun* **8**, 1499 (2017).

154. Redemann, S. & Muller-Reichert, T. Correlative light and electron microscopy for the analysis of cell division. *J Microsc* **251**, 109-112 (2013).

155. Bollen, M., Peti, W., Ragusa, M.J. & Beullens, M. The extended PP1 toolkit: designed to create specificity. *Trends Biochem Sci* **35**, 450-458 (2010).

156. Heroes, E. *et al.* The PP1 binding code: a molecular-lego strategy that governs specificity. *FEBS J* **280**, 584-595 (2013).

157. Holubcova, Z., Blayney, M., Elder, K. & Schuh, M. Human oocytes. Error-prone chromosome-mediated spindle assembly favors chromosome segregation defects in human oocytes. *Science* **348**, 1143-1147 (2015).

158. Flemming, W. Historical Paper. Contributions to the Knowledge of the Cell and Its Vital Processes. *J Cell Biol* **25**, SUPPL:1-69 (1965).

159. Kamath, R.S. *et al.* Systematic functional analysis of the Caenorhabditis elegans genome using RNAi. *Nature* **421**, 231-237 (2003).

# Appendix:

## Appendix A: RC localization using new in-house antibodies

MCAK(NH), CSC-1, BIR-1, KLP-19(stalk), KLP-19(motor), and CLS-2 recombinant proteins were made for future biochemistry experiments and for antibody production for the lab. Antibodies were generated by Covance in rabbits and then affinity purified and optimized for immunofluorescence (Protocols and final dilutions are described in the 'Materials and Methods' chapter.)

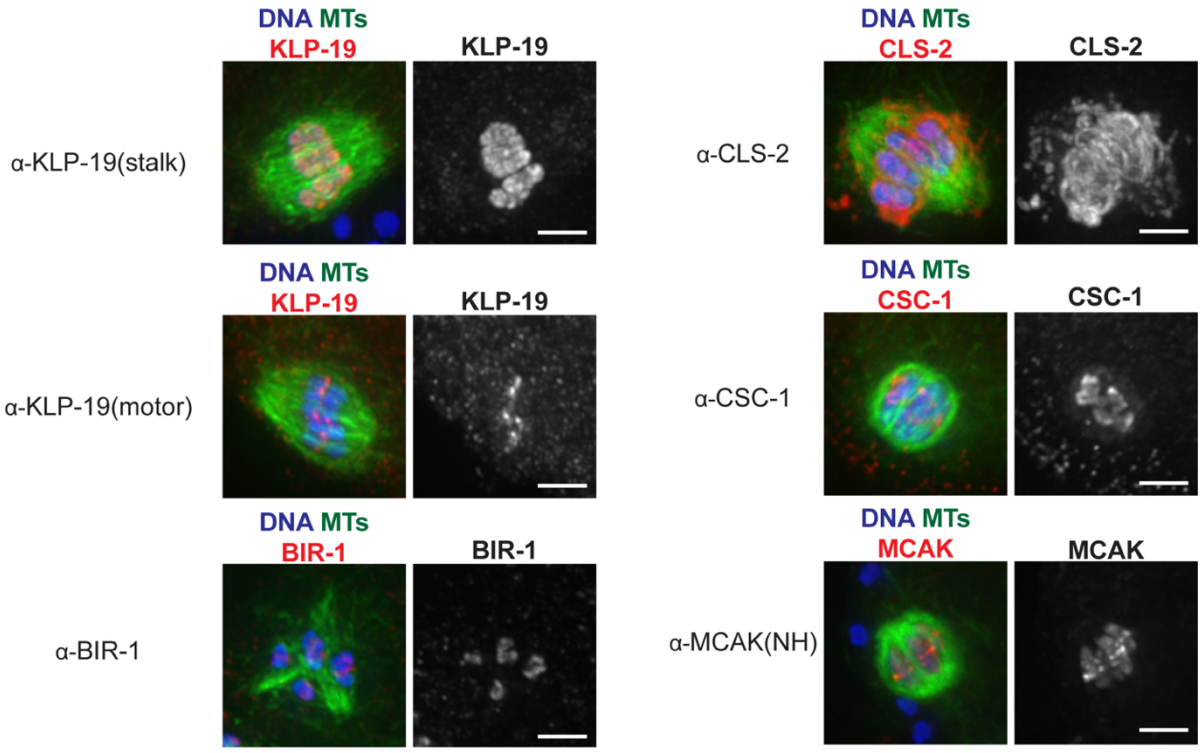


**Appendix Figure A. MCAK, CSC-1, BIR-1, CLS-2, and KLP-19 localization using new antibodies** Stained for DNA (blue), tubulin (green), and RC component (red). MCAK and KLP-19 are on the RCs and chromatin (stalk antibody only for KLP-19), BIR-1 and CSC-1 are RC localized. CLS-2 is on the kinetochore, kinetochore filaments, and faintly localized to the RCs.

**Appendix B: Many RC components can be SUMOylated *in vitro***

CSC-1, BIR-1, MCAK(NH), and CLS-2 were all capable of being SUMOylation *in vitro* (GEI-17 independent reaction) demonstrating that they could be candidates for *in vivo* RC SUMOylation. ULP-1 CD was also able to remove these modifications.

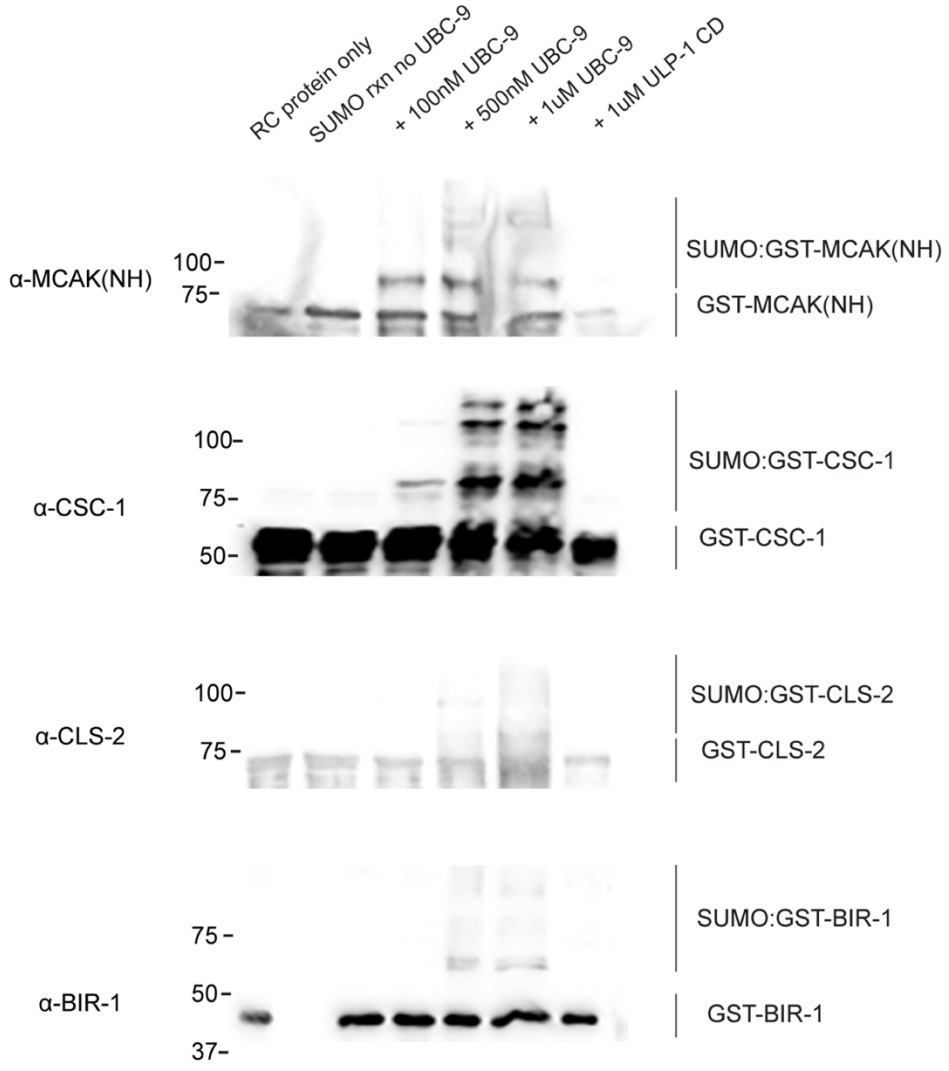


**Appendix Figure B. MCAK, CSC-1, CLS-2, and BIR-1 can be SUMOylation by UBC-9 and deSUMOylated by ULP-1 CD**
Western blots showing SUMOylation reactions with various RC proteins. Reactions were performed using 100nM, 500nM, and 1uM UBC-9 for 4 hours. Following that, 1uM ULP-1 CD was added and the reaction was incubated for another 6.5 hours.

**Appendix C: EBP-1 localization in oocyte meiosis**

EB1 proteins bind microtubule plus-ends and usually mark the growing plus-ends. In preliminary experiments, EBP-1 (the *C. elegans* homolog to EB-1) appeared to be enriched all over the spindle just prior to and also during anaphase when the spindle elongates.

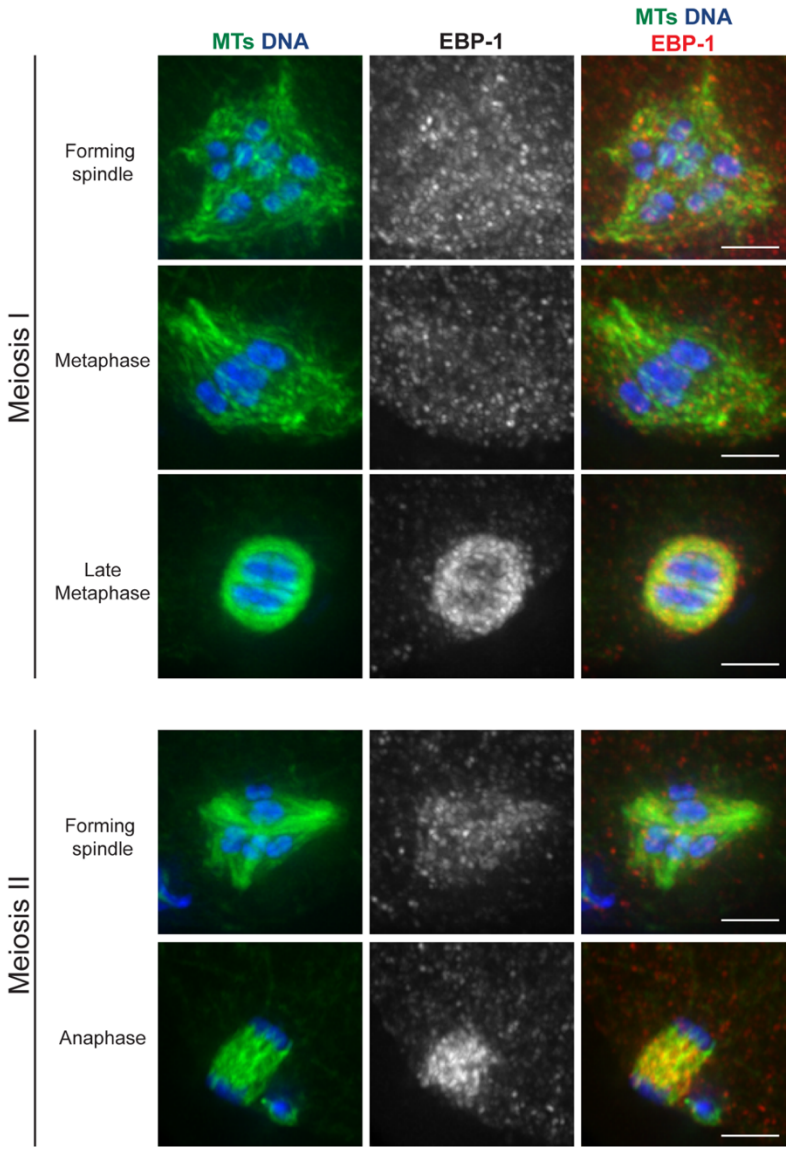


**Appendix Figure C. EBP-1 localization on oocyte spindles.**
Spindles stained for DNA (blue), tubulin (green), and GFP:EBP-1 (red)